

SHRP-A-630

Advanced High Performance Gel Permeation Chromatography Methodology

Dr. P.W. Jennings, Principal Investigator

Staff

Joan A. Pribanic

Dr. M.F. Raub

J.A. Smith

T.M. Mendes

Department of Chemistry and Biochemistry
Montana State University



Strategic Highway Research Program
National Research Council
Washington, DC 1993

SHRP-A-630
Contract AIIR-14

Program Manager: *Edward Harrigan*
Project Manager: *Jack Youtcheff*
Production Editor: *Marsha Barrett*
Program Area Secretary: *Juliet Narsiah*

April 1993

key words:
asphalt fractions
chromophores
diode-array detector
elution times
molecular size
molecular associations

Strategic Highway Research Program
National Academy of Sciences
2101 Constitution Avenue N.W.
Washington, DC 20418

(202) 334-3774

The publication of this report does not necessarily indicate approval or endorsement of the findings, opinions, conclusions, or recommendations either inferred or specifically expressed herein by the National Academy of Sciences, the United States Government, or the American Association of State Highway and Transportation Officials or its member states.

© 1993 National Academy of Sciences

Acknowledgments

The research described herein was supported by the Strategic Highway Research Program (SHRP). SHRP is a unit of the National Research Council that was authorized by section 128 of the Surface Transportation and Uniform Relocation Assistance Act of 1987.

Contents

Acknowledgement	iii
TABLE OF TABLES	ix
TABLE OF FIGURES	ix
Abstract	xi
I. EXECUTIVE SUMMARY	1
II. INTRODUCTION	4
A. <u>Background</u>	4
B. <u>Organization of report</u>	5
III. THEORETICAL APPROACH	7
A. <u>Asphalt: molecular structure and intermolecular interactions</u>	7
B. <u>Probing molecular structure and interactions</u>	9
IV. EXPERIMENTAL APPROACH	12
A. <u>The diode-array detector</u>	12
B. <u>The data and its interpretation</u>	13
C. <u>Columns and solvents</u>	17
D. <u>Reproducibility</u>	18
V. RESULTS AND DISCUSSION	21
A. <u>SHRP core samples in tetrahydrofuran</u>	21
1. Whole asphalts	21
2. IEC fractions	29
3. Oxidized asphalts	43
4. The SEC fractions	46

5. Derivatized samples	53
B. <u>General observations on solvent effects</u>	55
1. Effects on total conjugated volume	57
2. Effects on molecular size distribution	57
a. Asphalt AAA-1	58
b. Asphalt AAB-1	59
c. Asphalt AAC-1	60
d. Asphalt AAD-1	60
e. Asphalt AAF-1	61
f. Asphalt AAG-1	61
g. Asphalt AAK-1	62
h. Asphalt AAM-1	62
C. <u>Other MRL asphalts</u>	80
D. <u>Asphalt AAX (AC-20) and ROSE fractions</u>	92
E. <u>Relationship between data from HP-GPC analyses and other SHRP-generated information</u>	96
1. HP-GPC and other chemical data	96
2. HP-GPC and physical properties	97
F. <u>Summary descriptions of SHRP core asphalts</u>	99
G. <u>Miscellaneous topics</u>	103
1. Concentration effects	103
2. Effects of time in solution	104
3. Relationship of sample mass to detector response	108
VI. SUMMARY	111
VII. APPENDIX: EXPERIMENTAL PROCEDURES	116
A. <u>Short-term phase-transfer methylation</u>	116
B. <u>Friedel-Crafts acylation</u>	117
C. <u>HP-GPC analysis of asphalt samples</u>	117
VIII. REFERENCES	121

TABLE OF TABLES

Table 1.	Examples of uv-vis absorption of organic compounds	13
Table 2.	Elution times for polystyrene standards in different solvents.	18
Table 3.	Standard normal cumulative probabilities for conjugated volumes and conjugation indices for "standard" asphalt	20
Table 4.	HP-GPC and molecular weight data for core asphalts	23
Table 5.	HP-GPC characteristics of SHRP core asphalts	26
Table 6.	HP-GPC characteristics of IEC neutral fractions	30
Table 7.	HP-GPC characteristics of IEC weak acid and weak base fractions . . .	33
Table 8.	HP-GPC characteristics of IEC strong acid and strong base fractions .	34
Table 9.	Comparison of % LMS in whole asphalts with total % LMS for IEC fractions	35
Table 10.	Changes in HP-GPC parameters upon oxidation	45
Table 11.	Changes in %CV ₁₁₋₁₇ , % aromatic carbon and [OH+COOH] after TFO/POV oxidation	46
Table 12.	HP-GPC characteristics of SEC I and II fractions	48
Table 13.	Differences between % LMS observed in the whole asphalt and that calculated from amounts in SEC I and II	53
Table 14.	HP-GPC characteristics of Group 1 asphalts	83
Table 15.	HP-GPC characteristics of Group 2 asphalts	85
Table 16.	HP-GPC characteristics of Groups 3 and 4 asphalts	88
Table 17.	HP-GPC characteristics of AAX series materials	95
Table 18.	Effects of asphalt concentration on HP-GPC characteristics	104
Table 19.	Relationship of sample mass to detector response	110

TABLE OF FIGURES

Figure 1.	Examples of hydrocarbon and functional group types	8
Figure 2.	Comparison of uv-vis spectra	14
Figure 3.	Example of chromatogram at 340 nm	15
Figure 4.	Comparison of three-dimensional plots of two asphalts	15
Figure 5.	Example of seven-chromatogram plot with slice area cut points	16
Figure 6.	Seven-chromatogram plots of SHRP core asphalts	24
Figure 7.	3-D plots of SHRP core asphalts	25
Figure 8.	Plot of percent aromatic carbon vs CV_t	27
Figure 9.	Plot of percent aromatic carbon vs Cl_t	28
Figure 10.	Seven-chromatogram plots of IEC neutrals fractions	37
Figure 11.	Seven-chromatogram plots of IEC weak acids fractions	38
Figure 12.	Seven-chromatogram plots of IEC weak bases fractions	39
Figure 13.	Seven-chromatogram plots of IEC strong bases fractions	40
Figure 14.	Seven-chromatogram plots of IEC strong acids fractions	41
Figure 15.	Chromatograms at 230 nm of IEC fractions and the asphalts from which they were derived	42
Figure 16.	Chromatograms at 340 nm of untreated, POV and TFO/POV oxidized core asphalts	44
Figure 17.	Seven-chromatogram plots of SEC I fractions in THF	49
Figure 18.	Seven-chromatogram plots of SEC II fractions in THF	50
Figure 19.	Comparison of SEC I fractions from core asphalts at 340 nm	51
Figure 20.	Change in molecular size distribution of asphalt AAA-1 resulting from acylation reaction	55
Figure 21a and b.	Solvent effects on MSDs of Asphalt AAA-1 and its strong acid fraction	64
Figure 22a and b.	Solvent effects on MSDs of Asphalt AAB-1 and its strong acid fraction	66
Figure 23a and b.	Solvent effects on MSDs of Asphalt AAC-1 and its strong acid fraction	68
Figure 24a and b.	Solvent effects on MSDs of Asphalt AAD-1 and its strong acid fraction	70
Figure 25a and b.	Solvent effects on MSDs of Asphalt AAF-1 and its strong acid fraction	72

TABLE OF FIGURES (Continued)

Figure 26a and b. Solvent effects on MSDs of Asphalt AAG-1 and its strong acid fraction	74
Figure 27a and b. Solvent effects on MSDs of Asphalt AAK-1 and its strong acid fraction	76
Figure 28a and b. Solvent effects on MSDs of Asphalt AAM-1 and its strong acid fractions	78
Figure 29. Seven-chromatogram plots of Group 1 asphalts	84
Figure 30. Seven-chromatogram plots of Group 2 asphalts	86
Figure 31. Seven-chromatogram plots of Group 2 asphalts (continuation of Figure 30.)	87
Figure 32. Seven-chromatogram plot of sole asphalt in Group 3	89
Figure 33. Seven-chromatogram plots of Group 4 asphalts	89
Figure 34. Seven-chromatogram plots of AAX series materials	94
Figure 35. Effect of asphalt concentration on molecular size distribution	105
Figure 36. Changes in apparent molecular size distribution with time in 80 percent toluene/THF	107
Figure 37. Difference in response to time (hours) in solution for asphalts AAG-1 and ABD-1	108

Abstract

This report explores the use of high performance gel permeation chromatography (HP-GPC) as a means of studying asphalt composition and their intermolecular interaction. SHRP core asphalts, their acid-base fractions and laboratory-oxidized counterparts were analyzed. Based on the concept that distribution of molecular size and the ability of the molecules to assemble into larger entities in solution and into networks in neat asphalt are crucial to the performance of the asphalt. Attributes of the network formed will determine the ability of the asphalt to resist thermal shock, for example, by providing strength and elasticity.

I. EXECUTIVE SUMMARY

The purpose of the research conducted under the SHRP-AIIR-14 contract has been to explore enhancements of the HP-GPC (high performance gel permeation chromatography) technique and to apply the technique to the study of the chemical composition of the SHRP core asphalts and their modes of intermolecular interaction. The research has been premised on the idea that the distribution of apparent molecular sizes and the ability of the molecules to assemble into larger entities in solution -- and into networks in the neat asphalt -- are crucial to the performance of the asphalt. Attributes of this network will determine the ability of the asphalt to resist thermal shock, for example, by providing strength and elasticity.

From the technique used here, information has been obtained about apparent molecular size distribution, relative content of aromatic (conjugated) material and the relative size of the aromatic units (regardless of the size of the molecules in which they are embedded). SHRP core asphalts, their acid-base fractions, and their laboratory-oxidized counterparts have been analyzed. Further, through changes in the polarity of the solvent used in the analysis, the ability of the samples to undergo self-assembly by different interactive mechanisms has been probed.

As a result of this work, the core asphalts have been separated into four groups. The other asphalts in the SHRP Materials Reference Library collection were found to fall into similar patterns. Although there are many details which distinguish the asphalts within the groups (details which are discussed in this report), the authors suggest that

each group will be related to broad performance characteristics that will be somewhat modified by these details.

Group 1 asphalts are characterized by narrow molecular size distributions composed of smaller materials. These asphalts differ slightly in their tendency to assemble but as a group show very little such ability. Furthermore, their molecular size distributions undergo only minor changes upon laboratory oxidation. Thus, these asphalts, regardless of differences in detail, may be unable to assemble an effective intermolecular network incorporating several interaction mechanisms. As a result, they may exhibit "tenderness" and lack the ability to resist rutting and early cracking due to rapid temperature changes. Core asphalts AAC-1, AAF-1 and AAG-1 fall into this group. Preliminary gradings by the SHRP binder specification rate seven of the nine Group 1 asphalts as "failures."

Group 2 contains the "common" asphalt types characterized by broader molecular size distributions and by much better defined tendencies to form self-assembled entities. These asphalts should be able to assemble very effective intermolecular networks and so should not exhibit "tenderness" or early, temperature-associated cracking. However, these asphalts also undergo changes in molecular size distribution upon oxidation. This may add to the intermolecular network and lead, eventually, to age-associated cracking. Asphalts AAA-1, AAB-1 and AAK-1 are in this group. Group 2 asphalts are scattered through much of the climate-zone recommendations in the preliminary SHRP specification, most not being recommended for use below -10°F . We agree, in general. (This has unfortunate consequences for broad areas of the United States and

Canada where winter temperatures generally drop well below -10°F .)

Only one core asphalt is assigned to each of the remaining groups. Although asphalt AAD-1 resembles Group 2 asphalts in its network-forming ability and in changes on oxidation, its very broad molecular size distribution is marked by a unique concentration of quite small, slightly aromatic molecules. The effect of this is uncertain at this time, but it seems likely that this asphalt will be subject to volatile loss on heating leading to rapid hardening. Preliminary SHRP specifications rate asphalt AAD-1 for use in climates with a temperature range of -20 to 100°F . We would suggest -10°F as the lower limit to minimize age-related cracking at lower temperatures.

Asphalt AAM-1 represents Group 4. Characteristics of this group include a narrower molecular size distribution than Group 2 and 3 asphalts. However, the average molecular size is much larger, the chromophores are larger but the overall aromatic content is not high. There is some indication of intermolecular network formation, but, because of the very large aromatic structures and large aliphatic content, the performance is likely to be driven by these molecular types. Preliminary SHRP specifications place all Group 4 asphalts in "PG 3" category, for hotter climate zones (maximum 100°F). That is, interactions among these aromatic structures may be very effective in resisting deformation at high environmental temperatures.

II. INTRODUCTION

II. A. Background

Gel permeation chromatography (GPC) has a long history of use in the analysis of complex materials such as polymers, food products and petroleum products, including asphalt cements. There is, in fact, a substantial body of work on asphalts using the technique in its more efficient form, high performance GPC (HP-GPC). Most of this work has been reviewed for SHRP by ARE Inc (1), so an extensive review of the literature will not be undertaken here.

In principle, HP-GPC is simply a separation of molecules in a sample according to their sizes or, more specifically, their hydrodynamic volumes. This can be likened to a sieving process in which largest materials elute first, followed by successively smaller molecules. In asphalts, this is complicated by the fact that some of the largest "molecules" may be assemblies of smaller molecules held together by one or more intermolecular forces. As a result, HP-GPC can be useful in studying these modes of interaction which must contribute to the properties of the asphalt.

Brulé (1-4) has conducted extensive characterization studies of asphalts by HP-GPC. He has pioneered an "ultra-rapid" technique which discourages the break-up of intermolecular assemblies and causes them to elute at or near the exclusion volume of the column. Relationships of the elution characteristics with certain physical properties have been reported.

Plummer and Beazley (5,6), using a somewhat different system and analysis conditions, have reported a method by which certain physical properties of an asphalt can be predicted by HP-GPC analysis of the crude oil. Their work requires that no intermolecular assemblies be present, so they have used elevated temperature conditions with polar and nonpolar solvents.

Work in this laboratory has centered about relationships between the results from HP-GPC analyses and specific field performance characteristics of asphalts. However, extensive work has also been done to use HP-GPC to follow the results of mixing with aggregate, aging, mixing with other additives, etc. (1,7,8,9). The application of a multiple-wavelength, ultraviolet-visible detector (a diode array detector, "DAD") to the study of asphalt was explored in an effort with Elf, France (10).

The purpose of the research under the SHRP-AIIR-14 project has been to enhance the HP-GPC technique by exploration of the use of more advanced analytical column types with a diode array detector and then to apply that technique to study of the chemical composition of the SHRP core asphalts and their modes of intermolecular interaction.

II. B. Organization of report

This final report will be divided into seven major sections. Following this Introduction, Section III will deal with the theoretical approach to the study: molecular structure and interactions, the applications of HP-GPC to those problems, and the selection of appropriate samples. In Section IV, the experimental approach to HP-GPC

analyses will be discussed, although full experimental details will be reserved for the Appendices (Section VII). Section V will contain general discussions of the results of the study in addition to detailed descriptions of each of the core asphalts drawn from those results. A summary will be presented in Section VI.

III. THEORETICAL APPROACH

III. A. Asphalt: Molecular structure and intermolecular interactions.

Even a cursory review of the asphalt literature will reveal a variety of approaches to the problem of the chemical composition of asphalts and the question of how asphalt components interact. (J.C. Petersen has provided a fine review (11)). For example, Petersen and members of his research group (12) have been major contributors of methods for identifying functional groups in asphalt. T.F. Yen (13) and J. Speight (14) among others, have discussed theories for the intermolecular interactions which occur in asphaltenes. While recognizing the importance of this body of work, the authors have chosen to follow a different approach to these problems.

Although it is known that the molecules in an asphalt occur in a very broad range of molecular weights, shapes and chemical characteristics, a few generalizations may be made. First, all asphalts contain mostly carbon and hydrogen (90 percent or more by weight) and these may be arranged in aromatic, alicyclic or aliphatic portions (Figure 1). It is not necessary for all types of hydrocarbon to appear in one molecule.

Second, there are small amounts of heteroelements (nitrogen, oxygen and sulfur) arranged in a variety of functional groups.

These hydrocarbon and functional group characteristics are important because they are responsible for different kinds of interactions between molecules -- interactions which contribute to the behavior of the asphalt. For example, aromatic rings are flat and can stack one-above-another to form what are known as pi-pi interactions which can hold molecules together.

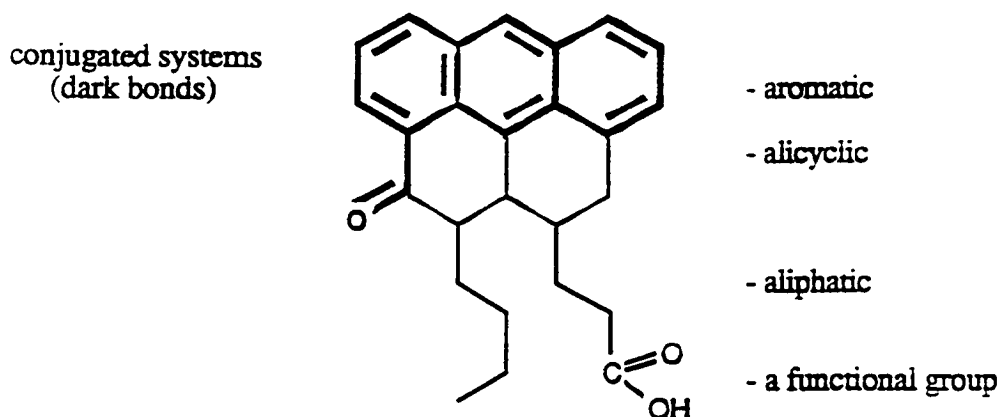


Figure 1. Examples of hydrocarbon and functional group types

These interactions are stronger between larger systems with fewer substituents.

Another mode of molecular interaction arises between aliphatic chains. These van der Waals interactions are stronger between longer chains with fewer branches.

Polar interactions, including hydrogen bonding, are also potential contributors to self-assembly among asphalt molecules. These involve heteroelements and could associate two molecules or perhaps two pi-bound stacks.

The precise ways in which these interactive forces affect asphalt properties are not yet entirely clear. However, the relationships should become more apparent when the results of this and other chemical studies are correlated with behavioral traits determined under SHRP contracts. Some thoughts on the subject will be put forward later in this report.

III. B. Probing molecular structure and interactions.

In an ideal HP-GPC experiment, molecules are separated by size with a minimum of interference from the chemical characteristics of the molecules. For example, the polarity of a molecule does not affect its elution volume. In certain systems for which accurate standards are available (e.g., polymers), molecular weight may be accurately determined.

For asphalt, however, accurate standards are not available for molecular weight determination because of the complexity of the mixture. Furthermore, chemical characteristics can interfere with a separation based strictly on molecular size if intermolecular associations are permitted under the analysis conditions. Since we theorize that the nature of intermolecular associations are critical to the physical and performance properties of an asphalt, the latter fact makes HP-GPC particularly useful for asphalt analysis.

Therefore, in this study, the apparent molecular size distributions of asphalts have been determined not only under the conditions ordinarily used in this laboratory but also with a variety of samples and analysis conditions designed to elucidate broad chemical characteristics as well as mechanisms of formation of intermolecular assemblies.

All samples have been analyzed in tetrahydrofuran (THF) which, like any effective solvent, must destroy most intermolecular associations but which apparently does leave some assemblies intact. If some of these assemblies result from polar interactions, the addition of a more polar solvent (e.g., methanol) should result in a

decrease in the apparent molecular size of the asphalt sample. However, if pi-pi and/or van der Waals interactions (nonpolar forces) can occur in the sample, an increase in solvent polarity will encourage them and thus, an increase in apparent molecular size will be observed. It is important to keep these opposing effects in mind throughout this discussion.

Similarly, addition of an aromatic compound such as toluene to the solvent system will discourage pi-pi interactions while encouraging polar forces. Hexane, a straight-chain hydrocarbon, will be particularly effective in interrupting van der Waals interactions. Both of these solvents have been used in this study.

Another approach to understanding the contribution of polar and non-polar forces to formation of assemblies is to interrupt them chemically by derivatization. Hydrogen bonding can be limited if the hydrogen atoms in phenols, alcohols and carboxylic acids are replaced with methyl groups. If hydrogen bonding is a key contributor to intermolecular assembly, one might expect to observe a decrease in apparent molecular size of the sample after such treatment. Similarly, pi-pi interactions may be interrupted by chemically attaching substituents to aromatic rings. Both of these approaches have been used in this research.

The SHRP core asphalts have been fractionated by SHRP A-002A contractors at Western Research Institute. Using ion exchange chromatography (IEC) (14), asphalts have been separated into five fractions by acid-base characteristics. These fractions are important in determining the chemical characteristics and modes of interactions of assembled entities and, thus, have been given attention in this work.

WRI has also supplied two fractions from their preparative size exclusion chromatography (SEC) (15) process. (This technique uses the same principle as GPC.) Fractions SEC I and II were provided from each core asphalt. SEC I is the first fraction to elute and thus contains the larger entities. Because it does not fluoresce, it is assumed to be composed of assemblies of smaller molecules. Since the non-polar solvent toluene was used in the separation, polar interactions are presumed to be strongly involved in SEC I fractions. SEC II contains fluorescing components, i.e., not association, of smaller molecular sizes. These samples have also been studied in the present research.

Finally, laboratory oxidized samples of the core asphalts (also supplied by WRI) have been analyzed to determine the effects of oxidation on apparent molecular size distribution.

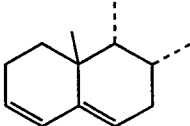
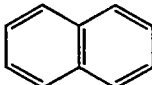
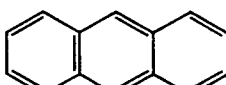
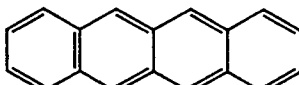
IV. EXPERIMENTAL APPROACH

IV. A. The diode-array detector.

Although no universal and absolute detection system is available for use in the HP-GPC analysis of asphalt, the diode-array detector (DAD) provides a great deal of useful chemical information. After a sample is separated by apparent molecular size in the HP-GPC column, the DAD analyzes the eluent by means of ultraviolet-visible spectroscopy in the range 200-600 nm. This takes advantage of the fact that molecules which are conjugated, including those which are aromatic (see Figure 1, page 8), absorb light in the uv-vis range to give information about their structures. The uv-vis spectrum of a given conjugated system will consist of rather broad peaks with maxima at specific wavelengths (λ_{\max}). In general, these maxima occur at shorter wavelengths for less extensive conjugated systems (i.e., smaller chromophores) and at longer wavelengths for more extensive conjugated systems (i.e., larger chromophores). Note that chromophore size is not necessarily the same as molecular size. For example, a small chromophore could be embedded in a large molecule. The intensity of the absorption expressed as the extinction coefficient (ϵ), is characteristic of the system. Some examples of conjugated systems are shown in Table 1.

A further contribution to uv-vis absorption can be expected from pi-pi interactions. These associations may change the wavelength at which absorption occurs depending on the nature of the molecules and their orientation.

Table 1. Examples of uv-vis absorption of organic compounds

	λ_{\max}	$\log \epsilon$
	234	4.3
	275	3.7
	254/356	5.4/3.9
	279/474	5.1/4.1

In Figure 2 are shown the uv-vis spectra of two asphalts taken at the same elution time (i.e., have the same apparent molecular size). The asphalt represented by spectrum I has a higher concentration of conjugated systems and/or more highly conjugated systems (larger chromophores) than does asphalt II. Thus, the combination of HP-GPC with uv-vis detection provides information about the conjugated molecular structure of asphalt across its full molecular size distribution.

IV. B. The data and its interpretation.

The data available from an HP-GPC experiment can be viewed and interpreted in a variety of ways. Both simple and useful is the chromatogram at a single wavelength such as that at 340 nm in Figure 3. The absorption due to large molecules and/or

intermolecular assemblies is recorded on the left with the absorption due to successively smaller molecules appearing to the right. Presumably, small associated units could appear toward the right, as well, but we have no means at present to determine this precisely. Therefore we will refer to "small molecules" with this understanding.

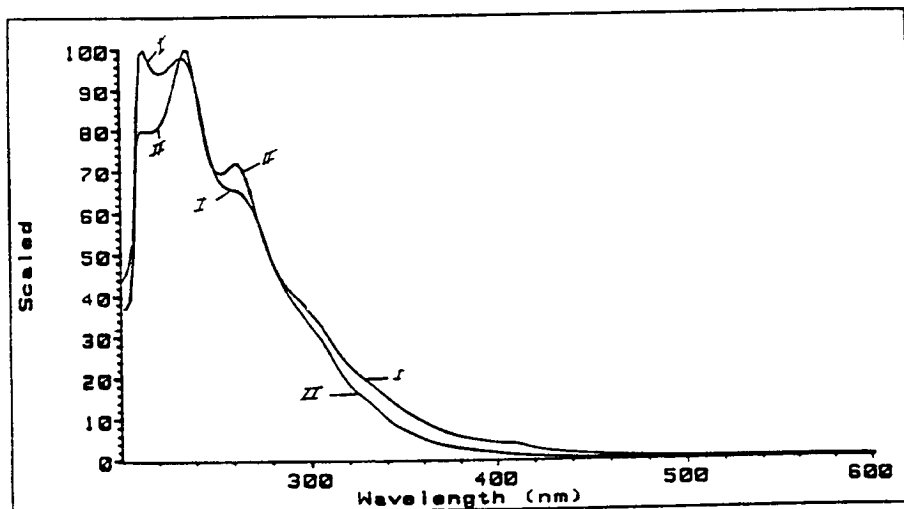


Figure 2. Comparison of uv - vis spectra

Also useful are the spectra at various elution times as described above. A combination of spectra and chromatograms at various wavelengths provides a visual tool for the qualitative assessment of an asphalt. Using two of these three-dimensional plots (Figure 4) one can compare the asphalts in terms of their breadth of molecular size distribution, evidence for presence of intermolecular assemblies (presence of the left-hand shoulder) and for the presence of extensive chromophores (in the relative intensities of absorption at longer wavelengths). These asphalts are clearly

different. It is the premise of this work that such differences will be reflected in the performance of the asphalts.

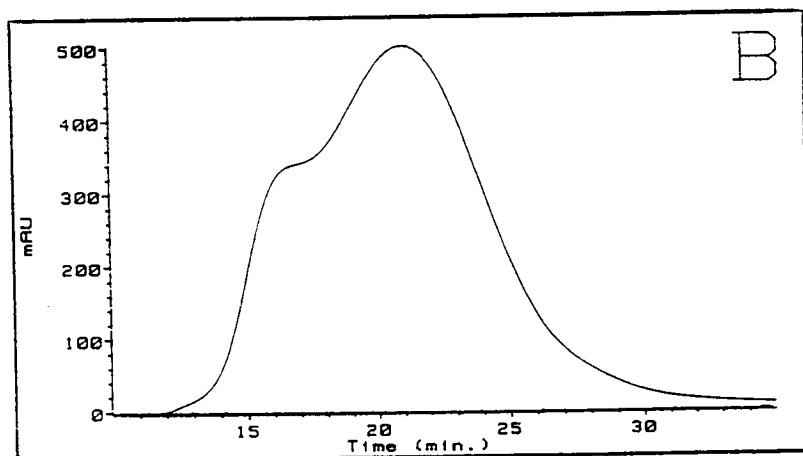


Figure 3. Example of chromatogram at 340 nm

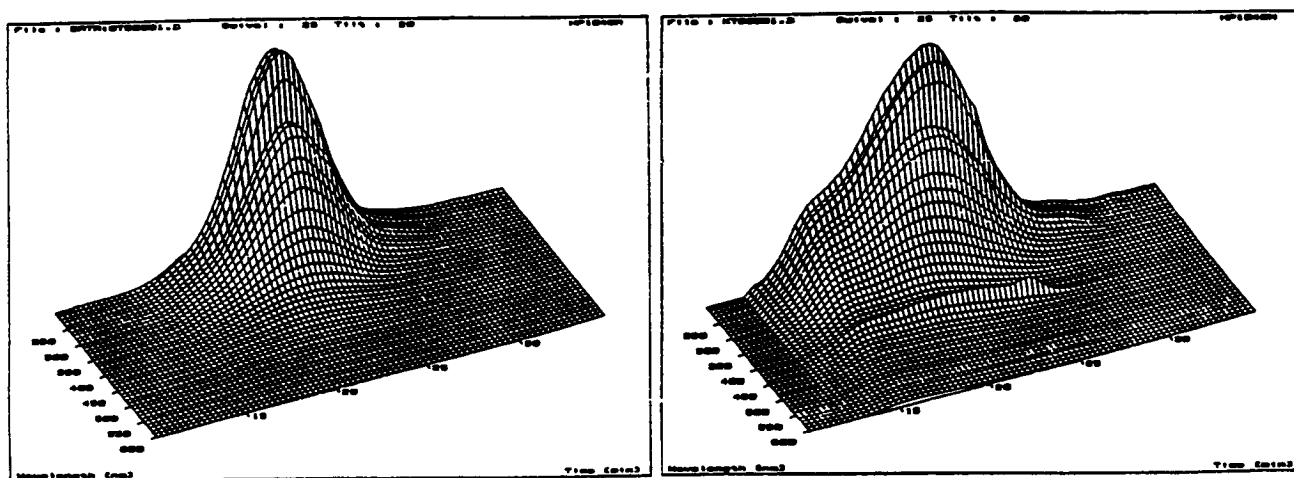


Figure 4. Comparison of three dimensional plots of two asphalts

Although qualitative differences may be easy to see when samples differ widely, smaller differences must be assessed in a more precise fashion. To that end, integrations of chromatogram areas are being used. In Figure 5 are shown chromatograms at seven wavelengths (230, 254, 280, 340, 380, 410 and 440 nm) as well as cut-points for calculation of areas of narrow slices or wider segments. The following parameters will be used in this report:

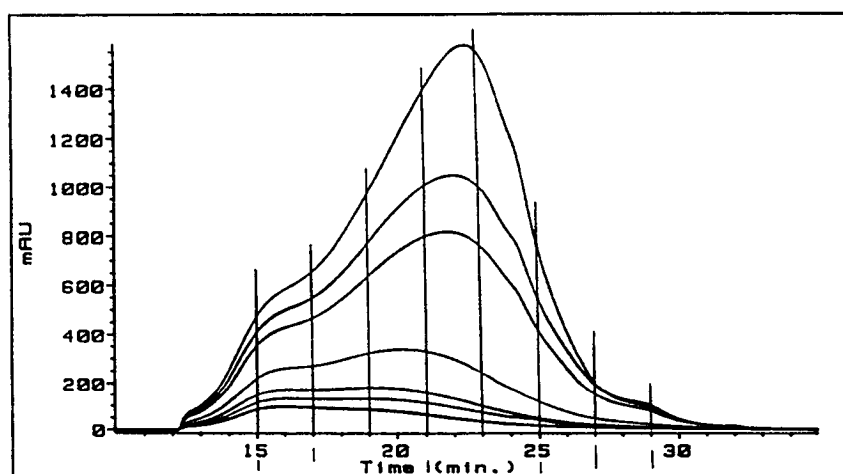


Figure 5. Example of seven-chromatogram plot with slice area cut points

- 1) Chromatogram area - the integrated area under the HP-GPC curve at a single wavelength.
- 2) Area percentage - the percentage of a chromatogram area in a given slice (e.g. 11-17 min).

- 3) Conjugated volume, total (CV_t) - the sum of areas under the seven chromatograms (230, 254, 280, 340, 380, 410 and 440 nm) to assess the relative conjugated character of a sample: larger value indicates more conjugated character.
- 4) Conjugation index, total (CI_t) - the result of dividing the area under the 340 nm chromatogram by that at 230 nm. This will be used in assessing the relative size of chromophores: smaller values indicate smaller chromophores, on average.
- 5) Percent conjugated volume, slice or segment ($\%CV_{x-y}$) - the percentage of CV_t represented between two given elution times. $\%CV_{11-17}$ may be termed %LMS, percent large molecular size or assembled materials.
- 6) Conjugation index, slice or segment (CI_{x-y}) - the ratio of the area at 340 nm to that at 230 nm between two given elution times.

The latter parameters ($\%CV_{x-y}$ and CI_{x-y}) will quantify differences between samples in terms of their molecular size distributions (MSD), their relative conjugated character at the same molecular size and their relative chromophore size at the same molecular size, as well as across the MSD.

IV. C. Columns and solvents.

Newer gel permeation column types made of highly crosslinked polystyrene-divinylbenzene are considerably more stable in different solvents than some common types. This characteristic is very important to this research because changes in the MSD

of an asphalt in different solvents must be attributed to changes in the asphalt rather than to solvent-induced changes in the columns. The stability of the analytical column was assessed using a series of polystyrene standards in the various solvents (see Appendix A). As can be seen in Table 2, the elution times of the standards remained remarkably constant, especially in the asphalt elution range from about 13 minutes on, in all of the solvent systems except hexane/THF in which elution times of lower molecular weight standards were gradually increased. This will be taken into account when describing the effects of this solvent system.

Table 2. Elution times for polystyrene standards in different solvents

	<u>M.W.(x10³)</u>	<u>1125</u>	<u>240</u>	<u>50</u>	<u>9</u>	<u>3.6</u>	<u>1.8</u>	<u>0.092⁽¹⁾</u>
<u>Solvent</u>	<u>Elution time (min.)</u>							
THF		11.53	12.06	12.53	15.82	17.4	18.51	29.02
20TOL ⁽¹⁾ /80THF		11.83	12.33	12.87	16.13	17.77	18.97	28.80
50TOL/50THF		11.73	12.23	12.80	16.13	17.70	18.83	29.20
80TOL/20THF		11.63	12.23	12.77	16.10	17.57	18.83	28.60
20HEX ⁽²⁾ /80THF			12.32	12.83	16.29		19.35	31.57
5MeOH ⁽³⁾ /95THF		11.62	12.23	12.74	16.11		19.12	29.51
MEAN		11.67	12.23	12.76	16.14	17.61	18.94	29.45
STANDARD								
DEVIATION		0.10	0.09	0.11	0.14	0.14	0.26	0.99

- (1) toluene
- (2) hexane
- (3) methanol

IV. D. Reproducibility.

In addition to using polystyrene standards for column calibration, our internal quality control program for the HP-GPC technique includes the analysis of an asphalt

sample of known performance characteristics, used for a number of years as a "standard". This asphalt standard is analyzed at the beginning of the sample run and a long-term running-account is made of the chromatogram data. An advantage this asphalt standard has over polystyrene is that the complex matrix of the asphalt exhibits a broad chromatographic profile so that subtle changes, i.e., elution time and intensity, are easily observed when compared with previous analyses. Preparation of mixed polystyrene standards of identical concentration is time consuming and changes that might occur are difficult to observe.

Table 3 is a compilation of the asphalt standard data acquired during sample analysis in each of the six solvents studied. The mean and confidence intervals (99.7%) for two parameters, CV and CI - both Total and Segment, are given. Confidence intervals for CV range from about 1% to 16% of the means given but average about 5%. Larger ranges are seen in the 11-15 minute and 25-29 minute time-segments of the CV-Segment data where slight changes in elution time combined with smaller CV's magnify the relative ranges. Confidence intervals for the CI parameter are smaller yet, from less than 0.1% to about 3%, and averaging less than 1%. Thus, what is demonstrated by this "asphalt standard" data is the reproducibility of the HP-GPC technique and the precision available when comparing sample data.

Table 3. Standard normal cumulative probabilities for conjugated volumes and conjugation indices for "standard" asphalt

	THF		20HEX ⁽²⁾		20TOL ⁽³⁾		50TOL ⁽⁴⁾		80TOL ⁽⁵⁾		5MeOH ⁽⁶⁾	
	MEAN	CI	MEAN	CI	MEAN	CI	MEAN	CI	MEAN	CI	MEAN	CI
CV _t (x10 ⁵)	11.94	±0.07	11.55	±0.10	11.70	±0.25	11.79	±0.37	10.97	±0.12	12.00	±0.08
CV-SEGMENT (x10 ⁵)												
11-17 min.(LMS)	1.84	±0.04	1.51	±0.04	1.82	±0.15	2.16	±0.09	1.90	±0.09	1.74	±0.10
17-21 min.	3.94	±0.03	3.27	±0.03	3.78	±0.05	3.65	±0.16	3.27	±0.04	3.82	±0.04
21-25 min.	4.62	±0.03	4.23	±0.07	4.72	±0.06	4.53	±0.14	4.20	±0.04	4.60	±0.13
25-29 min.	1.53	±0.03	2.54	±0.06	1.39	±0.02	1.45	±0.12	1.60	±0.06	1.83	±0.06
CI _t	0.478	±0.001	0.472	±0.001	0.491	±0.002	0.498	±0.006	0.510	±0.001	0.478	±0.000
CI-SEGMENT												
11-17 min	0.679	±0.003	0.667	±0.001	0.685	±0.006	0.682	±0.005	0.693	±0.003	0.675	±0.009
17-21 min.	0.539	±0.003	0.539	±0.004	0.557	±0.003	0.558	±0.005	0.571	±0.003	0.562	±0.005
21-25 min.	0.409	±0.001	0.407	±0.001	0.426	±0.002	0.429	±0.006	0.447	±0.002	0.409	±0.003
25-29 min.	0.414	±0.002	0.437	±0.002	0.412	±0.002	0.422	±0.007	0.441	±0.002	0.403	±0.002

(1) 99.7% confidence interval

(2) 20% hexane/THF

(3) 20% toluene/THF

(4) 50% toluene/THF

(5) 80% toluene/THF

(6) 5% methanol/THF

V. RESULTS AND DISCUSSION

This section of the report will focus on the results of this research effort as well as on the ramifications of those results. Because tetrahydrofuran has been used as the primary solvent for all samples, results from analyses of the core asphalts and samples derived from those asphalts in THF will be discussed in Part A. In Part B, general observations about the effects of other solvent systems will be presented. Descriptions of each of the SHRP core asphalts, drawing on this and some other SHRP research, will be found in Part C.

In the remaining parts of Section V, characteristics of other SHRP asphalts will be described, followed by presentation of several miscellaneous experiments.

V. A. SHRP core samples in tetrahydrofuran.

V. A.1. Whole asphalts. All samples in this study have been analyzed by HP-GPC in tetrahydrofuran (THF). Fundamental differences among the samples have been noted in these analyses and will be summarized here.

Seven chromatogram plots of the SHRP core asphalts (Figure 6) and three dimensional plots (Figure 7) show a range of molecular size distributions and varying indications of the existence of intermolecular assemblies. A bi- or trimodal peak shape showing the presence of two or three distinct populations of molecular sizes is regarded as evidence of intermolecular association in the large molecular size (LMS) region on the left of the chromatogram. Of the eight core asphalts, AAC-1, AAF-1 and AAG-1 have the narrowest MSD's (15-16 minutes) and AAG-1 gives no evidence for

intermolecular association. Asphalts AAC-1 and AAF-1 have marginally more self-assembly in THF, but the bimodality of their peaks is weak.

The molecular size distributions of asphalts AAA-1, AAB-1 and AAK-1 are broader (18.5-20 minutes) than those mentioned above, have earlier initial elution times and well-defined bi- or trimodal peaks. That is, these asphalts contain larger molecules and/or assemblies, a greater range of apparent molecular sizes and stronger evidence for assembled entities than do asphalts AAC-1, AAF-1 and AAG-1.

Asphalt AAM-1 fits neither of these groups. Its peak shape indicates little intermolecular association. Although its peak width is about average for the core asphalts, the peak maximum occurs a full minute earlier than any of the others indicating that the average molecular size is larger. Indeed the average molecular weight of AAM-1 is about 1300 as compared to 700-860 for other core asphalts (Table 4).

Asphalt AAD-1 is clearly unique among the core asphalts. It has a wide MSD but the main peak elutes two minutes later than any of the others. It appears to contain self-assembled materials by virtue of its strong trimodal distribution. A distinct peak about 24.5 minutes between 230 and about 330 nm seems to represent a concentration of a specific compound. The strong absorptions at smaller molecular sizes indicates a low average molecular weight for this asphalt. Indeed, AAD-1 and AAG-1 have the lowest average molecular weights of the core asphalts.

Table 4. HP-GPC and molecular weight data for core asphalts

<u>Asphalt</u>	<u>Approximate peak width, minutes</u>	<u>Time peak maximum</u>	<u>Ave MW⁽¹⁾</u>
<u>Group 1</u>			
AAG-1	15.5	22.2	710
AAC-1	15	21.2	870
AAF-1	16	21.4	840
<u>Group 2</u>			
AAB-1	18.5	21.5	840
AAA-1	20	22.1	790
AAK-1	20	22	860
<u>Group 3</u>			
AAD-1	19	24.1	700
<u>Group 4</u>			
AAM-1	18	20.2	1300

⁽¹⁾ By VPO in toluene. Data from Western Research Institute and SHRP
Materials Reference Library

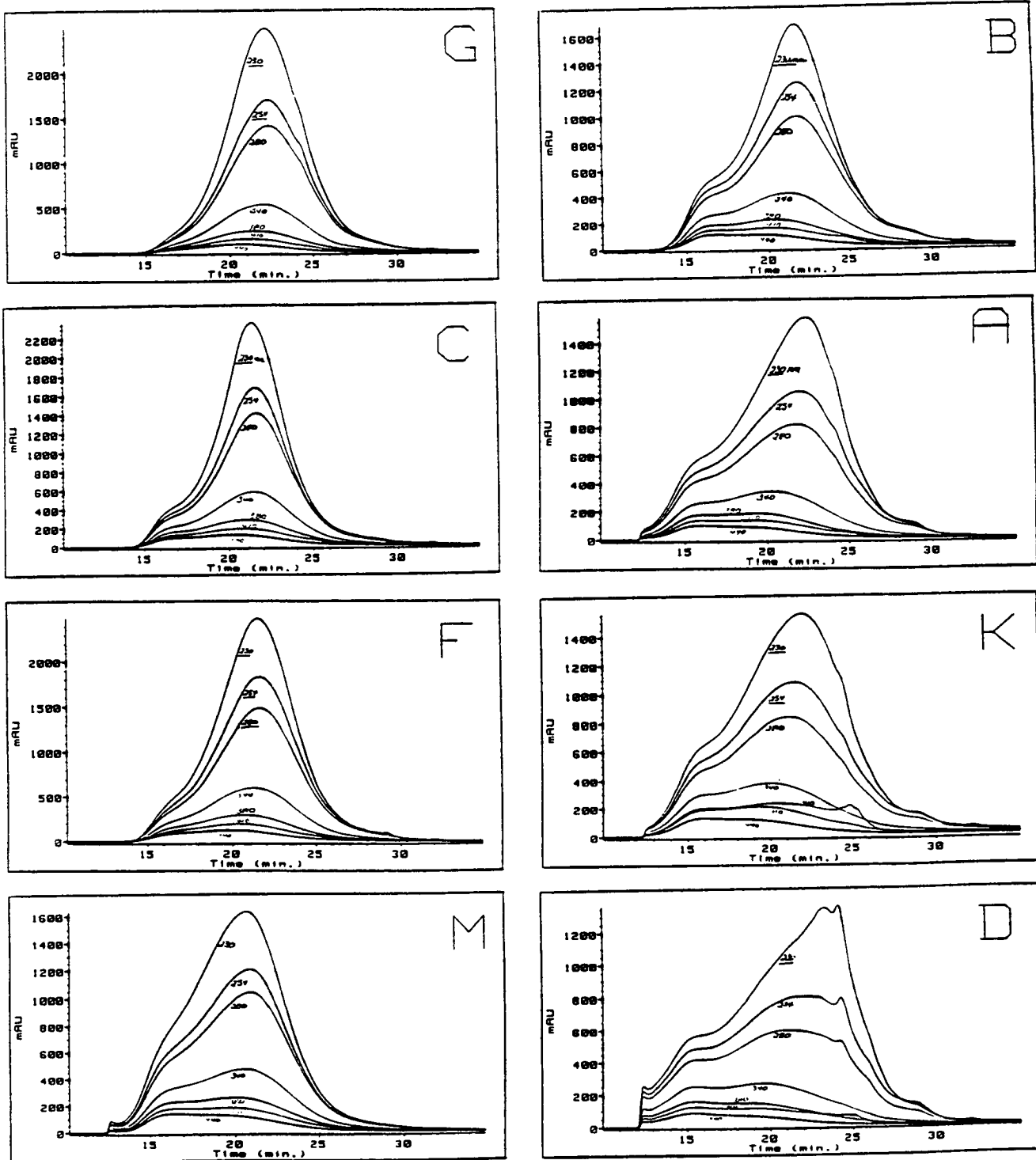


Figure 6. Seven-chromatogram plots of SHRP core asphalts

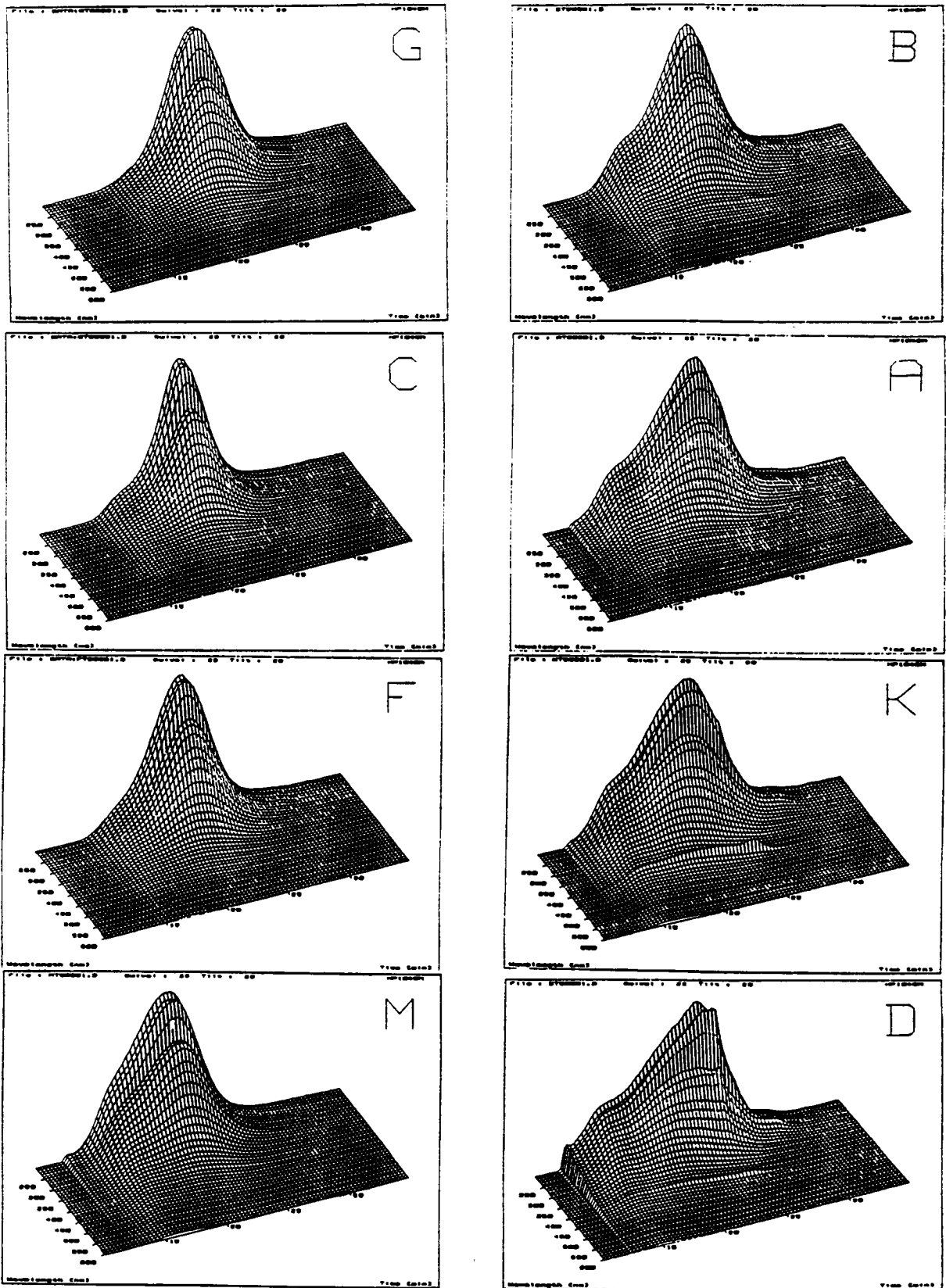


Figure 7. 3-D plots of SHRP core asphalts

Consideration of quantitative data in Table 5 permits further differentiation among these asphalts in terms of their conjugated volumes (CV_t and $\%CV_{x-y}$), conjugation indices (CI_t and CI_{x-y}) and percentage of aromatic carbon (17).

Table 5. HP-GPC characteristics of SHRP core asphalts⁽¹⁾

<u>Asphalt</u>	<u>CV_t</u>	<u>CI_t</u>	<u>%CV₁₁₋₁₇</u>	<u>%CV₁₇₋₂₁</u>	<u>%CV₂₁₋₂₅</u>	<u>%CV₂₅₋₃₄</u>	<u>CI₁₇₋₂₁</u>	<u>CI₂₁₋₂₅</u>	<u>% Arom. C⁽²⁾</u>	
			LMS							
AAA-1	22.6	0.264	19.2	34.2	36.7	9.9	0.451	0.169	27.9	
AAB-1	26.9	0.326	14.2	35.2	39.9	10.6	0.50	0.26	31.2	
AAC-1	23.9	0.327	8.2	38.5	45.3	8.0	0.53	0.28	27.8	
AAD-1	20.6	0.245	24.0	30.5	34.1	11.4	0.44	0.14	23.4	
AAF-1	27.6	0.299	8.3	39.0	44.2	8.5	0.478	0.251	32.8	
AAG-1	24.8	0.257	3.2	30.7	53.5	12.6	0.48	0.22	29.0	
AAK-1	24.6	0.274	19.5	35.3	33.8	11.4	0.453	0.180	26.2	
AAM-1	23.5	0.345	20.1	44.0	29.4	6.5	0.43	0.33	25.6	

⁽¹⁾ See page 16 for definition of parameters.

⁽²⁾ From carbon-13 nuclear magnetic resonance spectroscopy, SHRP A-002C final report (16).

A convention for ranking the asphalts in terms of a specific parameter has been adopted whereby the asphalt with the highest numerical value is listed first by its identifying letter. Parentheses indicate that, although there may be trends among the values, the differences may not be statistically significant.

Using this convention to rank the asphalts by CV_t :

$$F > B > (G > K) > (C > M) > A > D$$

and percent aromatic C:

$$(F > B) > (G > A = C > K > M) > D$$

A plot of these values (Figure 8) shows a general trend for percent aromatic carbon to follow conjugated volume. A precise correlation would not be expected because conjugated volume reflects not only the amount of aromatic carbon but also the way that carbon is arranged, particularly the size of chromophores. This is demonstrated in Figure 9, wherein the conjugation index (indicating the relative size of chromophores) is plotted against percent aromatic carbon. For example, asphalts AAA-1 and AAC-1 contain similar amounts of aromatic carbon, but their CI_t values indicated that the chromophores in AAC-1 are generally larger than those in AAA-1.

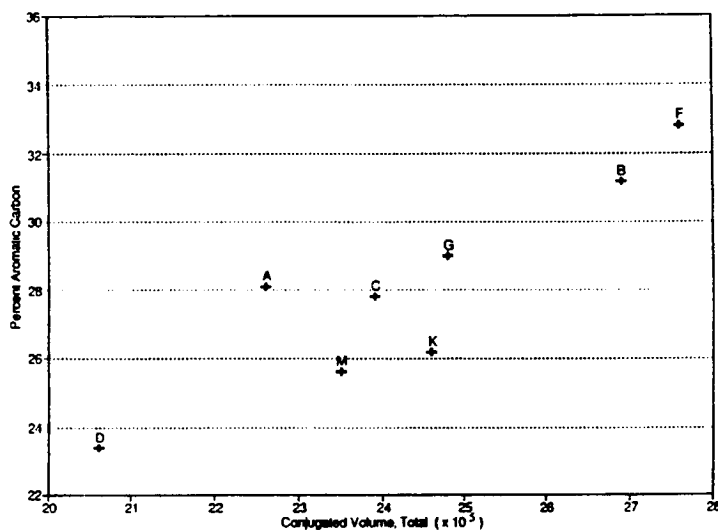


Figure 8. Plot of percent aromatic carbon vs CV_t

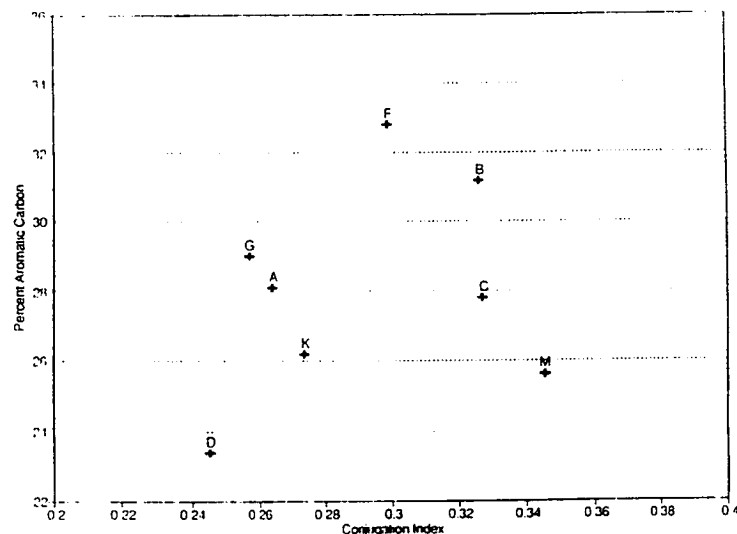


Figure 9. Plot of percent aromatic carbon vs Cl_t

Earlier in this part of the report, asphalts AAC-1, AAF-1 and AAG-1 were grouped together on the basis of their HP-GPC peak shapes, particularly their narrow molecular size distributions and relative lack of evidence for self-assembled entities in the curve shapes. The $\%CV_{x-y}$ data in Table 5 quantitates these characteristics. There is very little absorption before 17 minutes and most of the absorption is recorded between 21 and 25 minutes. Asphalt AAF-1 is considerably more aromatic than the other two asphalts (from $\%$ aromatic carbon and CV_t data) and, in fact, than all other core asphalts. However, the average chromophore is larger for AAC-1 (Cl_t ranking: $C > F > G$). Only for asphalt AAM-1 among all core asphalts is the average chromophore larger than that for AAC-1. Thus, the Group 1 asphalts seem to be quite different in terms of chemical composition and are grouped, at this level, on the basis of

MSD.

Asphalt AAM-1 is unique among the core asphalts in that the chromophore size remains quite large across the MSD. For the other asphalts, the largest chromophores are found in the LMS region but there is a significant decrease in the value of CI as molecular size decreases.

Asphalt AAD-1 continues to stand out because it is lowest in percent aromatic carbon, in CV_t and CI_t . In other words, it has more aliphatic and alicyclic molecules or portions of molecules than the other asphalts. The conjugated entities are broadly distributed in molecular size but, on average the chromophores are small.

For the eight core asphalts, CI_t values decrease in the order:

$M > (B = C) > F > K > (A > G) > D$.

Asphalts AAA-1, AAB-1 and AAK-1 were grouped together earlier on the basis of HP-GPC peak characteristics. They differ somewhat in terms of percent aromatic carbon, $B > (A > K)$. However, chromophores are significantly larger in AAB-1 than in AA-1 or AAK-1.

V. A.2. IEC fractions

Ion exchange chromatography (IEC) was used by SHRP-A-OO2A contractors at Western Research Institute to fractionate the core asphalts by acid-base characteristics (14). All five fractions have been analyzed by HP-GPC in THF to determine their molecular size distributions and to find evidence for self-assembly.

Seven chromatogram plots of the IEC neutral fractions (Figure 10) show no

outstanding features except for AAD-1. The distinctive peak at 24.5 minutes in the chromatogram of the whole asphalt AAD-1 is clearly present in the neutrals fraction.

Table 6. HP-GPC characteristics of IEC neutral fractions

<u>Asphalt</u>	CV_t ($\times 10^5$)	CI_t	$\%CV_{11-17}$	$\%CV_{17-21}$	$\%CV_{21-25}$	$\%CV_{25-34}$	$\%$ of whole <u>Asphalt</u> ⁽¹⁾	$\%$ CV_t <u>Whole asphalt</u> ⁽²⁾
LMS								
<u>Group 1</u>								
AAG-1	16.6	0.162	0.0	17.8	63.8	18.4	50.3	33.7
AAC-1	14.2	0.196	0.1	27.9	63.7	8.3	68.2	40.5
AAF-1	16.9	0.194	0.2	27.8	60.3	11.7	56.7	34.7
<u>Group 2</u>								
AAB-1	15.8	0.173	0.3	25.1	59.0	15.6	56.9	35.4
AAA-1	14.7	0.125	0.7	24.3	57.0	18.0	59.6	38.8
AAK-1	14.9	0.121	0.6	27.5	55.0	16.9	52.2	31.6
<u>Group 3</u>								
AAD-1	11.8	0.083	0.4	19.4	56.5	23.7	51.6	29.6
<u>Group 4</u>								
AAM-1	13.8	0.210	5.3	48.9	41.0	4.8	53.4	31.4
⁽¹⁾ Percent of whole asphalt found in neutrals fraction, from WRI () ⁽²⁾ Percent of CV_t of whole asphalt accounted for by neutrals								

The neutrals peak closely resembles the main peak of the whole asphalts (Figure 6) and there is no evidence for self-assembly in any sample. The values for CV_t (Table 6) decrease in the order: (F>G)>B>(K>A>C>M)>D, which is roughly similar to the order of CV_t for the whole asphalts. In terms of CI_t , the neutrals rank: M>(C=F)>B>G>(A>K)>D.

Except for AAM-1 and AAD-1, the chromophore sizes of the neutrals fraction do not directly mirror those in the whole asphalts. Nevertheless, chromophores in neutrals are quite small.

Although the neutrals fractions are not highly aromatic, they contribute 30 to 40 percent of the conjugated volume of the whole asphalts because they constitute at least 50 percent of the asphalt by weight (last two columns of Table 6). Note that the neutrals account for 68 percent of the whole asphalt AAC-1, presumably because of the "waxy" nature of that material.

The weak acids and weak bases fractions together account for less than 20 percent of the asphalts but generally are responsible for nearly 20 percent or more of the CV_t of the asphalt. Asphalt AAD-1 derives only about 16 percent of its CV_t from these fractions (Table 7) but shows a substantial absorbance among smaller molecular sized materials at 254 nm in the weak acids fraction.

Seven chromatogram plots of the weak acids (Figure 11) and weak bases (Figure 12) show that the MSD's of the weak acids are generally broader than those of the weak bases. However, there is no indication of self-assembly in any of the samples.

There is more obvious variation among the strong bases fractions (Figure 13 and Table 8). There is little evidence for self-assembly among the Group 1 fractions. However, the chromatograms for AAB-1, AAA-1 and AAM-1 are bimodal and those for AAK-1 and AAD-1 trend strongly toward the larger molecular sizes. Their CV_t 's are in the same range as those of the weak acids but, since their concentrations are low, they do not contribute a great deal to the CV_t of the whole asphalt. The strong

absorbance at 410 nm in the weak bases from asphalt AAK-1 indicates the presence of the vanadyl porphyrins in this fraction.

It is in the strong acids fractions that the largest contrasts among the core asphalts are found (Table 8 and Figure 14). These samples have the highest CV_t and CI_t values of the IEC fractions. Further, since they are present in the highest concentrations of the acid/base fractions, they make substantial contributions to the CV_t of the whole asphalt. This is particularly true of the strong acids from AAD-1. Although these have the lowest conjugated volume and the second lowest conjugation index of the strong acids, they contribute almost 39% of the CV_t of the whole asphalt because they comprise about 26% of the asphalt.

On the other hand, asphalt AAC-1 contains only 7.5% strong acids. Although these are highly conjugated and have fairly large chromophores, they contribute only about 13% of the total CV.

It would be tempting to assume that strong acids thus are responsible for intermolecular associations, but this can not be substantiated. First, because of the IEC separation procedure, the strong acids fraction will contain all those molecules with a strong acid functional group regardless of what other functional groups may be present. That is, this fraction is more likely to contain multifunctional molecules which could assemble into longer "chains" of associated molecules. (This likelihood decreases through the isolation sequence SA>SB>WA>WB>N.) The observed intermolecular association in this isolated fraction thus may not accurately reflect the interactions among the same molecules in the whole asphalt. This can be seen in Figure 15 in which

Table 7. HP-GPC characteristics of IEC weak acid and weak base fractions

<u>Asphalt</u>	CV_t ($\times 10^5$)	CI_t	$\frac{\%CV_{11-17}}{LMS}$	$\%CV_{17-21}$	$\%CV_{21-25}$	$\%CV_{25-34}$	<u>% of whole Asphalt</u>	<u>% CV_t Whole asphalt</u>
Weak Acids								
<u>Group 1</u>								
AAG-1	31.8	0.341	1.1	35.2	54.4	9.3	11.4	14.6
AAC-1	35.6	0.414	1.1	41.6	50.5	6.8	8.3	12.4
AAF-1	35.6	0.380	5.2	50.2	39.4	5.1	9.8	12.6
<u>Group 2</u>								
AAB-1	35.2	0.416	9.2	48.3	35.4	7.1	8.6	11.2
AAA-1	33.0	0.370	13.7	50.1	30.8	5.3	8.6	12.6
AAK-1	28.3	0.364	12.8	52.3	29.2	5.8	8.5	9.8
<u>Group 3</u>								
AAD-1	28.3	0.294	7.9	46.5	39.7	6.0	7.8	10.7
<u>Group 4</u>								
AAM-1	31.6	0.418	16.8	49.8	28.5	5.0	10.0	13.4
Weak Bases								
<u>Group 1</u>								
AAG-1	26.8	0.306	0.8	42.6	47.2	9.4	9.0	9.7
AAC-1	29.7	0.377	0.9	45.3	43.4	10.4	7.2	8.9
AAF-1	34.4	0.412	3.9	51.7	35.8	8.5	8.5	10.6
<u>Group 2</u>								
AAB-1	33.4	0.422	6.7	50.7	34.0	8.6	6.8	8.4
AAA-1	27.5	0.366	10.2	55.0	29.0	5.9	5.0	6.1
AAK-1	30.5	0.346	8.5	53.2	32.7	5.6	7.6	9.4
<u>Group 3</u>								
AAD-1	19.7	0.257	9.3	52.0	31.0	7.8	5.5	5.3
<u>Group 4</u>								
AAM-1	28.3	0.406	20.2	51.6	23.2	5.0	9.1	11.0

(1) Percent of whole asphalt found in weak acid or base fractions from WRI

(2) Percent of CV_t of whole asphalt accounted for by weak acids or base

Table 8. HP-GPC characteristics of IEC strong acid and strong base fractions

<u>Asphalt</u>	CV_t ($\times 10^5$)	CI_t	$\%CV_{11-17}$	$\%CV_{17-21}$	$\%CV_{21-25}$	$\%CV_{25-34}$	$\%$ of whole Asphalt ⁽¹⁾	$\% CV_t$ Whole asphalt ⁽²⁾
Strong Acids								
<u>Group 1</u>								
AAG-1	35.0	0.394	16.9	36.3	37.9	8.9	18.0	25.4
AAC-1	40.9	0.455	9.9	44.0	39.8	6.3	7.5	12.8
AAF-1	40.2	0.397	25.8	40.9	26.3	7.0	15.4	22.4
<u>Group 2</u>								
AAB-1	39.6	0.483	41.2	30.2	22.2	6.4	15.0	23.4
AAA-1	33.6	0.429	55.8	26.5	14.5	3.2	17.4	25.9
AAK-1	33.7	0.441	48.4	28.3	15.9	7.4	18.7	25.6
<u>Group 3</u>								
AAD-1	30.7	0.418	54.6	25.0	15.2	5.3	26.0	38.7
<u>Group 4</u>								
AAM-1	38.3	0.465	45.0	29.9	18.6	6.6	13.7	22.3
Strong Bases								
<u>Group 1</u>								
AAG-1	29.7	0.319	4.6	49.0	40.9	5.5	12.0	14.4
AAC-1	30.5	0.351	3.9	52.7	38.8	4.5	7.4	9.4
AAF-1	35.1	0.386	17.0	51.5	26.7	4.9	6.1	7.8
<u>Group 2</u>								
AAB-1	36.7	0.419	27.8	44.3	21.9	6.0	9.1	13.1
AAA-1	30.1	0.372	31.7	44.9	19.0	4.4	6.4	8.5
AAK-1	28.9	0.339	26.0	49.7	19.6	4.7	8.0	9.4
<u>Group 3</u>								
AAD-1	25.6	0.294	16.7	50.4	26.5	6.3	7.8	9.7
<u>Group 4</u>								
AAM-1	28.9	0.399	36.0	43.9	15.8	4.3	10.4	12.8

(1) Percent of whole asphalt found in neutrals fraction from WRI

(2) Percent of CV_t of whole asphalt accounted for by neutrals

the 230 nm chromatogram for each of the fractions is plotted in approximate proportion to its concentration in the whole asphalt, which is represented by its 230 nm trace. The largest molecular sized entities in the isolated strong acids fractions are larger than the largest materials in the whole asphalt for asphalts AAG-1 and AAB-1. It also appears that the strong acids contain more of the largest materials than the whole asphalts AAA-1, AAK-1 and AAD-1.

However, even if the intermolecular association in the strong acids is "artificially" high, the total of self-assembled materials in all of the fractions is much lower than in the whole asphalt. This may be assessed by use of the conjugated volume in segment 11-17 minutes, the percent LMS, in the following way: $(\% \text{ LMS}_{\text{strong acids}} \times \text{weight percent}_{\text{strong acids}}) + \text{a similar factor for each IEC fraction} = \text{total LMS of the IEC fractions} \times 100$. The total LMS for the IEC fractions of the eight core asphalts are compared with the percent LMS observed in the whole asphalt in Table 9. The "loss" in

Table 9. Comparison of % LMS in whole asphalts(a) with total %LMS for IEC fractions (b)

<u>Asphalt</u>	a % LMS _{whole}	b total LMS for IEC	a - b
AAA-1	19.2	13.4	15.8
AAB-1	14.2	9.9	4.3
AAC-1	8.2	1.3	6.9
AAD-1	24.0	16.3	7.2
AAF-1	8.3	6.0	2.3
AAF-1	3.2	3.8	-0.6
AAK-1	19.5	13.2	6.3
AAM-1	20.1	16.3	3.8

LMS material resulting from the separation of the asphalt into IEC fractions indicates that numerous interactions in addition to those within the strong acids fraction contribute to self-assembly in asphalt. An exception is found in asphalt AAG-1 in which there is no apparent difference in total self-assembly in spite of the larger entities observed in its strong acid fraction.

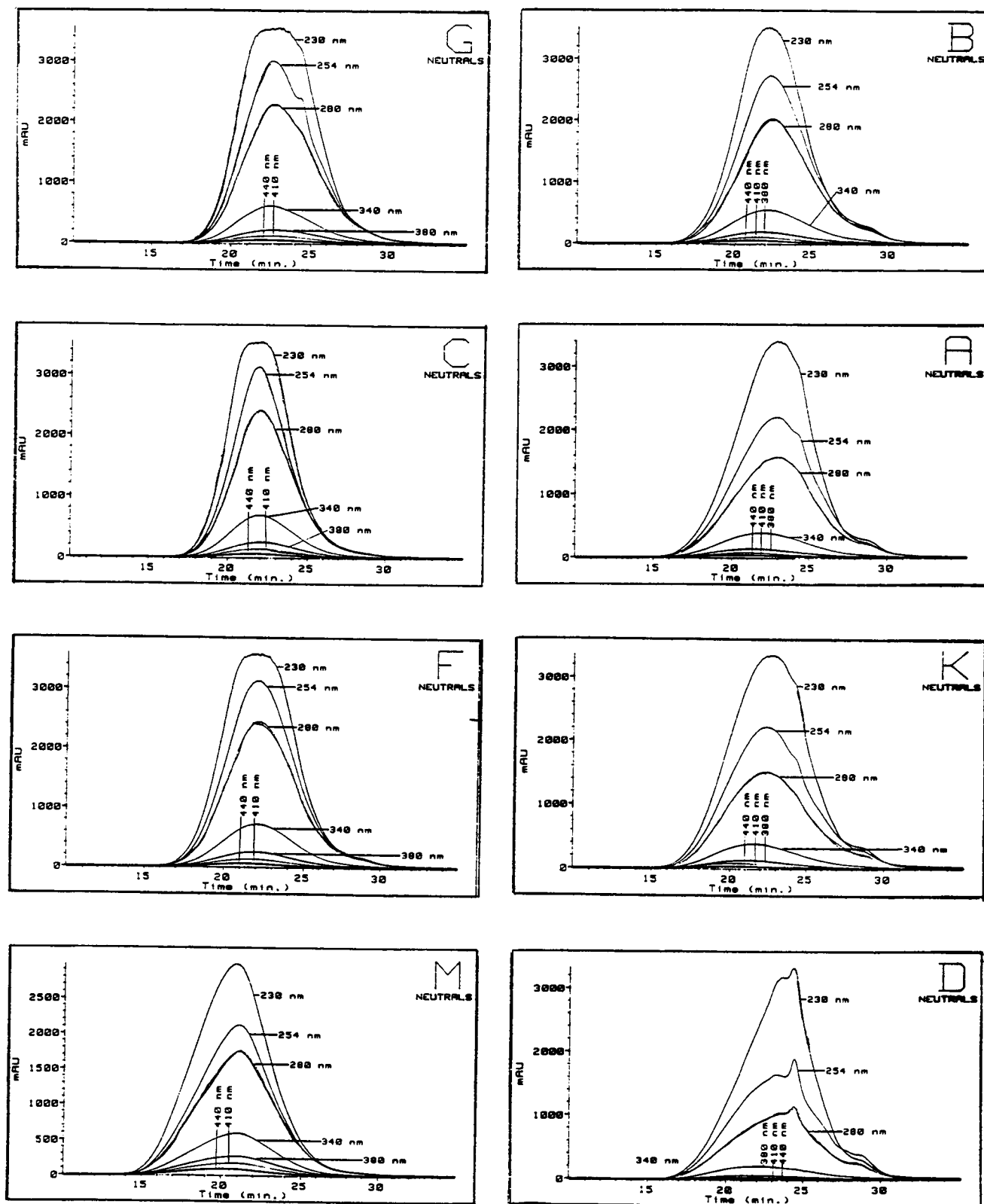


Figure 10. Seven-chromatogram plots of IEC neutrals fractions

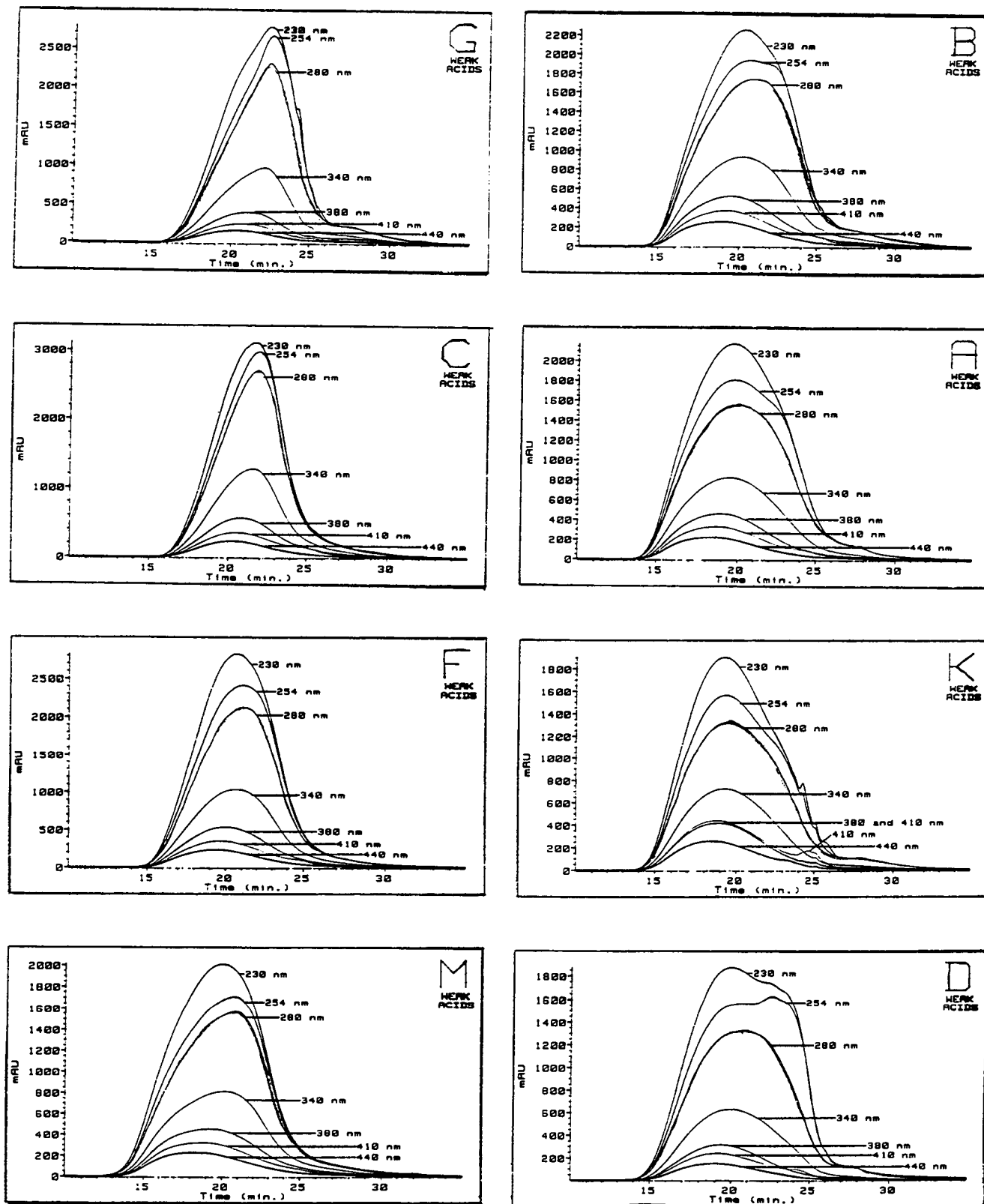


Figure 11. Seven-chromatogram plots of IEC weak acids fractions

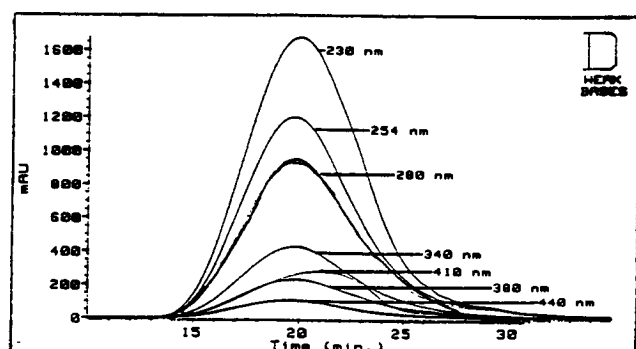
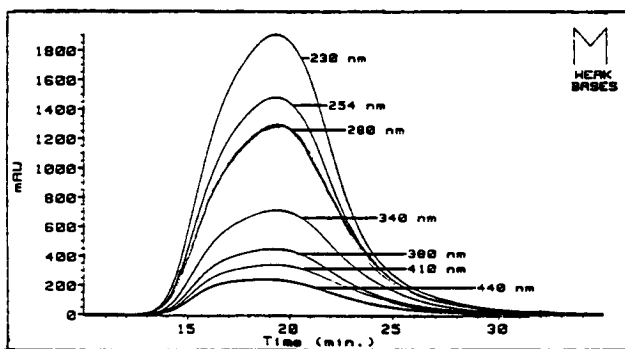
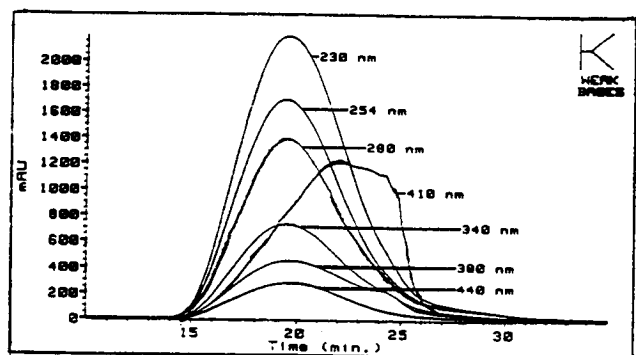
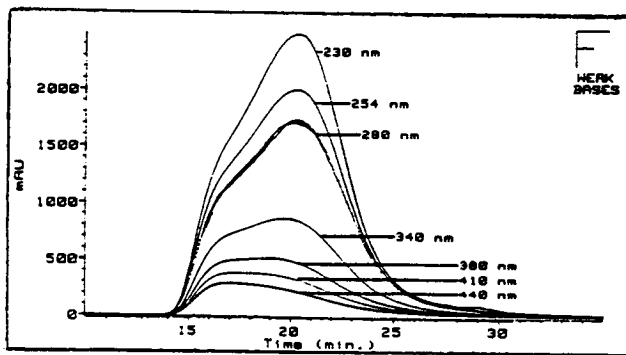
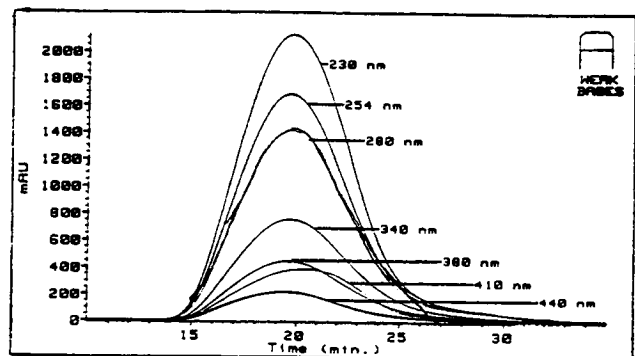
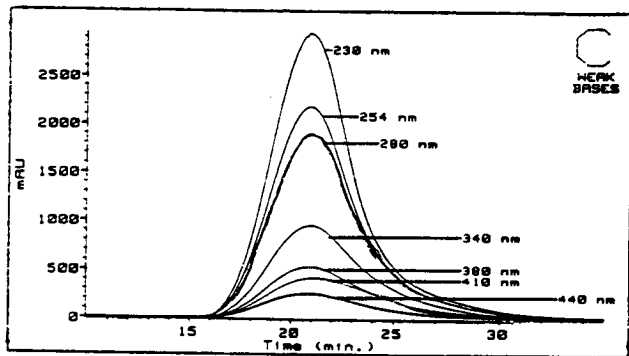
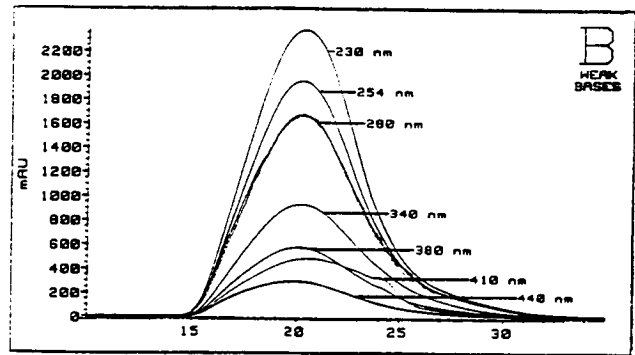
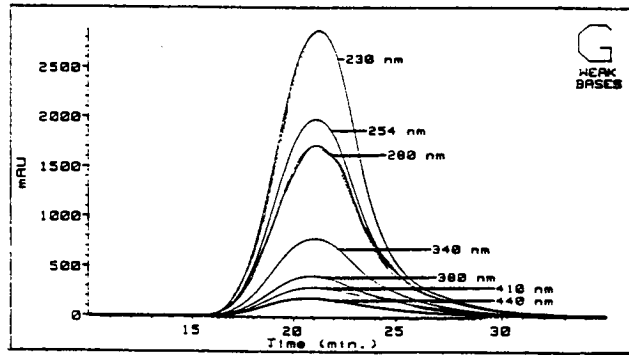


Figure 12. Seven-chromatogram plots of IEC weak bases fractions

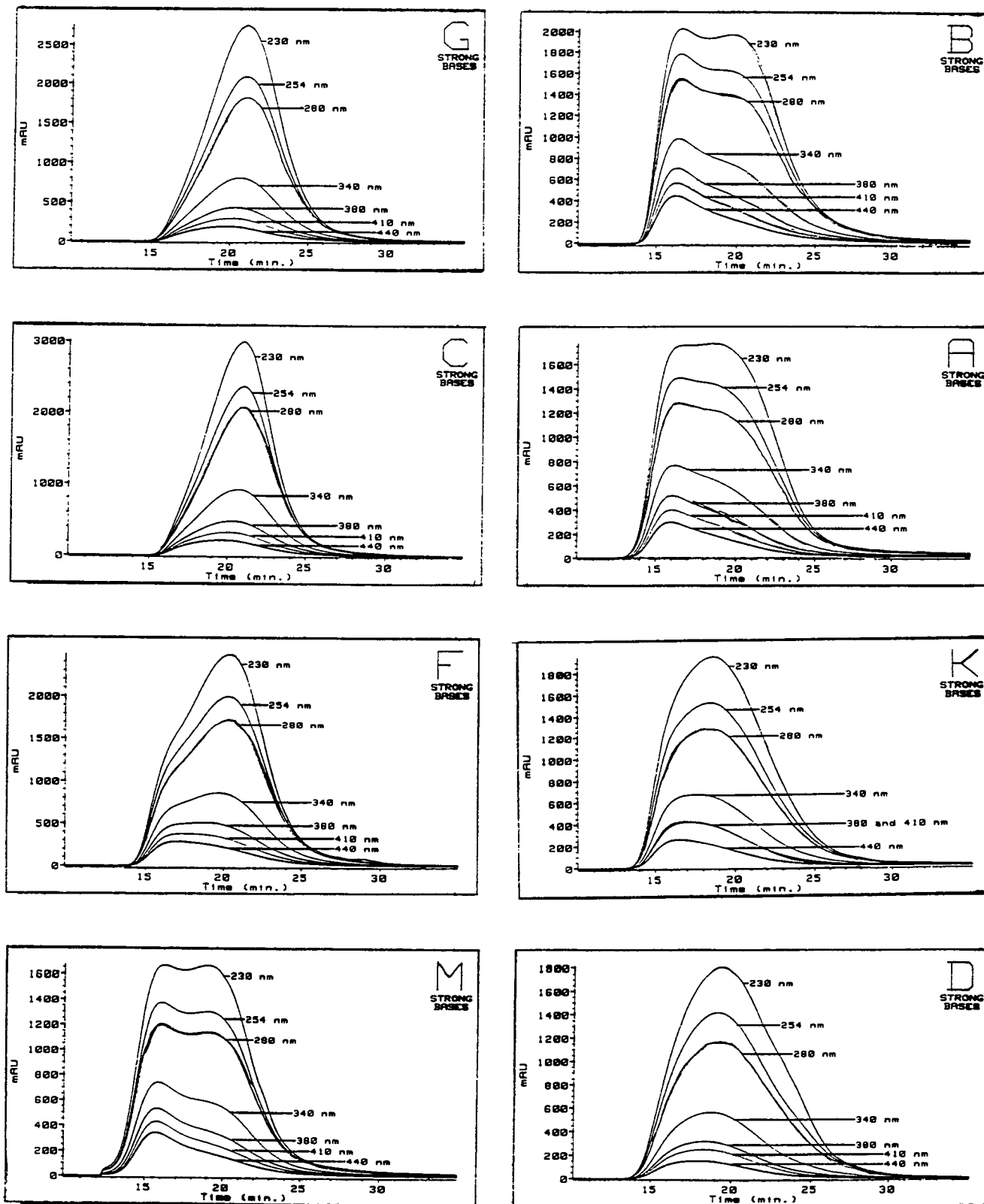


Figure 13. Seven-chromatogram plots of IEC strong bases fractions

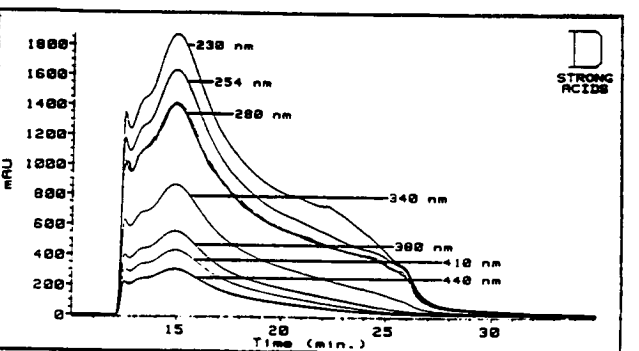
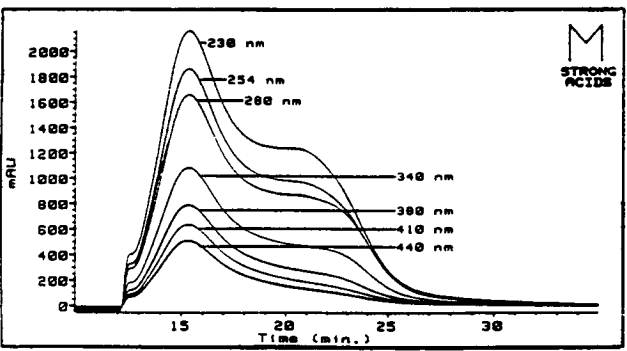
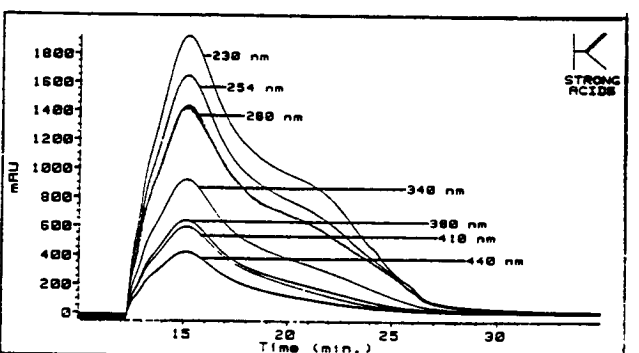
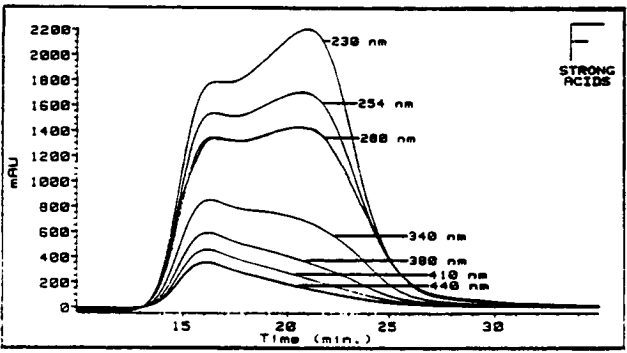
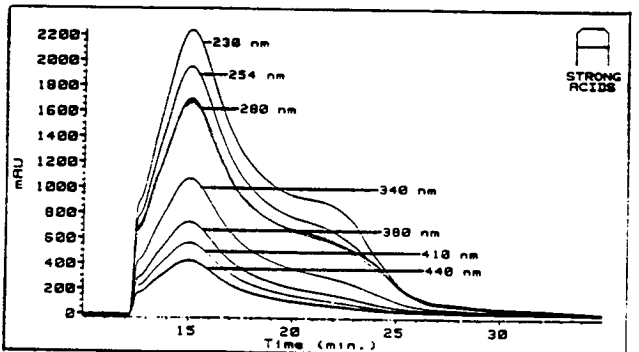
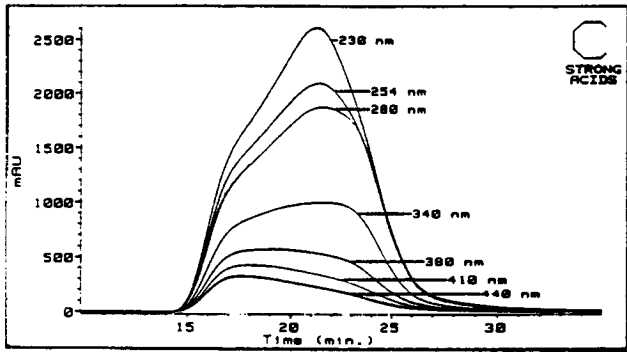
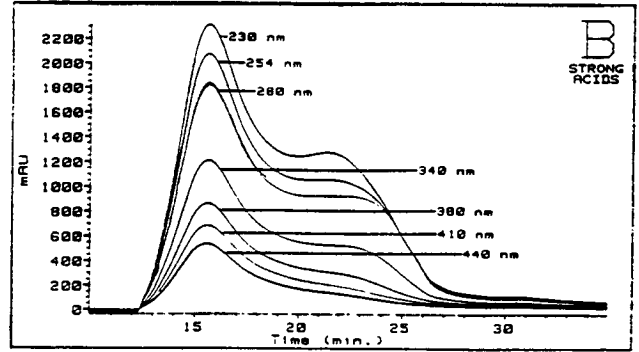
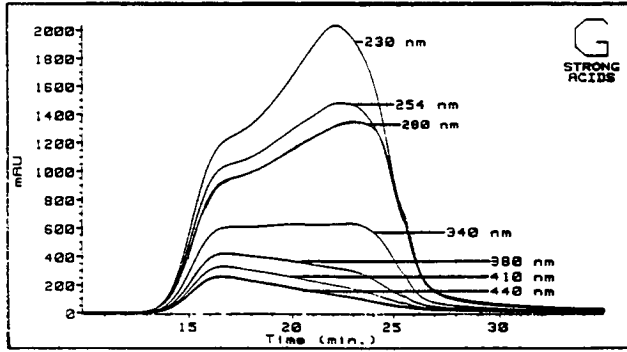


Figure 14. Seven-chromatogram plots of IEC strong acids fractions

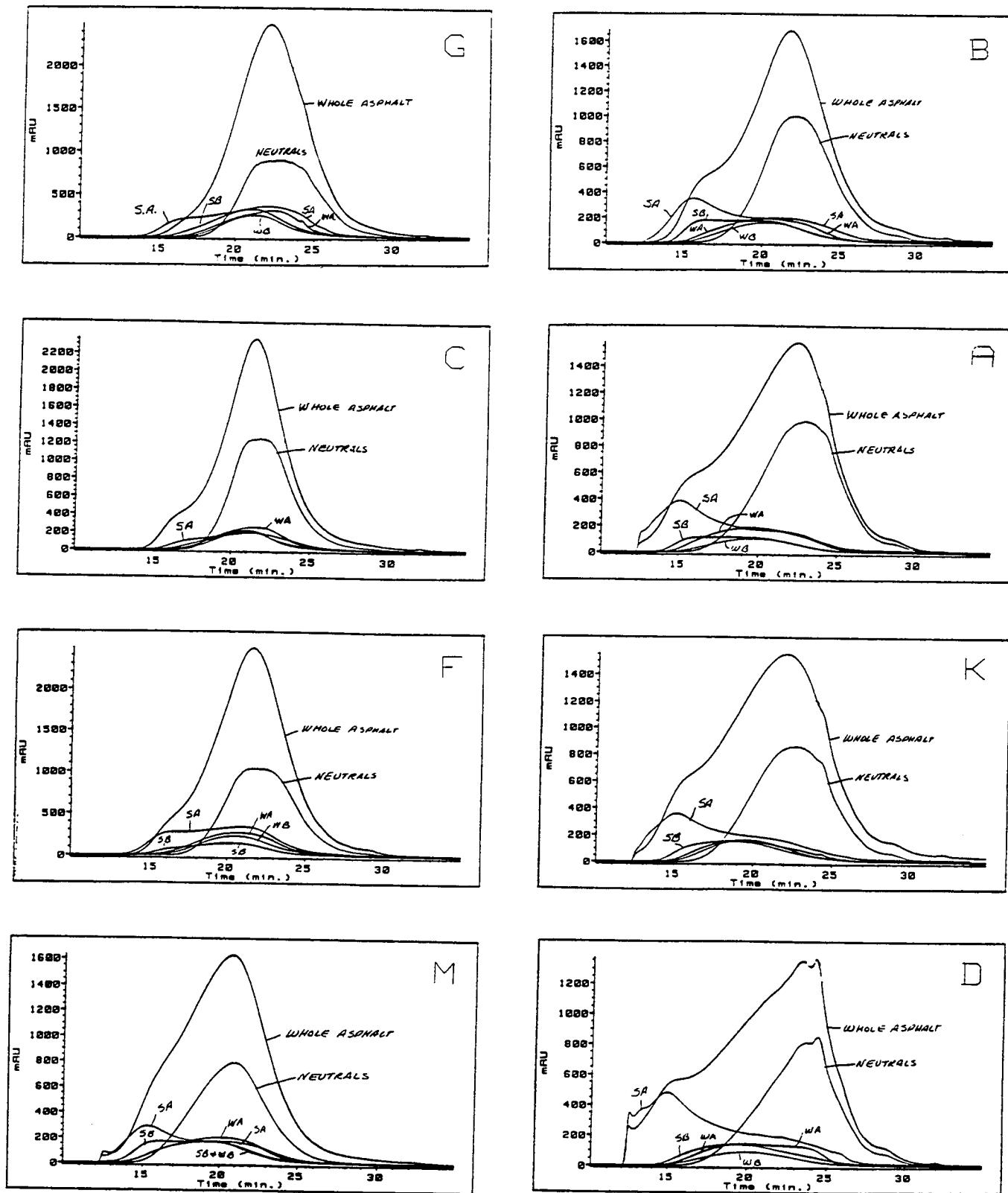


Figure 15. Chromatograms at 230 nm of IEC fractions and the asphalt from which they were derived

V. A.3. Oxidized asphalts

Oxidation is perceived to be very important to the performance of asphalt cements. SHRP researchers at Western Research Institute provided samples of the core asphalts which had been subjected to a pressure oxygen vessel (POV) treatment, to simulate long-term pavement aging, and samples which were subject to thin film oven (TFO) treatment to simulate oxidation in the mix plant, prior to POV aging. These were analyzed by HP-GPC in THF to monitor the effects of these oxidation procedures on the molecular size distribution and intermolecular assembly of the asphalts.

One way to visualize the effects of POV and TFO/POV treatment is to compare the resulting chromatograms at 340 nm with those of the untreated asphalts. This has been done for each of the core asphalts in Figure 16. In general, the intensity of the main peak decreases with POV treatment and decreases still further after TFO/POV aging. Simultaneously, the intensity of the LMS region increases. These changes appear to be similar to those seen in this laboratory after asphalt has been mixed with aggregate. However, since these SHRP asphalts have not been subjected to aggregate treatment, it is unknown whether the changes observed after laboratory oxidation are of the same extent and kind as would be caused by aggregate.

As documented in Table 10, the conjugated volumes of some of these asphalts were observed to change upon oxidation but those changes are generally quite small. The increases in the intensity of absorption in the LMS regions vary but appear to be less significant for asphalts AAF-1 and AAG-1 than for the remaining core asphalts.

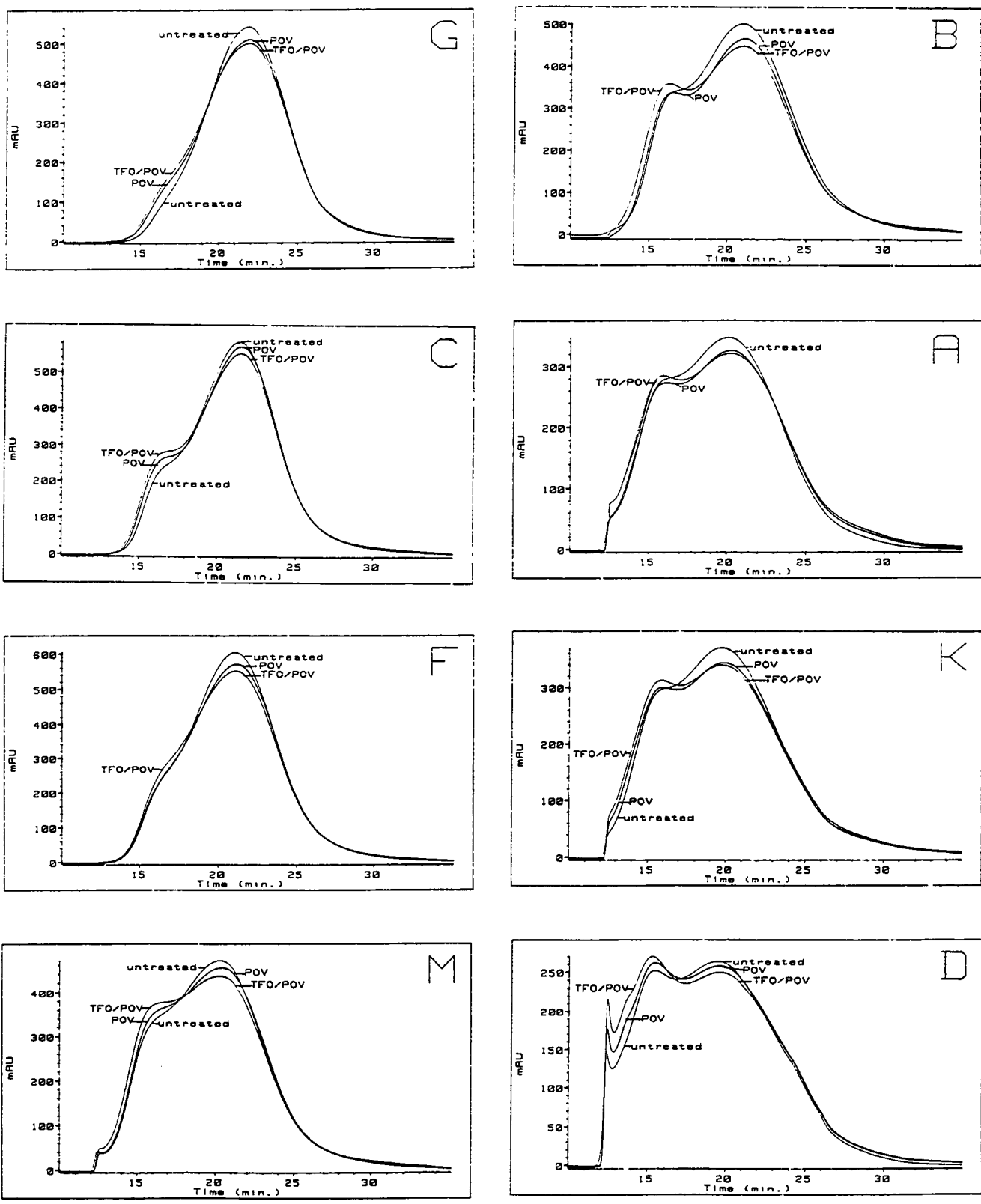


Figure 16. Chromatograms at 340 nm of untreated, POV, and TFO/POV oxidized core asphalts

Table 10. Changes in HP-GPC parameters upon oxidation

Asphalt		% CV CV _t (x10 ⁵)	%CV Segment 11-17	%CV Segment 17-21	%CV Segment 21-25	Segment 25-
AAA-1	U ⁽¹⁾	22.6	19.2	34.2	36.7	9.9
	P ⁽²⁾	22.4	19.8	32.5	36.5	11.2
	T/P ⁽³⁾	22.5	21.4	31.9	3.58	10.9
AAB-1	U	26.9	14.2	35.3	39.9	10.6
	P	26.6	15.0	33.5	39.4	12.1
	T/P	26.7	17.2	33.3	37.9	11.6
AAC-1	U	23.9	8.2	38.5	45.3	8.0
	P	24.3	10.4	37.4	44.1	8.1
	T/P	24.2	11.3	37.4	43.3	8.0
AAD-1	U	20.6	24.0	30.5	34.1	11.4
	P	20.8	25.2	29.2	33.5	12.2
	T/P	20.6	27.0	28.5	32.8	11.7
AAF-1	U	27.6	8.3	39.0	44.2	8.5
	P	27.1	8.9	38.7	43.1	9.4
	T/P	26.9	9.9	38.8	42.4	8.9
AAG-1	U	24.8	3.2	30.7	53.5	12.6
	P	24.2	4.8	31.2	52.1	11.9
	T/P	24.2	5.5	31.5	51.2	11.8
AAK-1	U	24.6	19.5	35.3	33.8	11.4
	P	24.0	21.7	33.9	33.1	11.3
	T/P	23.7	22.9	33.9	32.8	10.4
AAM-1	U	23.5	20.1	44.0	29.4	6.5
	P	23.6	22.0	43.1	28.0	6.9
	T/P	23.5	24.1	42.4	26.8	6.6

(1) untreated

(2) POV oxidized

(3) TFO plus POV oxidized

Since changes in aromatic carbon content and/or in the concentrations of functional groups could effect changes in intermolecular association, it is of interest to compare the data from HP-GPC analyses with data on aromatic carbon content and

concentrations of phenols and carboxylic acids (from NMR studies, 16). The requisite data, presented in Table 11, shows no direct correlations among the change in % LMS, change in aromatic carbon percentage or change in [OH+COOH] after TFO/POV oxidation. It is obvious that additional parameters are involved.

Table 11. Changes in % CV₁₁₋₁₇, % aromatic carbon and [OH+COOH] after TFO/POV oxidation

<u>Asphalt</u>	Increase <u>%CV₁₁₋₁₇</u> ⁽¹⁾ LMS	change in <u>% aromatic carbon</u>	Increase <u>[OH+COOH]</u>
AAA-1	2.2	+0.7	2.6
AAB-1	3.0	+0.1	1.1
AAC-1	3.1	+0.3	4.0
AAD-1	3.0	+1.0	4.3
AAF-1	1.6	-2.7	4.3
AAG-1	2.3	-3.0	1.7
AAK-1	3.4	+1.0	5.0
AAM-1	4.1	+1.1	-0.8

⁽¹⁾ % CV₁₁₋₁₇ after TFO/POV minus % CV₁₁₋₁₇ untreated

V. A.4. The SEC fractions

Preparative size exclusion chromatography (SEC) was used at WRI to separate each of the eight core asphalts into two fractions (15). SEC I is the non-fluorescing fraction in the toluene-mediated apparent molecular size separation and contains the largest entities. The lack of fluorescence is attributed to the presence of intermolecular associations. Fluorescence characterizes the SEC II fractions which thus are thought to contain no associated material.

The SEC I and II fractions were analyzed by HP-GPC in THF. Figures 17 and 18 contain the chromatograms obtained; corresponding data are in Table 12. In all cases studies, SEC I is more aromatic and has more LMS material than the corresponding whole asphalt, whereas SEC II is much less aromatic and shows no evidence in the LMS region for intermolecular association. However, there are significant differences among the asphalts. For example Group 2 asphalts AAA-1 and AAK-1, and Group 3 asphalt AAD-1 show strong evidence for intermolecular interactions in both the whole asphalts and SEC I fractions. Molecules in asphalt AAG-1 apparently do not easily associate in the whole asphalt; those in the SEC I fraction exhibit the least evidence for self-assembly of all SEC I samples tested (Figure 19). Similarly, the SEC I fractions for other Group 1 asphalts (AAC-1, AAF-1) have less absorption in the LMS region of the chromatogram. However, these Group 1 fractions begin to elute as much as two minutes earlier than the parent asphalt. Also, they are incompletely soluble in THF whereas the parent asphalts are easily soluble.

These observations call the role of solvents to question. In toluene, polar interactions should be enhanced and pi-pi associations should be disrupted. After separation into fractions and removal of solvent, the new arrangements may remain intact, at least partly because components that might have modified these associations in the whole asphalt are now removed. That is, the associated species in the fraction may not be completely the same as those originally present in the whole asphalt.

Table 12. HP-GPC characteristics of SEC I and II fractions

<u>Asphalt</u>	<u>CV_t</u>	<u>CI_t</u>	<u>%CV</u> <u>11-15</u>	<u>%CV</u> <u>15-17</u>	<u>%CV</u> <u>11-17</u> LMS	<u>%CV</u> <u>17-21</u>	<u>%CV</u> <u>21-25</u>	<u>%CV</u> <u>25-</u>
SEC I								
<u>Group 1</u>								
AAG-127.8	0.452		4.8	29.4	34.2	60.0	11.0	3.9
AAC-140.2	0.541		12.2	40.3	52.5	38.8	6.2	2.5
AAF-145.5	0.482		16.8	37.0	53.8	36.9	6.3	3.1
<u>Group 2</u>								
AAB-138.2	0.512		20.1	38.0	58.1	33.6	5.8	2.5
AAA-133.9	0.460		37.9	32.5	70.4	23.9	3.8	1.9
AAK-133.3	0.465		32.3	32.8	65.1	27.0	5.1	2.8
<u>Group 3</u>								
AAD-132.0	0.454		41.4	30.1	71.5	22.7	4.0	1.9
<u>Group 4</u>								
AAM-125.6	0.448		27.0	38.2	65.2	27.0	4.9	2.9
SEC II								
<u>Group 1</u>								
AAG-125.5	0.235				0.8	30.5	58.2	10.6
AAC-121.4	0.273				0.2	40.8	53.0	6.0
AAF-125.5	0.257				1.0	43.2	49.0	6.8
<u>Group 2</u>								
AAB-122.5	0.243				0.8	37.1	53.0	9.1
AAA-115.3	0.180				1.6	38.4	50.5	9.5
AAK-120.9	0.190				2.3	40.6	46.6	10.5
<u>Group 3</u>								
AAD-118.4	0.161				3.2	34.9	48.5	13.4
<u>Group 4</u>								
AAM-121.5	0.332				5.3	53.4	36.5	4.8

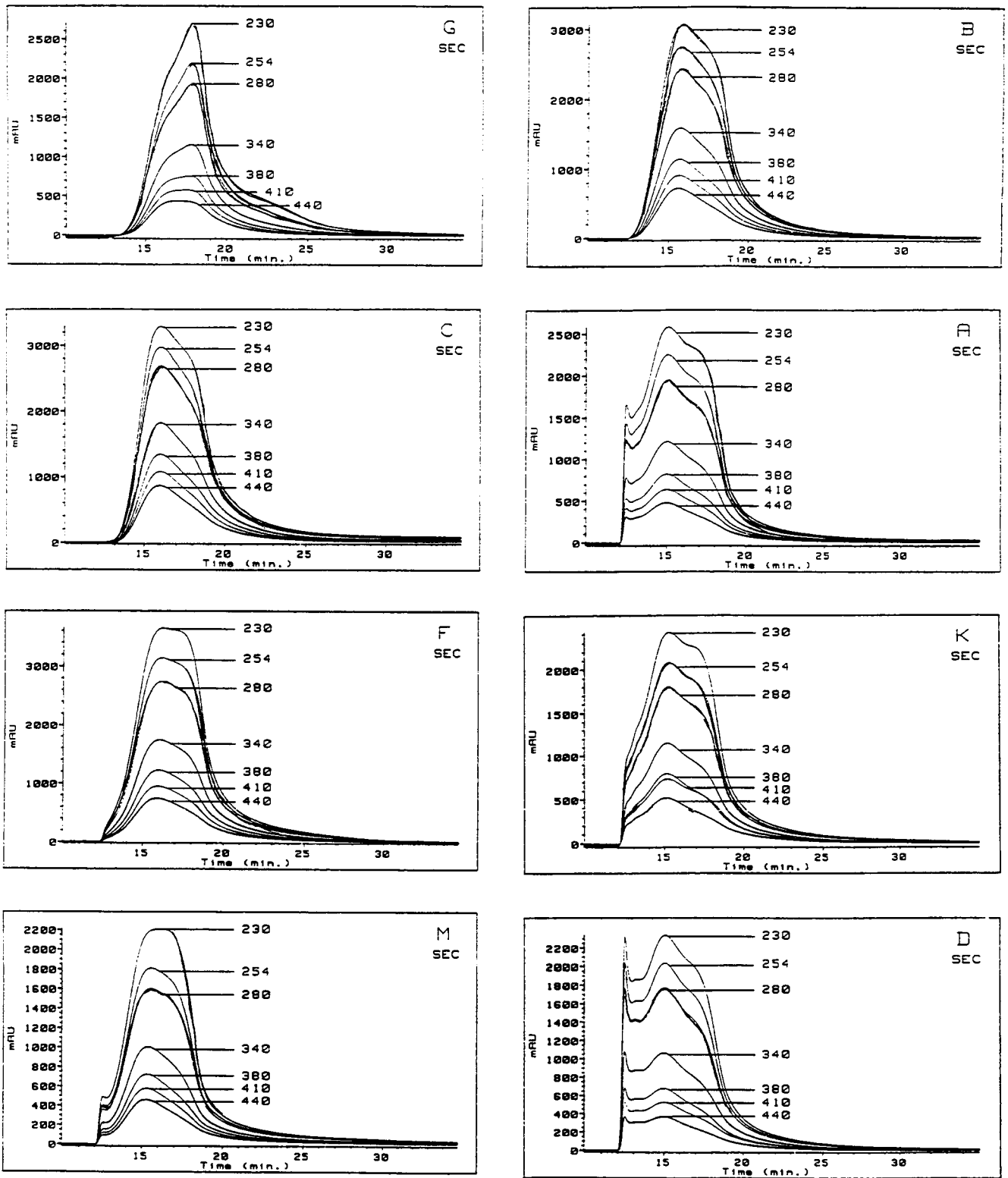


Figure 17. Seven-chromatogram plots of SEC I fractions in THF

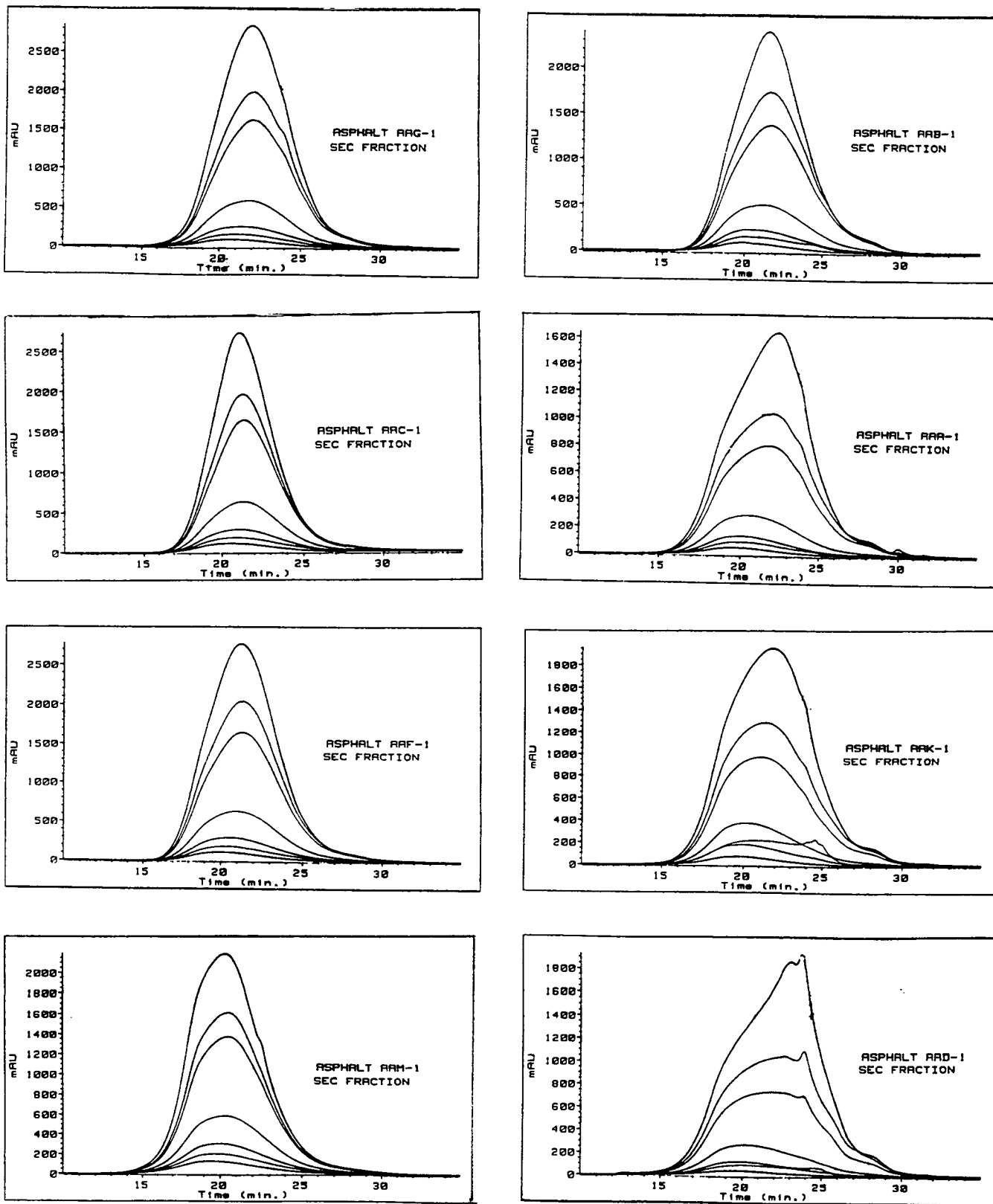


Figure 18. Seven-chromatogram plots of SEC II fractions in THF

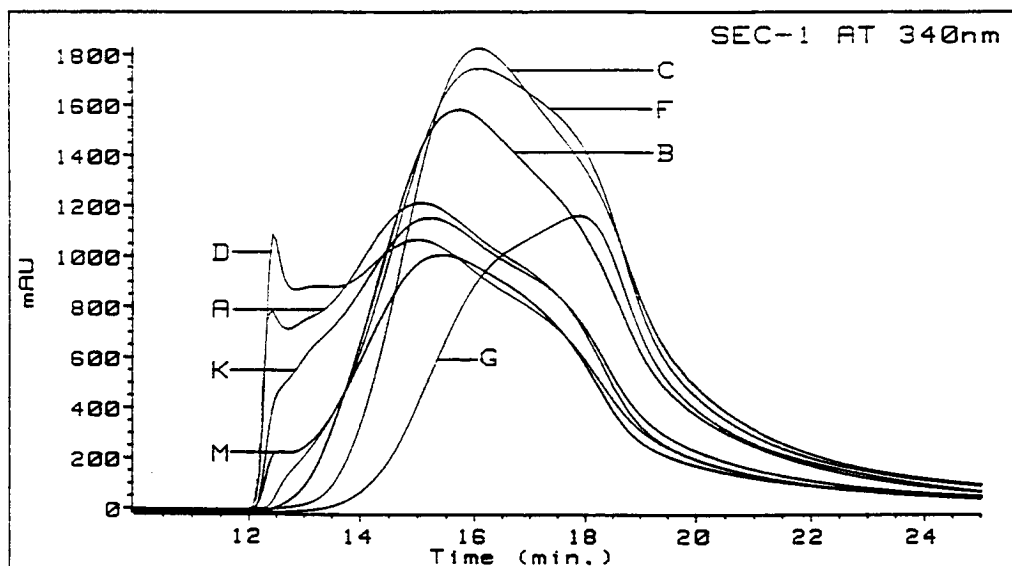


Figure 19. Comparison of SEC-1 fractions from core asphalts at 340 nm.

Comparable preparative-scale isolations have not been made with regard to the activity of THF as a solvent. However, evidence will be presented later in this paper that THF, in the process of dissolving an asphalt sample, disrupts most of the intramolecular associations present in the whole asphalt. However, the strongest associative bonds, both polar and non-polar, apparently do survive in THF solution. (See sections B. 2a, b and c, and F.1.) For that reason, the authors believe that THF is the solvent of choice for indicating the tendency of molecules in an asphalt to assemble into larger entities by any of the possible bonding mechanisms.

When the strong response in the LMS region for SEC I fractions is observed, it would be easy to assume that all the LMS material in the whole asphalt is accounted for by the SEC I fraction. However, when the amount of LMS material explained by SEC I and II is compared with that found by analysis of the whole asphalt, differences among

the asphalts are observed (Table 13). For example, for asphalts AAA-1, AAB-1 and AAD-1, less LMS material is calculated from the SEC I and II fractions than is observed in the whole asphalt. Since the SEC preparation using toluene should encourage polar interactions while disrupting pi-pi bonds, the HP-GPC data may indicate that pi-pi interactions are somewhat more important than polar interactions in these three asphalts.

For asphalts AAC-1, AAF-1 and AAK-1, the difference between calculated and observed LMS percentages is small (within experimental error). This may mean either a) that neither interactive mechanism is important, or b) that both interactions contribute about equally in the whole asphalt. Studies with changes in solvent polarity (to be described later in this report) indicate that the latter is true for asphalt AAK-1. For asphalts AAC-1 and AAF-1, in which little intermolecular interaction is noted, it may be that both polar and non-polar associations contribute about equally to the low LMS content.

Asphalts AAG-1 and AAM-1 present a different picture in that the total LMS percentage in SEC I and II is higher than in the whole asphalt. This difference is substantial in asphalt AAM-1, less so in asphalt AAG-1. We suggest that the SEC separation of AAG-1 in toluene encourages polar interactions not present in the whole asphalt, as mentioned earlier. In the whole asphalt, in fact, neither polar nor non-polar interactions seem to be important.

Asphalt AAM-1, well known as an unusual material, does not change its reputation here. We suggest that, not only does the SEC separation encourage polar bonds

Table 13. Differences between % LMS observed in the whole asphalt and that calculated from amounts in SEC I and II

Asphalt	a % LMS observed	b % LMS calculated ⁽¹⁾	difference a - b
AAA-1	19.2	16.5	2.7
AAB-1	14.2	11.7	2.5
AAC-1	8.2	7.3	0.9
AAD-1	24.0	20.0	4.0
AAF-1	8.3	8.3	0.0
AAG-1	3.2	4.7	-1.5
AAK-1	19.5	18.6	0.9
AAM-1	20.1	24.2	-4.1

⁽¹⁾ Percent LMS whole asphalt, calc. $\times 100 - (\% \text{ LMS SEC I})(\text{wt } \% \text{ SEC I}) + (\% \text{ LMS SEC II})(\text{wt } \% \text{ SEC II})$

not present in the whole asphalt, but also it disrupts non-polar interactions that are particularly strong in this asphalt. That is, toluene may actually invert the interactions prevalent in the neat asphalt. It should be noted that asphalt AAM-1 is known as a highly compatible material from which little if any asphaltene can be precipitated by heptane. That is, heptane can not induce the separation of polar materials perhaps because they are so strongly solubilized by virtue of pi-pi interactions. This would be consistent with the HP-GPC results.

V. A.5. Derivatized samples

Several derivatization reactions were explored as means of interrupting intermolecular interactions. A phase-transfer methylation (PTM) procedure (Appendix A) was used to replace hydrogen atoms on phenol and carboxylic acid groups with

methyl groups and, thus, to decrease hydrogen bonding potential. It was anticipated that a decrease in the absorption in the LMS region would be observed. Instead a very strong relative increase in that absorption combined with an overall decrease in CV_t were seen. An increase in LMS absorption under the desired reaction could possibly be explained if hydrogen bonds held large molecules in folded configurations that would unfold to larger hydrodynamic volumes upon interruption of the hydrogen bonds. However, the large loss in CV_t is not readily explained. Furthermore, results from other studies (16) indicate that the PTM reaction causes other changes in the asphalt. Therefore, the authors are concerned that the changes in molecular size distribution may result from artifacts of the PTM reaction in addition to the desired reaction.

A reaction with diazomethane designed to methylate carboxylic acids (Appendix B) also produced questionable data, including loss of CV_t and poor reproducibility in terms of HP-GPC characteristics. These may arise from ancillary reactions which have little to do with the interruption of hydrogen bonding through carboxylic acids.

Iron hexacarbonyl was used in a reaction designed to interrupt pi-pi interactions by bonding to aromatic rings. The products were not analyzed on the HP-GPC columns used for the rest of this project because of the risk of damage to the column packing material. However, they were analyzed on an older column set and showed an overall decrease in molecular size and loss of CV_t . These are the expected results, but they cannot be quantitated.

Finally, an acylation reaction (Appendix C) was used to attach a small group to aromatic rings and thus to interrupt pi-pi interactions. Results from acylation of asphalt

AAA-1 are shown in Figure 20. Because the reaction requires the presence of acid, the asphalt was treated with acid alone to determine its effect. Obviously, most of the decrease in LMS absorption is attributable to the acylation reaction and presumably involves interruption of pi-pi interactions.

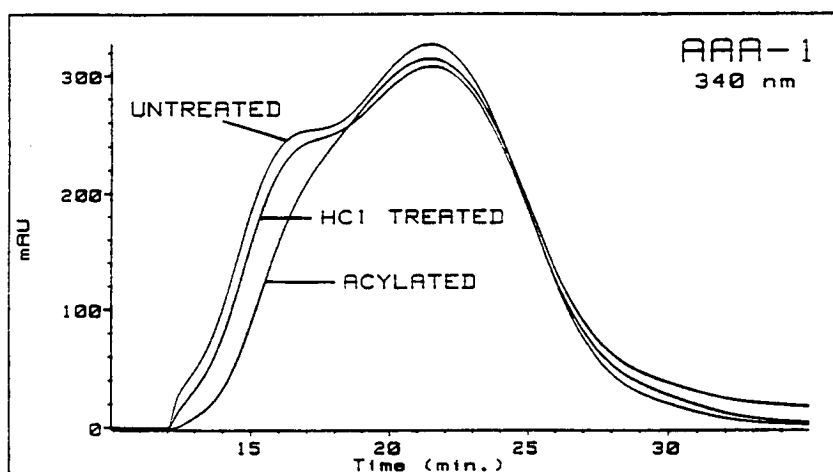


Figure 20. Change in molecular size distribution of asphalt AAA-1 resulting from acylation reaction.

V.B. General observations on solvents effects

As explained earlier, changes in polarity of the HP-GPC solvent were explored as probes of the mechanism of self-assembly in various samples. For example, an increase in solvent polarity is expected to disrupt polar interactions whereas a decrease in polarity would be expected to enhance these interactions. Of course, asphalt is not so simple and it must be kept in mind that a more polar solvent might not only interfere with polar interactions in the asphalt but also could induce non-polar interactions. A

similar dichotomy exists in the case of less polar solvents. That is, unless one type of interaction is strongly dominant, one might observe a shift in behavior with different solvents.

Changes in intermolecular associations will be evident particularly in the LMS region of the chromatograms. Changes will not be very large for at least two reasons. First, the samples are in dilute solution (0.5% weight/volume). At this concentration, column overload is avoided, but many intermolecular interactions will have been disrupted in the dissolution process. Only the stronger associations will remain. Second, the concentrations of modifying solvent in the HP-GPC mobile phase had to be controlled so as to cause as little effect as possible on the column packing material itself. Therefore, the range of polarities useable was limited.

The following solvent systems were used:

100% THF

5% methanol (MeOH) in THF - more polar

20, 50 and 80% toluene (tol) in THF - increasingly non-polar and more aromatic

20% hexane (hex) in THF - less polar by virtue of a straight chain hydrocarbon.

In the discussion of each asphalt, "changes" will be defined in each solvent system relative to THF. In general, the solvent systems extended the elution times of polystyrene standards by 0.2 to 0.4 minutes. Hexane had a larger effect (see Table 2, page 18). That is, in the solvent systems (except hexane), if there is no effect on self-

assembled units, the chromatogram simply would be observed to shift to the right by 0.2 to 0.4 minutes. This will be taken into account.

V. B.1. Effects on total conjugated volume

Methanol in the mobile phase caused no significant changes in the CV_t of the whole asphalts but did increase the CV_t for some SEC I fractions in the order: B>C>G>K>A while decreasing CV_t for the SEC I fraction from asphalt AAF-1 slightly. Increases in the CV_t possibly for strong acid fractions of AAC-1 and AAB-1 were observed in methanol.

Increases in toluene concentration in the mobile phase resulted in very small but consistent decreases in CV_t possibly as a consequence of the uv absorption of the toluene itself.

No significant changes in CV_t were noted when using hexane: THF, except for decreased values for the whole asphalt AAF-1 and its SEC I fraction.

These observations would seem to indicate that the uv-vis absorption characteristics are not significantly changed by solvent, with the exceptions noted. A possible source for change in the CV_t with solvent could be changes in the nature of intermolecular associations.

V. B.2. Effects on the molecular size distribution.

In this work, the whole asphalts and strong acid fractions were analyzed in all solvent systems listed above. The SEC I fractions were analyzed in THF and MeOH/THF. Each of the SHRP core asphalts will be discussed individually then comparisons will be noted. Figures will contain chromatograms at 340 nm comparing

results in the particular solvent system to results in THF. Note that shifts on the far right of the chromatogram are in accord with column changes unless otherwise described.

V. B.2.a. Asphalt AAA-1 (Figure 21a and b)

Seven-chromatogram plots of asphalt AAA-1 (Figure 6, page 24) show a trimodal molecular size distribution with strong evidence for intermolecular association. Various plots in Figure 21 show the effects of solvent polarity. Methanol induces an increase in LMS absorption indicating the formation of non-polar associations to more than offset any polar bond disruptions.

In toluene/THF, different effects are observed, depending on the concentration of toluene. The most polar interactions are produced in 50% toluene/THF. This data suggests that, in 20% toluene, some polar interactions offset any disruption of non-polar bonds; at 50% toluene, this effect is strengthened. However, at 80% toluene, the disruption of non-polar associations is decreasing the overall LMS effect. Similarly, hexane seems to induce polar association.

The SEC I fraction behaves similarly to the whole asphalt in methanol/THF, showing the availability of non-polar interactions to counteract the loss of polar bonds in this fraction. Strong acids demonstrate a similar although less intense result. The effect of toluene on the strong acids resembles that on the whole asphalt but, again, is not as strong.

These data indicate the ready availability of both polar and non-polar associations in asphalt AAA-1. A comparison of chromatograms in the two solvents most differing

in polarity (methanol/THF and 80% toluene/THF) indicates that the polar solvent induces more LMS and, therefore, that non-polar associations may play a more prominent role in this asphalt. This agrees with data from analysis of SEC I and II fractions (page 51).

V. B.2.b. Asphalt AAB-1 (Figure 22a and b)

Asphalt AAA-1 has a bimodal molecular size distribution (Figure 6, page 24) indicating a moderate amount of self-assembly. Methanol induces only a slight increase in the LMS region indicating a minor predominance of non-polar interactions. Increasing concentrations of toluene in the mobile phase causes a pattern of results similar to those described for asphalt AAA-1, above. The additional LMS absorption in 50% toluene/THF is not as great as in asphalt AAA-1, however, hexane also induces an increase in the LMS region.

The behavior of the SEC I fraction in methanol/THF, like that of AAA-1, indicates the ability to form non-polar bonds. However, in the same solvent, the strong acids appear to be less prone to establish non-polar interactions (also like AAA-1). In increasing concentrations of toluene, the strong acids of AAB-1 are less likely than those of AAA-1 to establish polar associations to counterbalance the disruption of non-polar associations.

Data from SEC I and II analyses indicate that non-polar associations are predominant in this asphalt. Comparison of chromatograms at the available polarity extremes shows agreement concerning the largest materials but, at somewhat longer

elution times (still within the LMS region) polar forces seem to be more important. In any case, the maximum molecular size in AAB-1 is not so large as that in AAA-1 and it appears that the influence of self-assembled units is somewhat smaller in AAB-1.

V. B.2.c. Asphalt AAC-1 (Figure 23a and b)

A narrow MSD with little indication of self-assembly in the LMS region characterizes asphalt AAC-1 in THF. No change is observed in either whole asphalt or strong acids when methanol is added to the mobile phase (the shift is no more than that caused by column changes noted earlier), but there is a small increase in LMS of the SEC I fraction.

The effects of toluene are generally small for whole asphalt and strong acids but the trend is that 50% toluene/THF induces some polar bond formation. Thus, polar associations may be somewhat more important in asphalt AAC-1, but their total contributions to network formation in the neat asphalt are small. Analysis of SEC I and II fractions suggests that contributions from polar and non-polar sources are similar.

V. B.2.d. Asphalt AAD-1 (Figure 24 a and b)

The HP-GPC chromatogram of asphalt AAD-1 in THF shows a strong, tri-modal MSD and a substantial main peak trending toward smaller molecular sizes with small chromophores. The presence of methanol in the mobile phase induces non-polar interactions which increase the percent LMS compared to the whole asphalt in THF. Toluene at 20 and 80 percent decreases the amount of LMS although at 50 percent,

polar forces increase the amount of LMS observed, especially in the first peak. No changes are observed in hexane.

SEC I in methanol/THF likewise demonstrates the ability to form non-polar associations but polar forces are destroyed to a greater extent in the strong acids fraction. Toluene has the same general effects on the strong acids as on AAD-1 itself. These data indicate the importance of both polar and non-polar interactions in this asphalt, although the latter dominate somewhat, as supported both by the comparison of methanol/THF and 80% toluene/THF peaks and by the SEC I and II information.

V. B.2.e. Asphalt AAF-1 (Figure 25a and b)

The MSD of asphalt AAF-1 is narrow and has very little LMS shoulder. The effect of increased solvent polarity on whole asphalt and SEC I fraction is to move the peak to the right in accordance with column changes. Decreasing solvent polarity induces small increases in LMS due to polar interactions in whole asphalt and strong acids. Hexane produces no meaningful change. Comparison of the chromatograms of the whole asphalt in methanol/THF and 80% toluene/THF suggests that there is very little difference between these solvent systems, (in agreement with analyses of SEC fractions) and, in any case, that any associations are relatively weak.

V. B.2.f. Asphalt AAG-1 (Figure 26a and b)

Of all the SHRP core asphalts, this has the narrowest MSD and the least evidence for intermolecular assembly. Changes induced by the various solvent systems

amount to little more than that attributable to column changes except that the higher concentrations of toluene (80%) and hexane seem to disrupt non-polar forces. This suggests that non-polar forces may be slightly more important, in agreement with SEC I and II information. Nevertheless, the vast majority of interactions that may be present in the neat asphalt are not strong enough to survive dissolution.

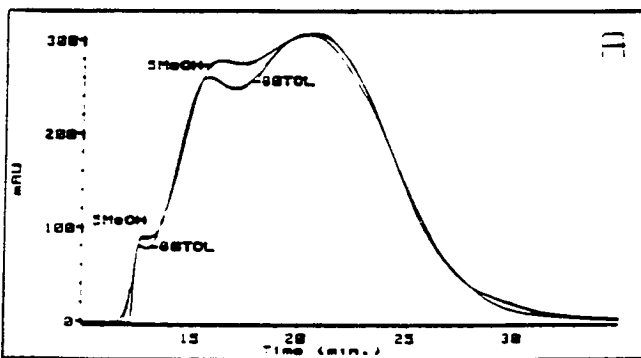
V. B.2.g. Asphalt AAK-1 (Figure 27a and b)

The HP-GPC chromatogram of asphalt AAK-1 shows a tri-modal MSD with ample evidence for self-assembled materials. Methanol induces non-polar interactions in the whole asphalt and SEC I fraction as well as in the strong acids. Toluene induces polar interactions, especially at 50% concentration in both whole asphalt and strong acids. Hexane behaves similarly. In comparing the effects of methanol and 80% toluene, one notices that the chromatograms cross at several points, indicating nearly equal responses. This would agree with data from SEC I and II fractions. However, except for this small detail, the behavior of asphalt AAK-1 is very much like that of AAA-1 and AAB-1.

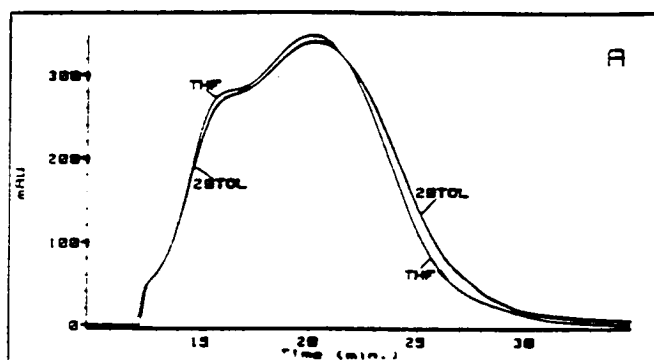
V. B.2.h. Asphalt AAM-1 (Figure 28a and b)

This asphalt is unusual among the SHRP core asphalts in that its moderately wide MSD is shifted strongly to larger molecular sizes. Its trimodal distribution, if present at all, is not well-defined. Methanol provides a small increase in the peak at the far left but otherwise shifts the entire peak in accordance with column changes. The

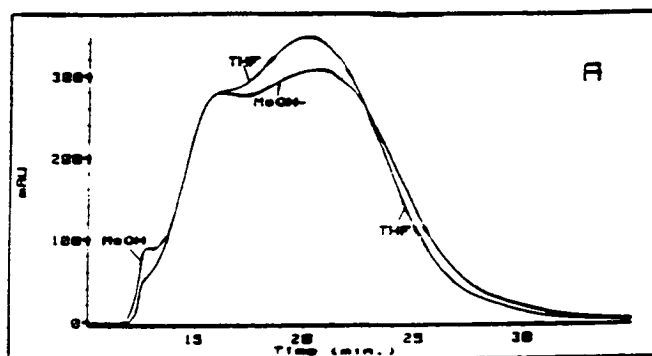
effects of toluene also are not prominent, although some tendency to induce polar associations is evident. In hexane, polar association also outweighs any non-polar dissociation, but the effect is small. A similar series of comments can be made about the SEC I and strong acids fractions. Comparison of chromatograms obtained at opposite ends of the available polarity limits indicates that polar associations are more easily induced than non-polar ones. The SEC data discussed earlier (page 51) suggests that non-polar associations are most important in this asphalt.



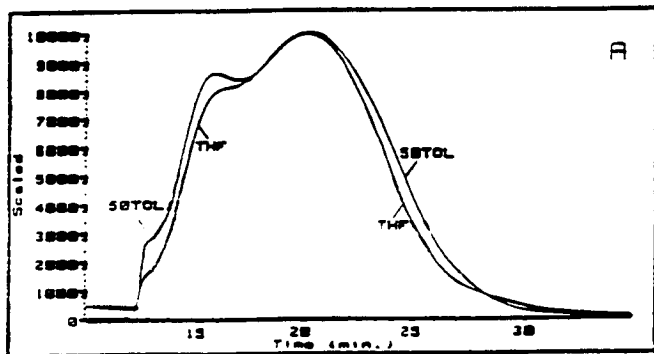
Whole asphalt in most polar and least polar solvents.



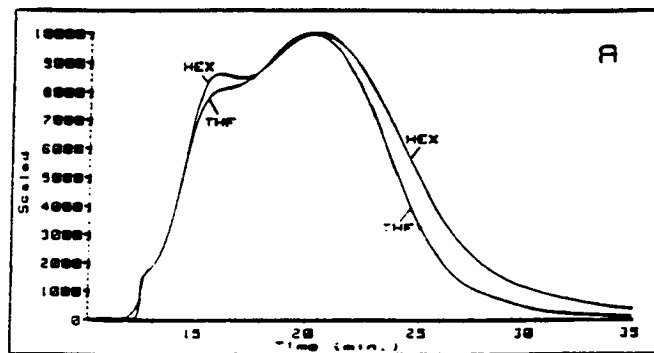
Whole asphalt - THF vs 20% Toluene



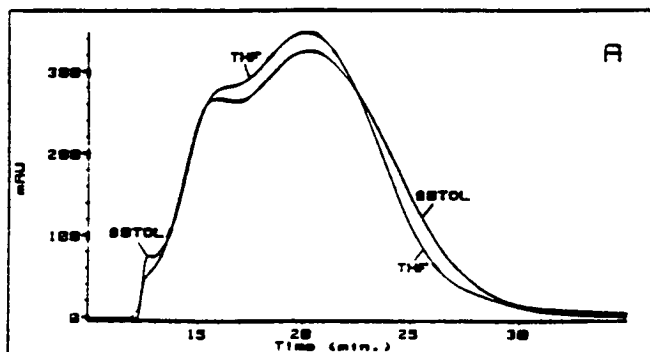
Whole asphalt - THF vs Methanol



Whole asphalt - THF vs 50% Toluene

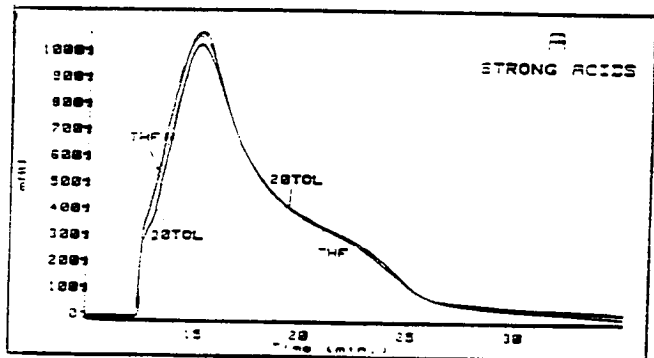


Whole Asphalt - THF vs Hexane

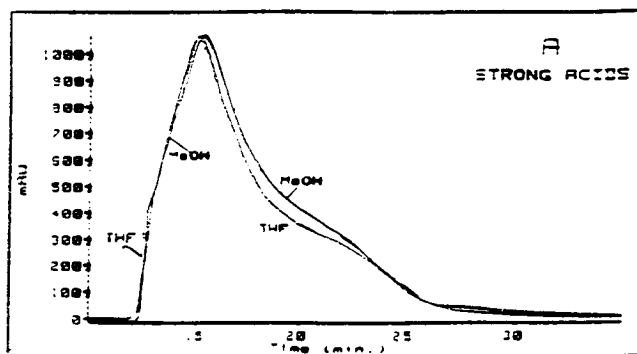


Whole asphalt - THF vs 80% Toluene

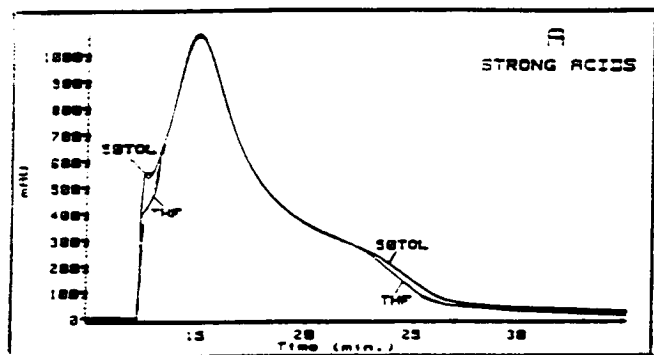
Figure 21a. Solvent effects on MSD's of asphalt AAA-1.



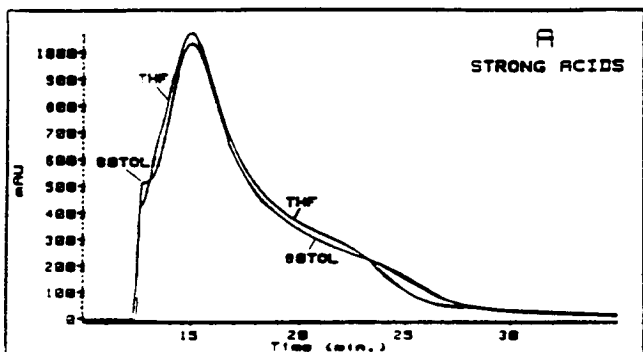
Strong acids fraction - THF vs 20% Toluene



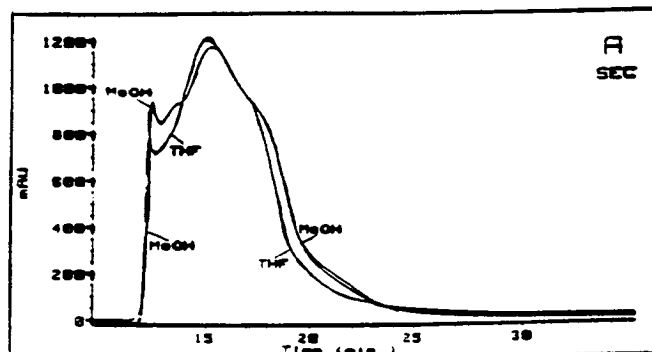
Strong acids fraction - THF vs Methanol



Strong acids fraction - THF vs 50% Toluene

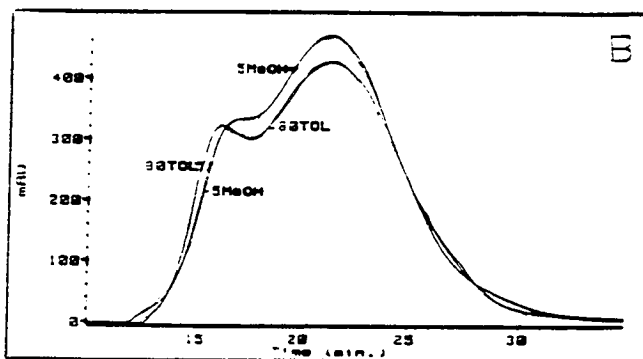


Strong acids fraction - THF vs 80% Toluene

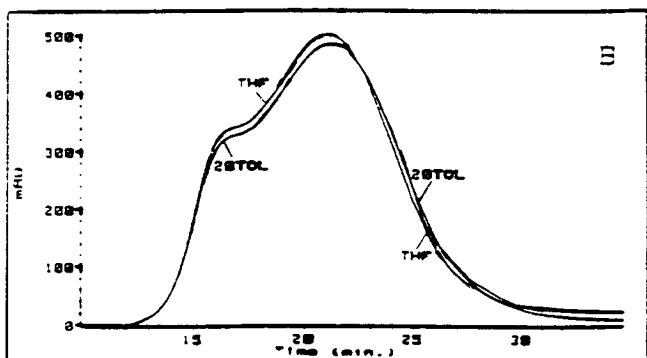


SEC I fraction - THF vs Methanol

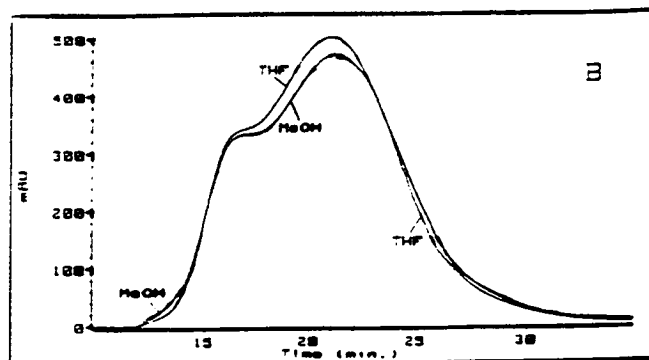
Figure 21b. Solvent effects on MSDs of asphalt AAA-1 strong acids fraction and SEC I fraction



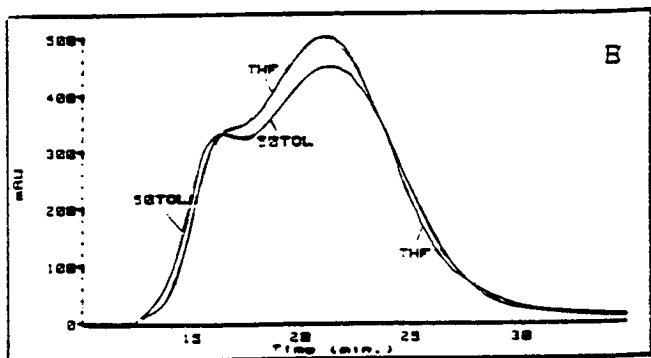
Whole asphalt in most polar and least polar solvents.



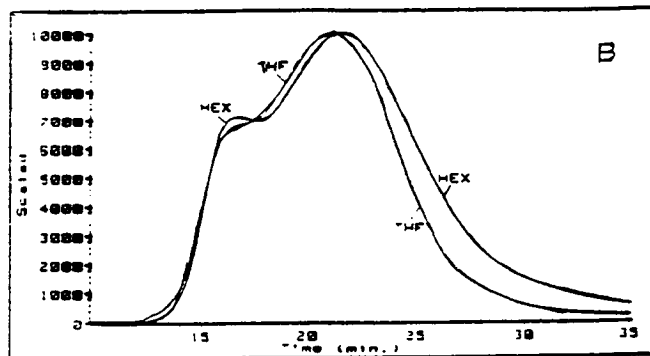
Whole asphalt - THF vs 20% Toluene



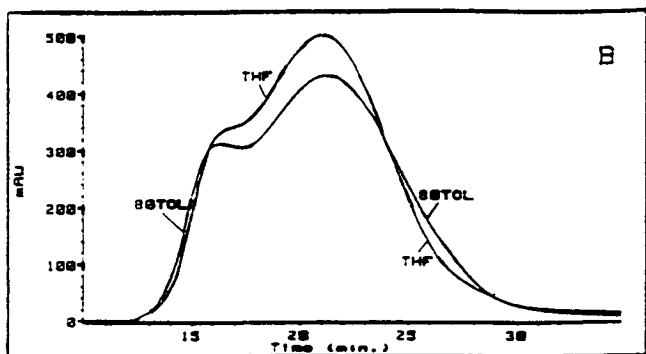
Whole asphalt - THF vs Methanol



Whole asphalt - THF vs 50% Toluene

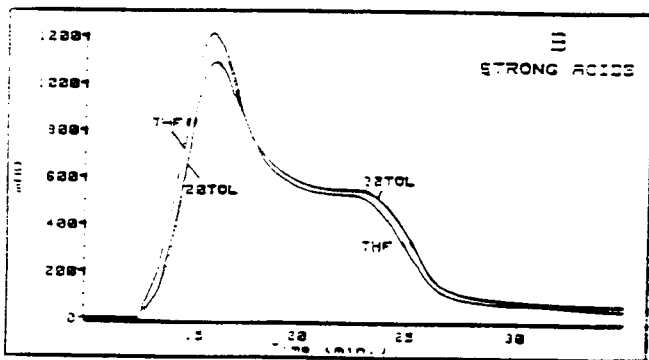


Whole Asphalt - THF vs Hexane

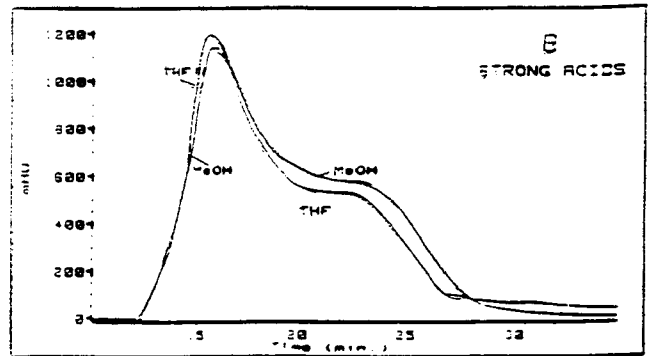


Whole asphalt - THF vs 80% Toluene

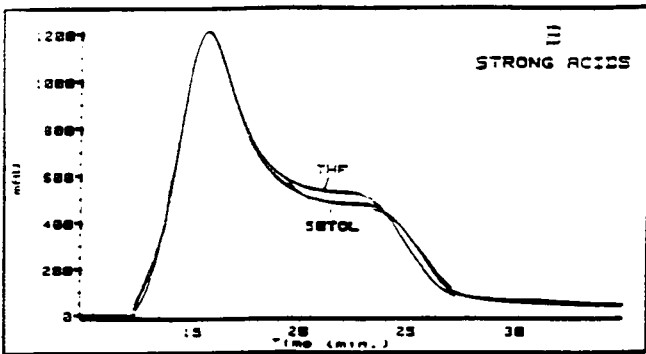
Figure 22a. Solvent effects on MSD s
of asphalt AAB-1.



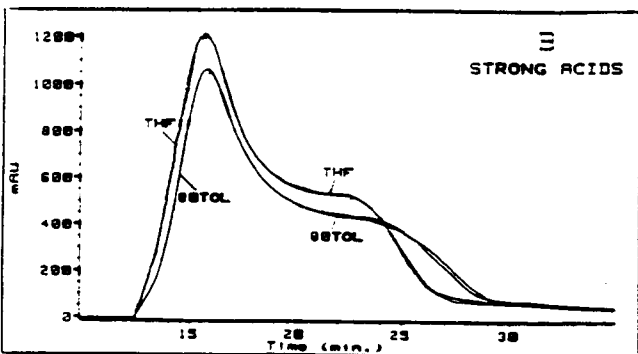
Strong acids fraction - THF vs 20% Toluene



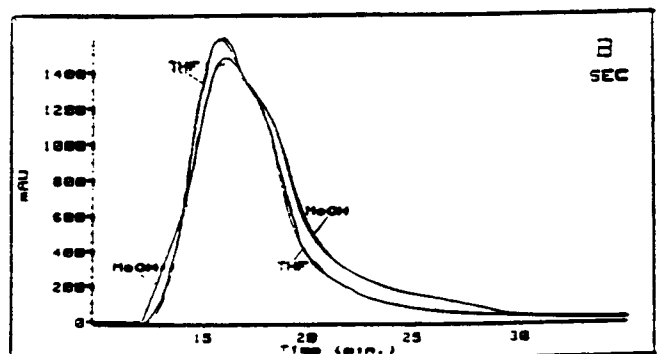
Strong acids fraction - THF vs Methanol



Strong acids fraction - THF vs 50% Toluene

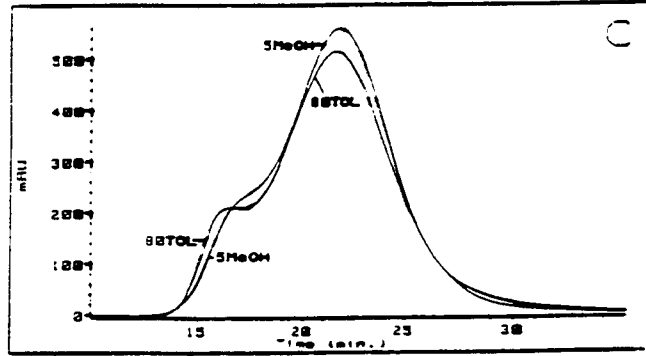


Strong acids fraction - THF vs 80% Toluene

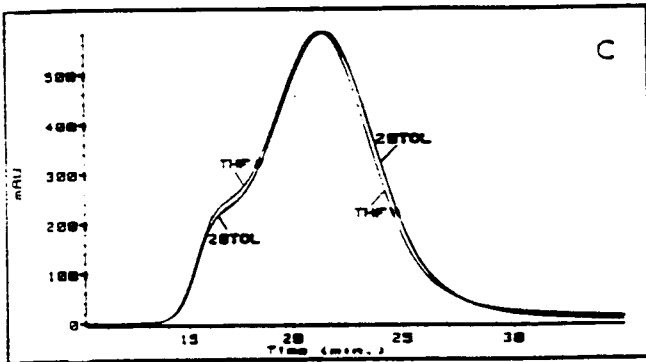


SEC 1 fraction - THF vs Methanol

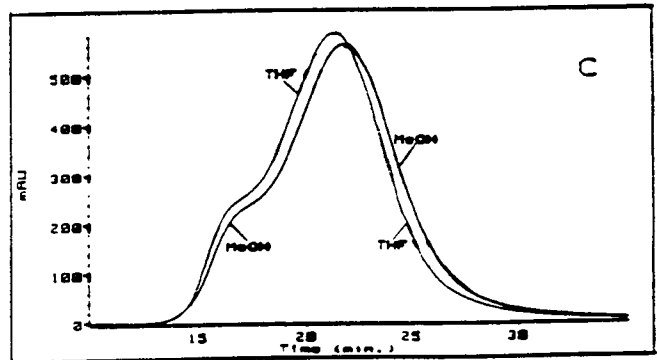
Figure 22b. Solvent effects on MSDs of asphalt AAB-1 strong acids fraction and SEC 1 fraction



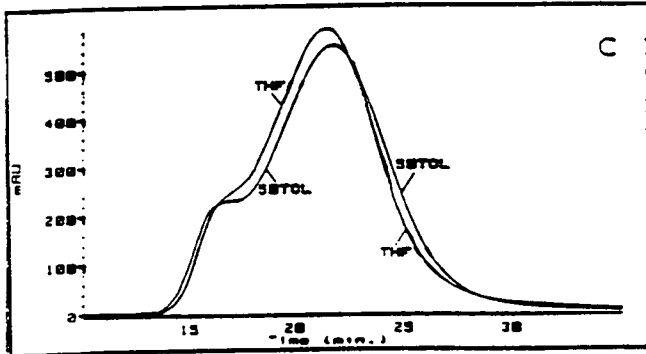
Whole asphalt in most polar and least polar solvents.



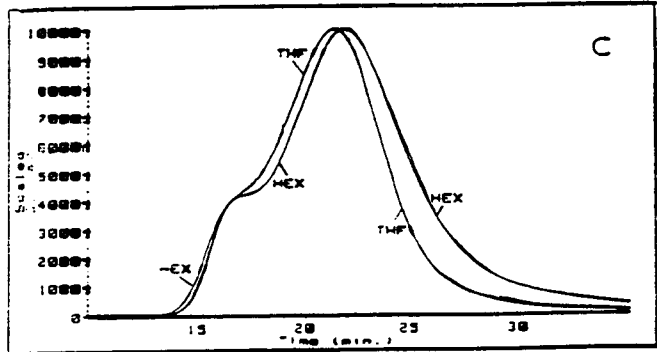
Whole asphalt - THF vs 20% Toluene



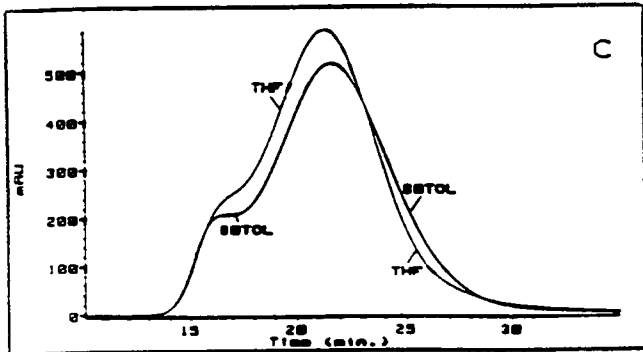
Whole asphalt - THF vs Methanol



Whole asphalt - THF vs 50% Toluene

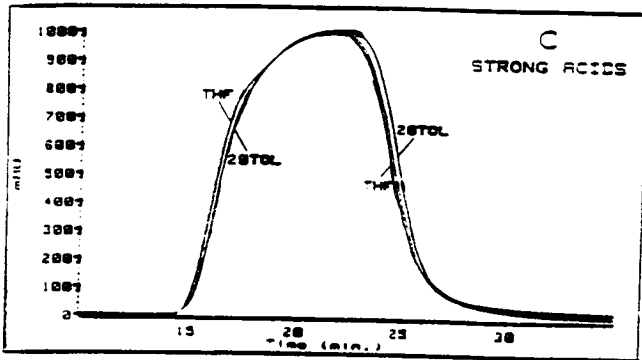


Whole Asphalt - THF vs Hexane

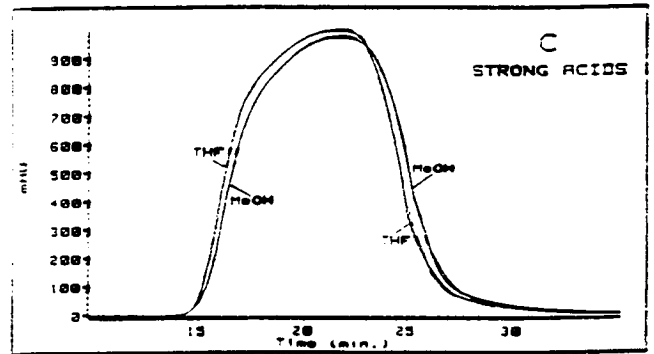


Whole asphalt - THF vs 80% Toluene

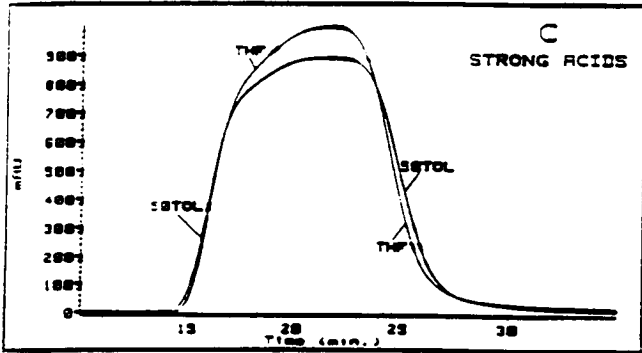
Figure 23a. Solvent effects on MSD's
of asphalt AAC-1.



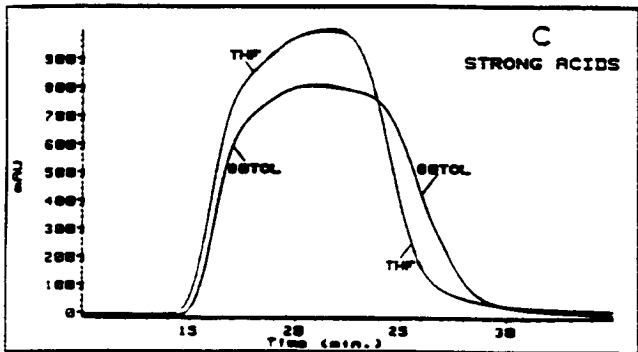
Strong acids fraction - THF vs 20% Toluene



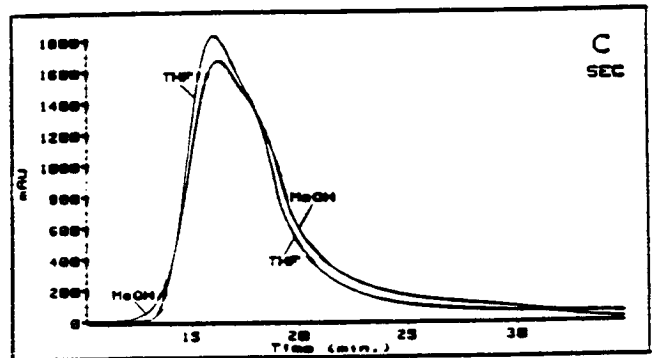
Strong acids fraction - THF vs Methanol



Strong acids fraction - THF vs 50% Toluene

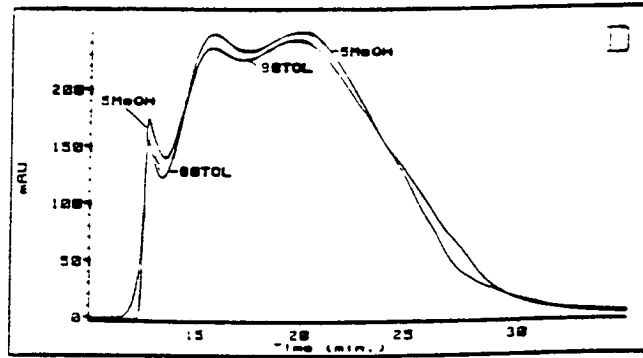


Strong acids fraction - THF vs 80% Toluene

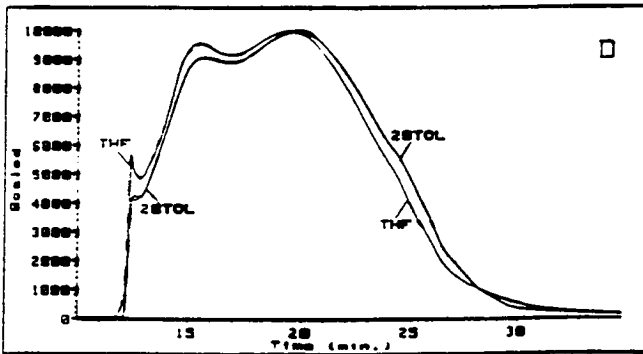


SEC I fraction - THF vs Methanol

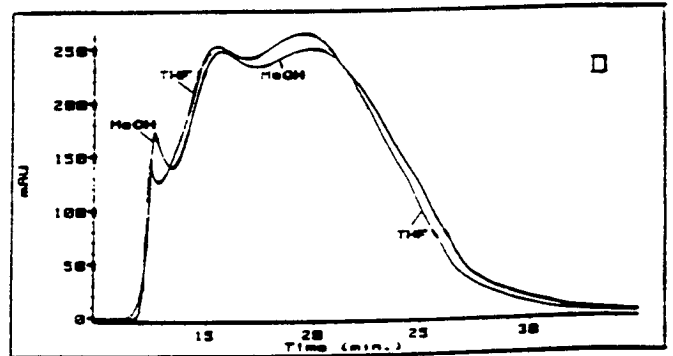
Figure 23b. Solvent effects on MSD s of asphalt AAC-1 strong acids fraction and SEC I fraction



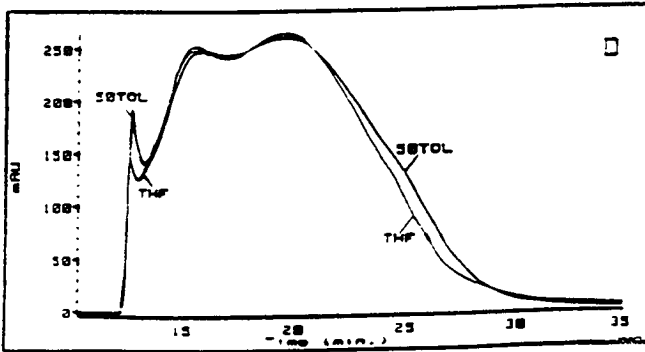
Whole asphalt in most polar and least polar solvents.



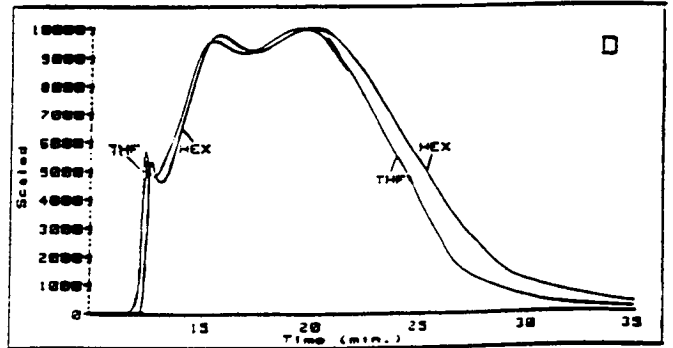
Whole asphalt - THF vs 20% Toluene



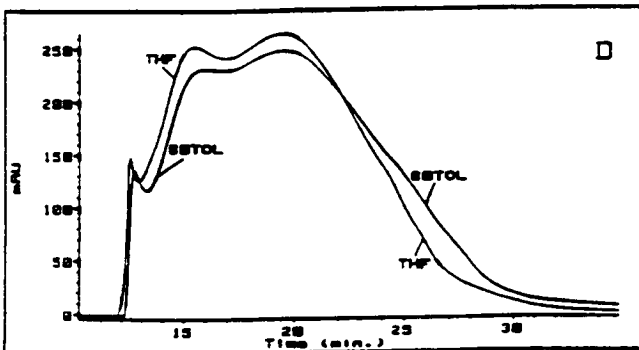
Whole asphalt - THF vs Methanol



Whole asphalt - THF vs 50% Toluene

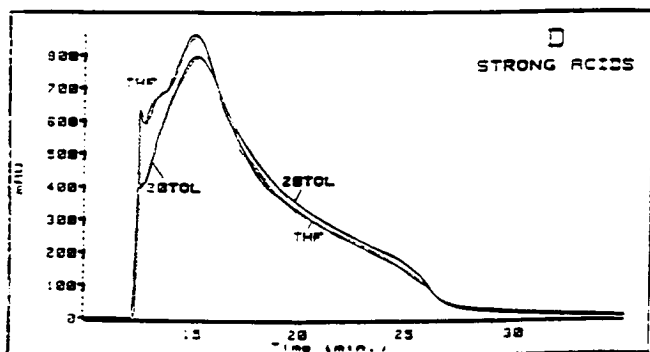


Whole Asphalt - THF vs Hexane

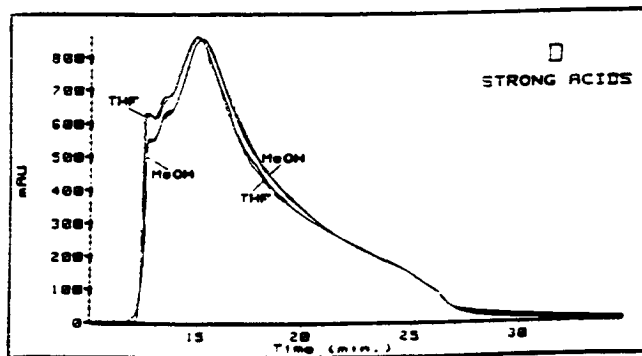


Whole asphalt - THF vs 80% Toluene

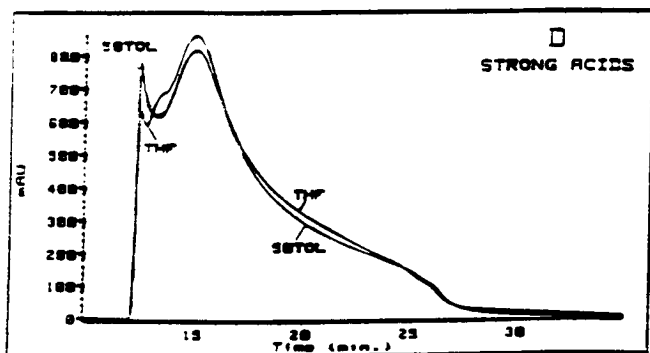
Figure 24a. Solvent effects on MSD's of asphalt AAD-1.



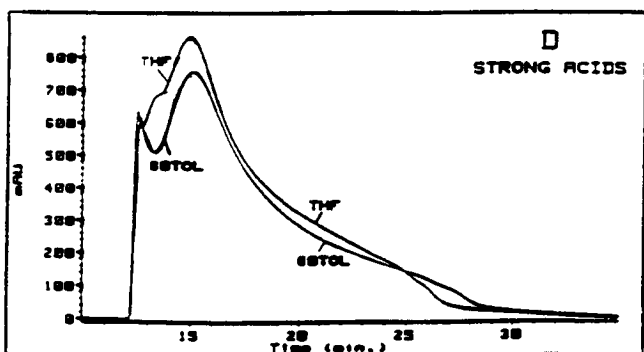
Strong acids fraction - THF vs 20% Toluene



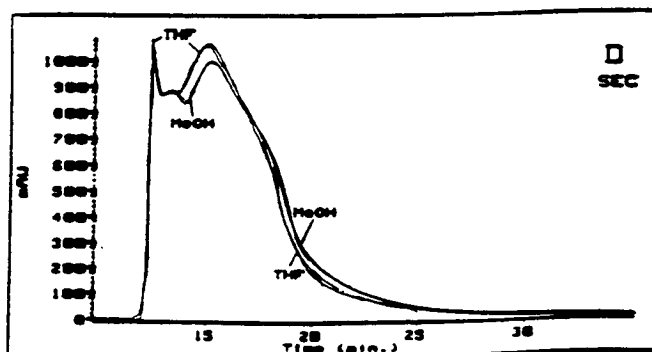
Strong acids fraction - THF vs Methanol



Strong acids fraction - THF vs 50% Toluene

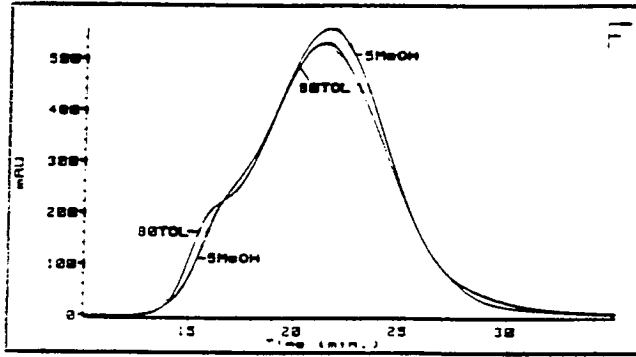


Strong acids fraction - THF vs 80% Toluene

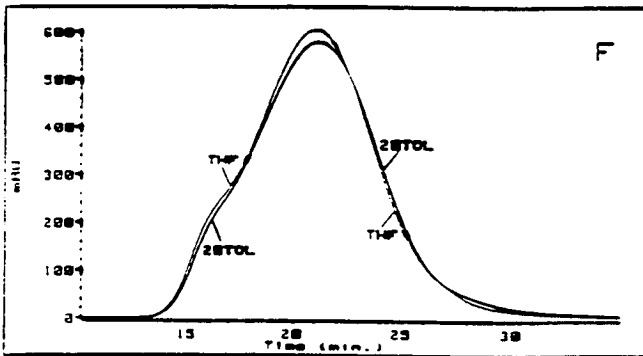


SEC I fraction - THF vs Methanol

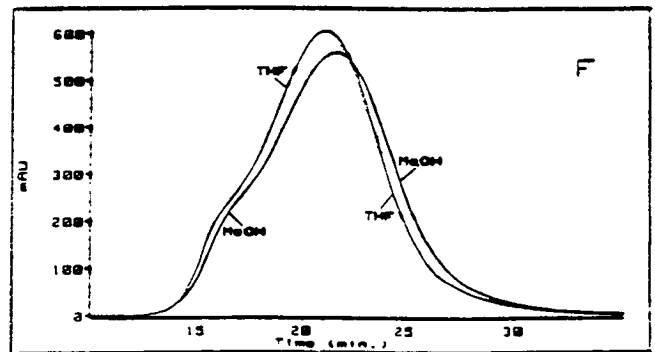
Figure 24b. Solvent effects on MSDs of asphalt AAD-1 strong acids fraction and SEC I fraction



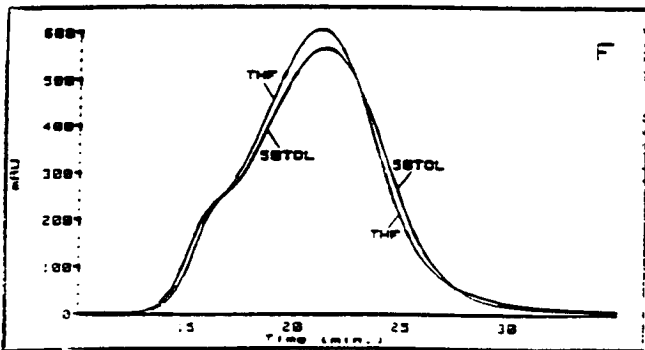
Whole asphalt in most polar and least polar solvents.



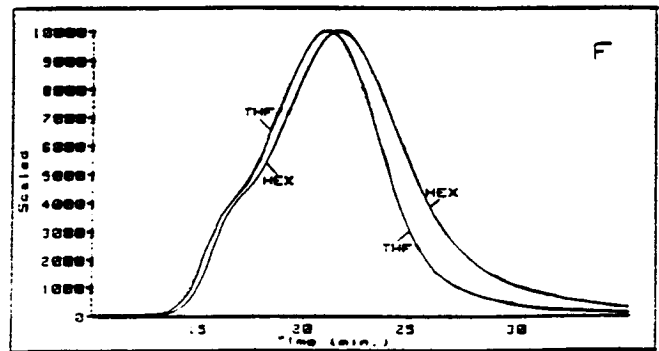
Whole asphalt - THF vs 20% Toluene



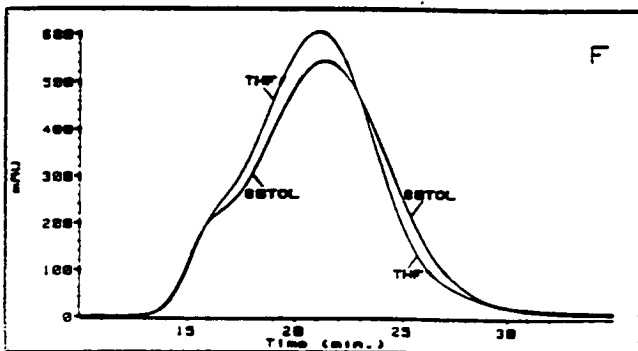
Whole asphalt - THF vs Methanol



Whole asphalt - THF vs 50% Toluene

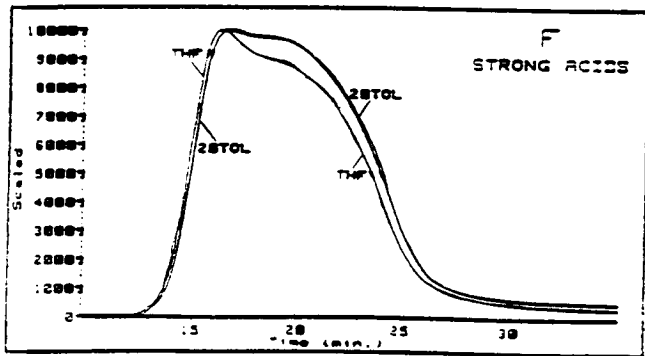


Whole Asphalt - THF vs Hexane

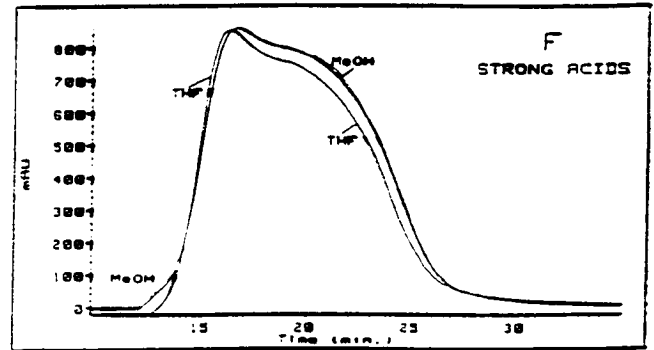


Whole asphalt - THF vs 80% Toluene

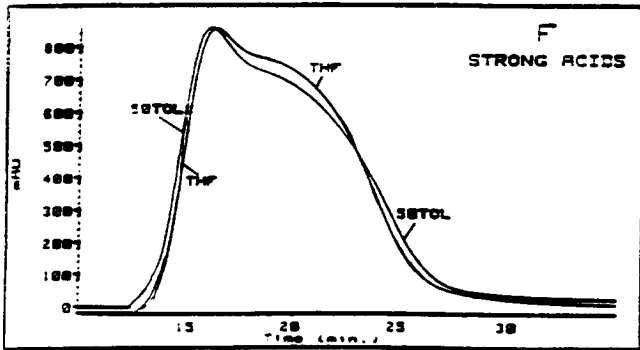
Figure 25a. Solvent effects on MSDs of asphalt AAF-1.



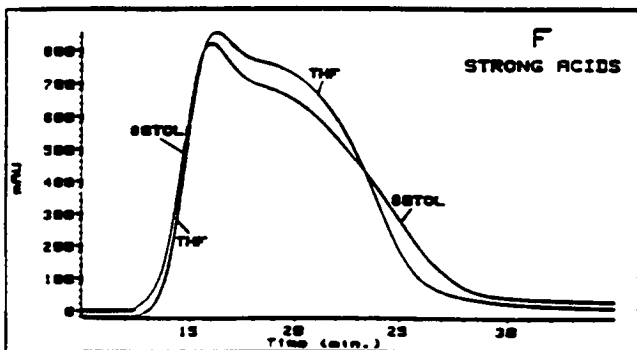
Strong acids fraction - THF vs 20% Toluene



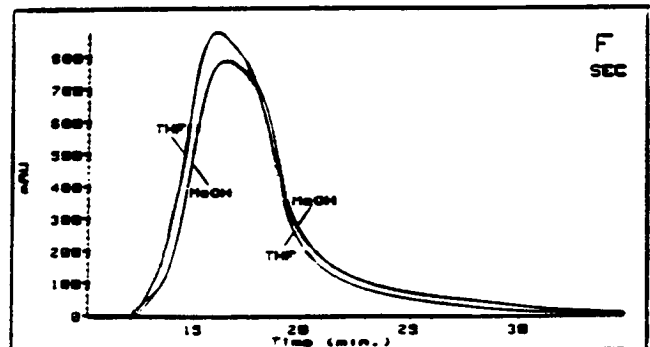
Strong acids fraction - THF vs Methanol



Strong acids fraction - THF vs 50% Toluene

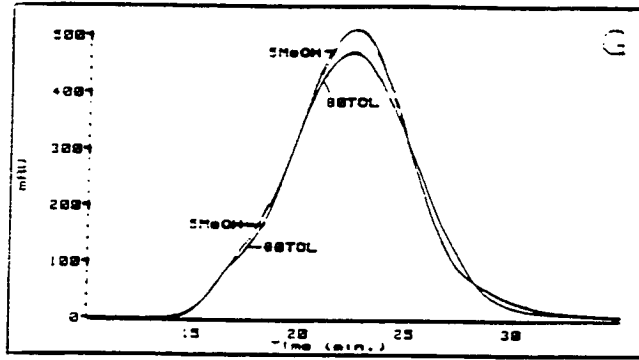


Strong acids fraction - THF vs 80% Toluene

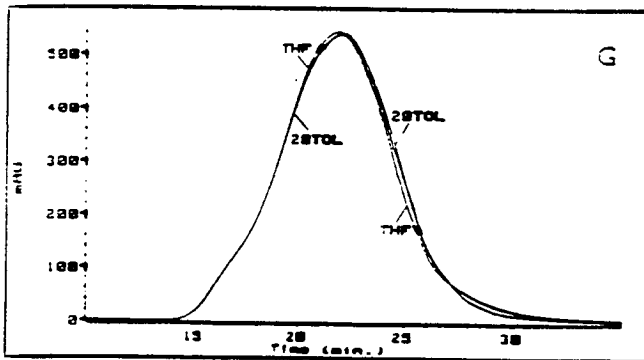


SEC I fraction - THF vs Methanol

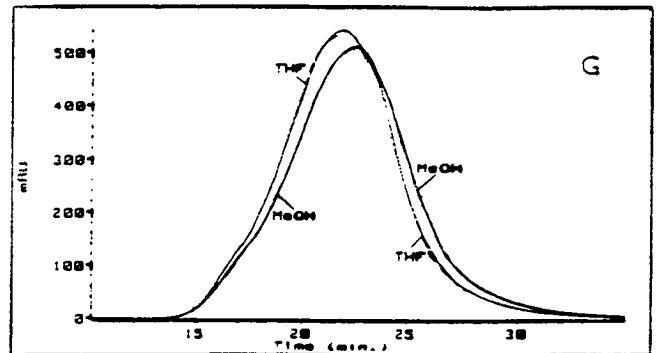
Figure 25b. Solvent effects on MSD's of asphalt AAF-1 strong acids fraction and SEC I fraction



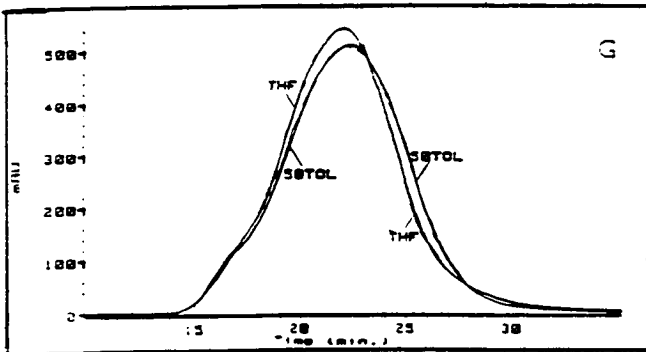
Whole asphalt in most polar and least polar solvents.



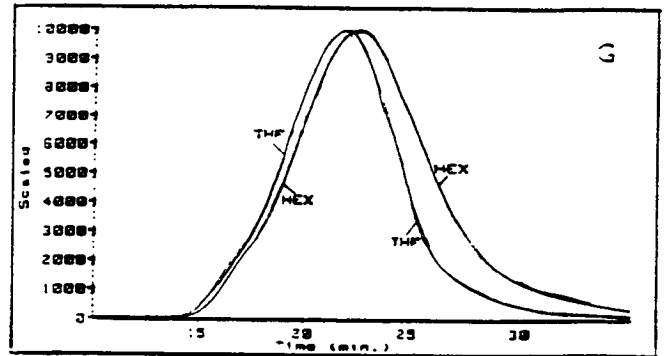
Whole asphalt - THF vs 20% Toluene



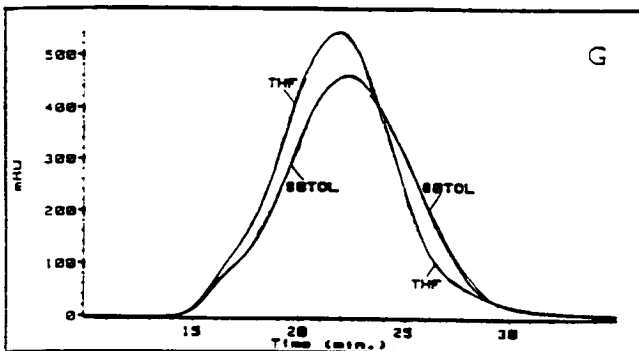
Whole asphalt - THF vs Methanol



Whole asphalt - THF vs 50% Toluene

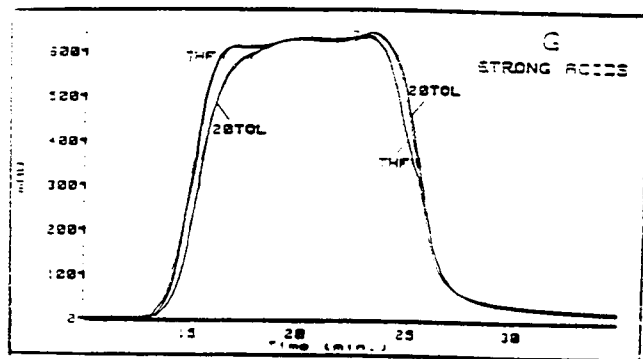


Whole Asphalt - THF vs Hexane

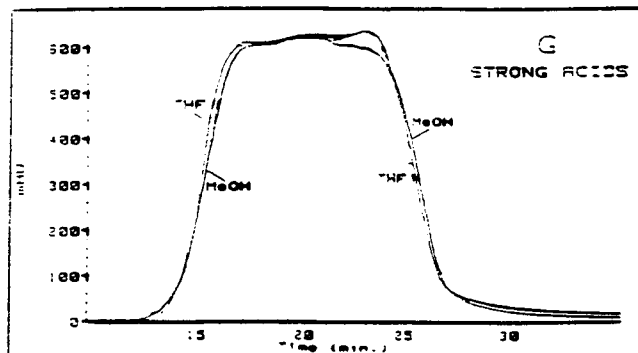


Whole asphalt - THF vs 80% Toluene

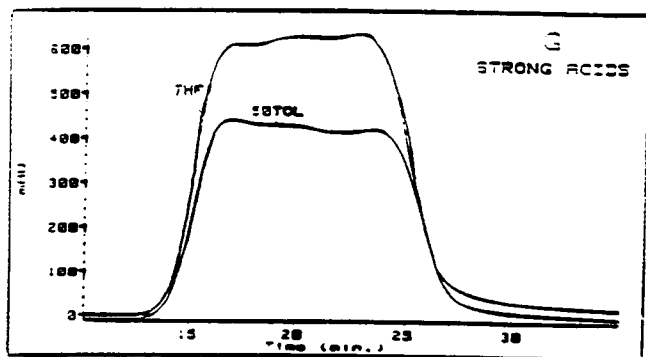
Figure 26a. Solvent effects on MSD's of asphalt AAG-1.



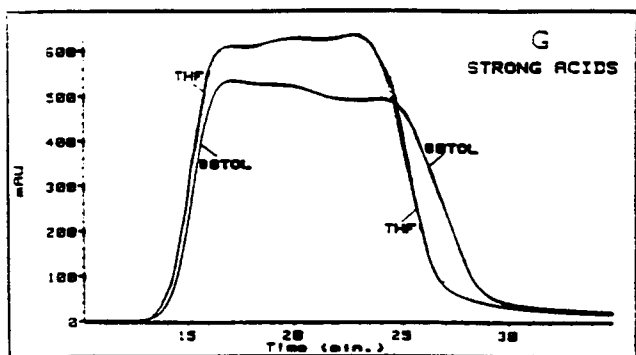
Strong acids fraction - THF vs 20% Toluene



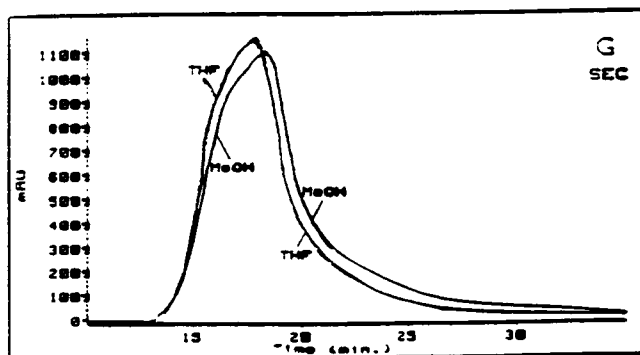
Strong acids fraction - THF vs Methanol



Strong acids fraction - THF vs 50% Toluene

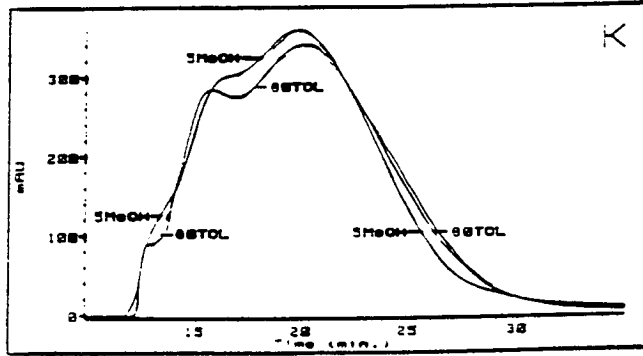


Strong acids fraction - THF vs 80% Toluene

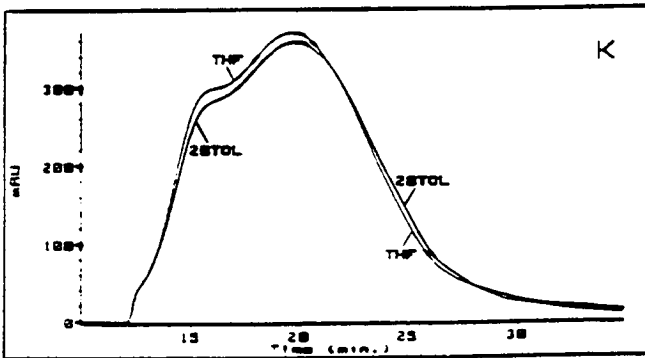


SEC I fraction - THF vs Methanol

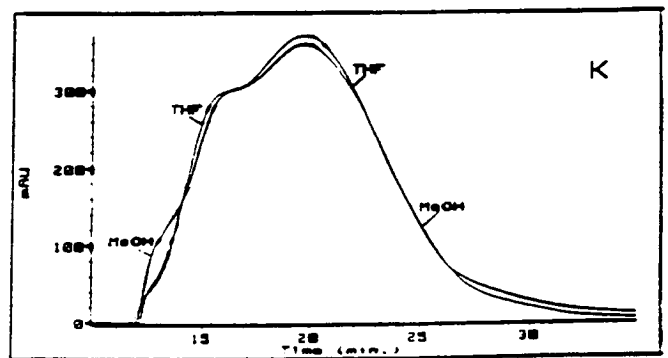
Figure 26b. Solvent effects on MSDs of asphalt AAG-1 strong acids fraction and SEC I fraction



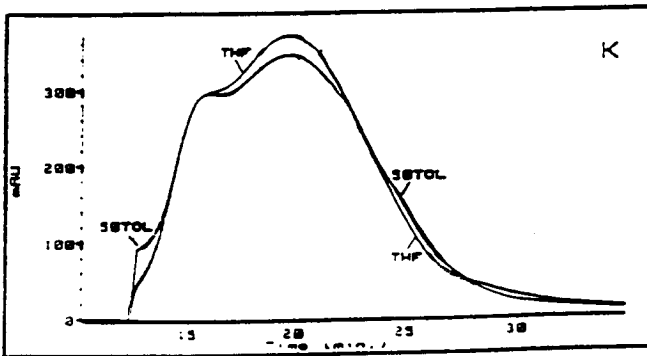
Whole asphalt in most polar and least polar solvents.



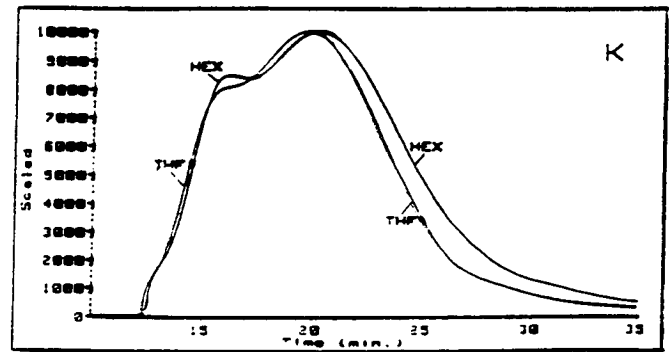
Whole asphalt - THF vs 20% Toluene



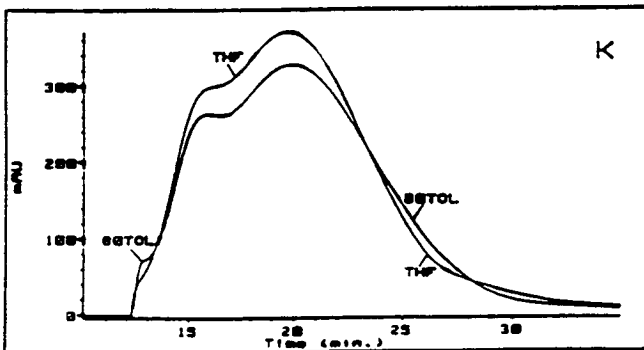
Whole asphalt - THF vs Methanol



Whole asphalt - THF vs 50% Toluene

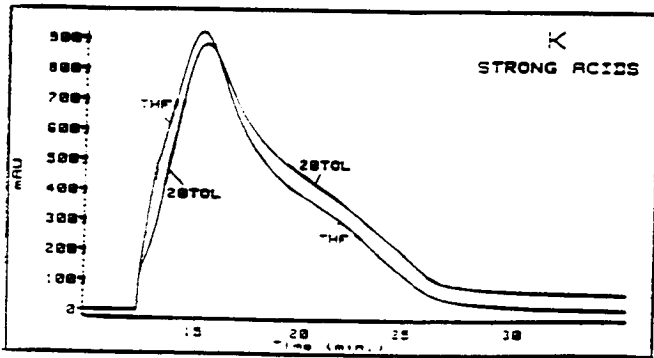


Whole Asphalt - THF vs Hexane

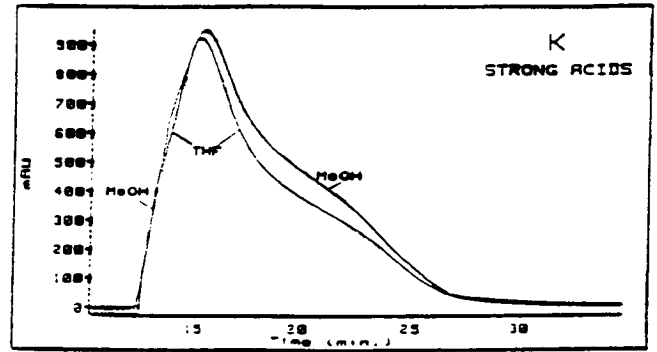


Whole asphalt - THF vs 80% Toluene

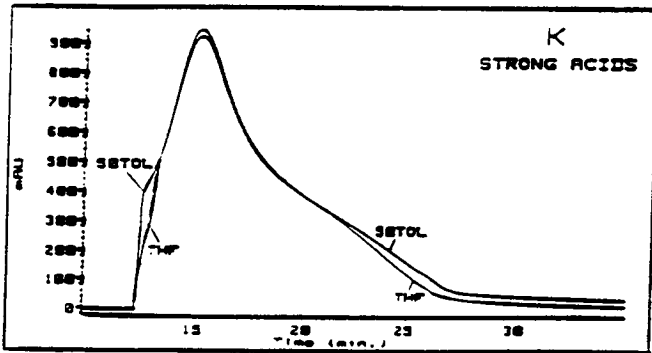
Figure 27a. Solvent effects on MSD's of asphalt AAK-1.



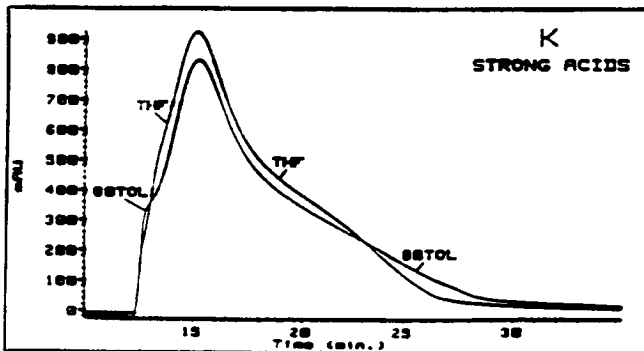
Strong acids fraction - THF vs 20% Toluene



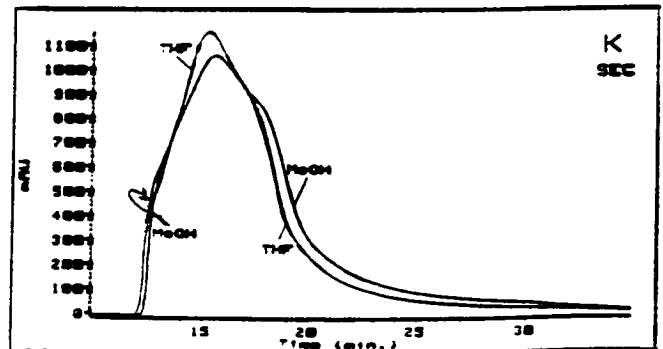
Strong acids fraction - THF vs Methanol



Strong acids fraction - THF vs 50% Toluene

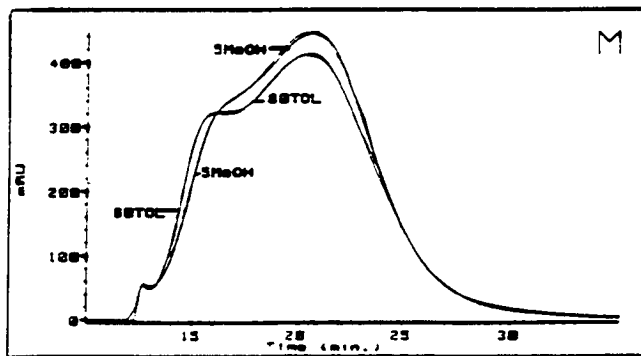


Strong acids fraction - THF vs 80% Toluene

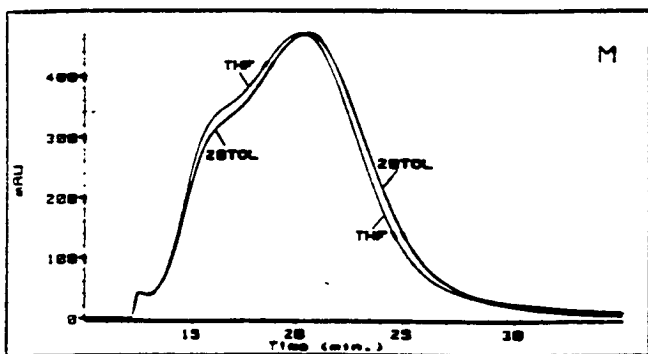


SEC I fraction - THF vs Methanol

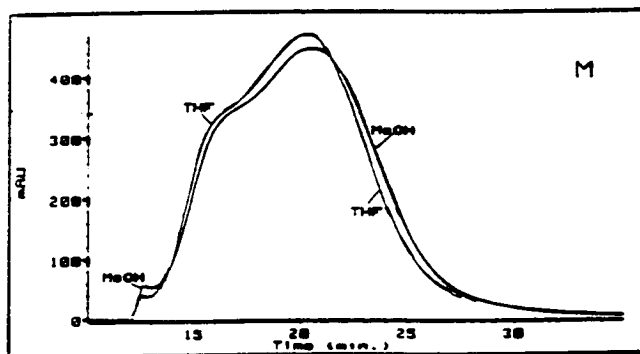
Figure 27b. Solvent effects on MSDs of asphalt AAK-1 strong acids fraction and SEC I fraction



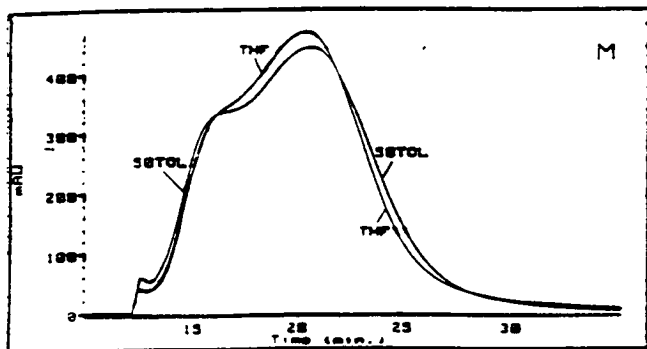
Whole asphalt in most polar and least polar solvents.



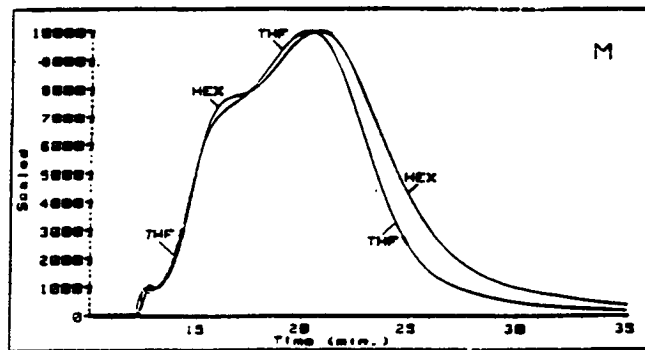
Whole asphalt - THF vs 20% Toluene



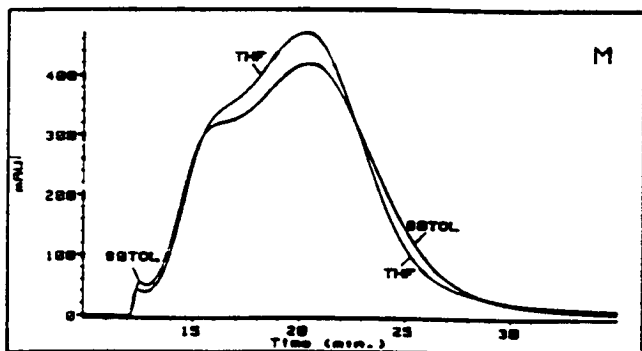
Whole asphalt - THF vs Methanol



Whole asphalt - THF vs 50% Toluene

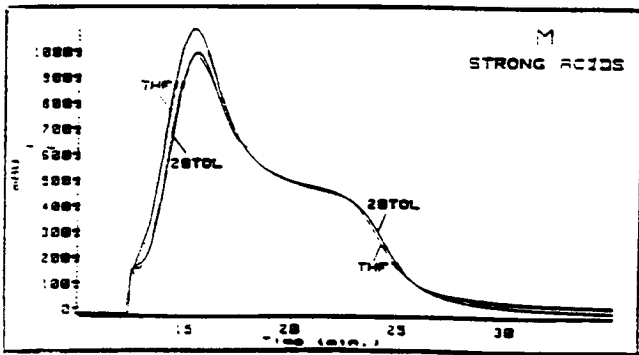


Whole Asphalt - THF vs Hexane

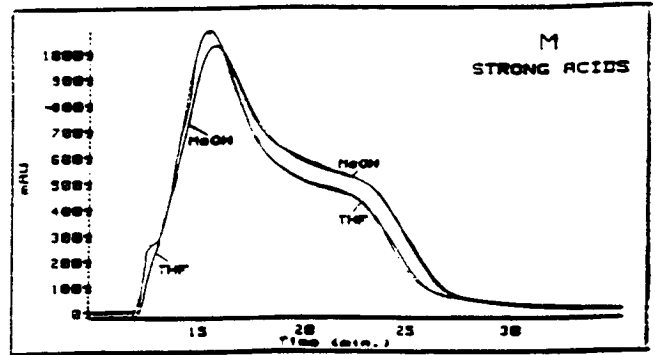


Whole asphalt - THF vs 80% Toluene

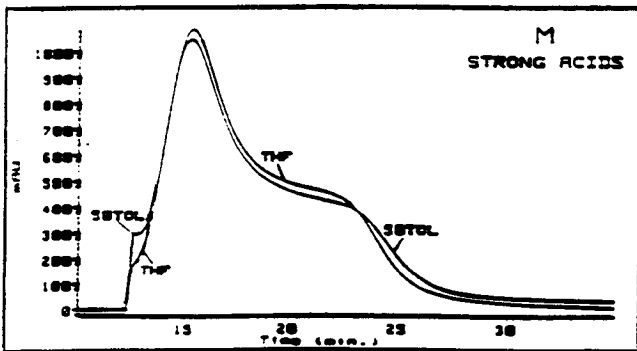
Figure 28a. Solvent effects on MSD's of asphalt AAM-1.



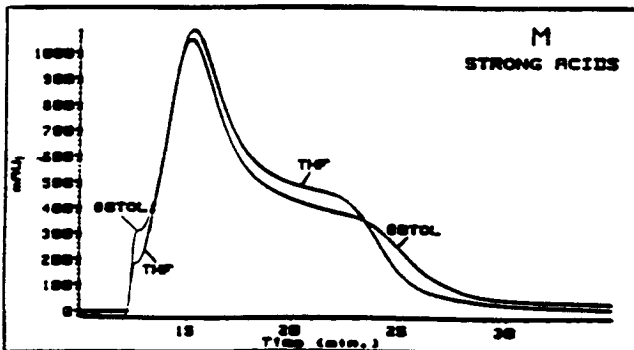
Strong acids fraction - THF vs 20% Toluene



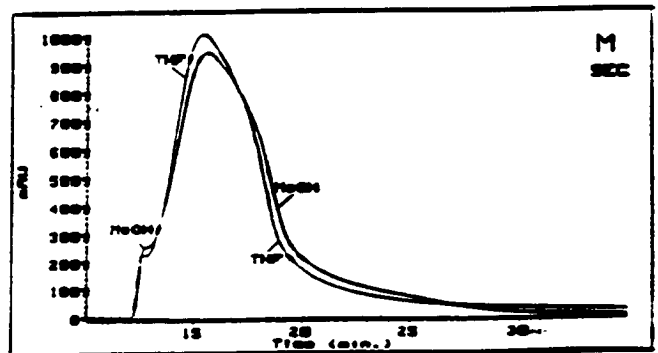
Strong acids fraction - THF vs Methanol



Strong acids fraction - THF vs 50% Toluene



Strong acids fraction - THF vs 80% Toluene



SEC I fraction - THF vs Methanol

Figure 28b. Solvent effects on MSD's of asphalt AAM-1 strong acids fraction and SEC I fraction

V. C. Other MRL asphalts

SHRP has collected a number of asphalts in addition to the core asphalts which form the bulk of the study. Although little other testing has been done on these "extra" MRL asphalts, they have been analyzed by HP-GPC in THF. Their characteristics will be the next topic for discussion.

As indicated earlier, the eight core asphalts have been separated into four groups based on their overall molecular size distribution characteristics, particularly peak width and shape. The MRL asphalts fall rather neatly into the same categories (although asphalt AAD-1 remains unique). However, grouping the asphalts is not intended to imply that all asphalts within a group are similar by all measures. As has been and will be seen, there is considerable variability within each group in terms of the content of conjugated materials and the size of the chromophores in those materials. These parameters may prove to be important to the physical and performance properties of the asphalts.

Table 14 provides some HP-GPC characteristics of eight asphalts, including three core asphalts, which have been placed in Group 1. Chromatograms in Figure 29 show only small shoulders, if any, in the region representing larger molecular sizes. The initial elution time ranges from about 14 to just over 15 minutes indicating that the largest molecules in Group 1 asphalts are significantly smaller than the largest molecules (or molecular assemblages) in other MRL asphalts. This fact is reflected in the %LMS, a value ranging between 3.2 and 10.2% for Group 1.

CV_t values for this group range from 17.7×10^5 to 28.3×10^5 mAU in the order

AAQ > AAF-1 > AAZ-1 > (AAG-1 > AAV-1 > AAC-1 = ABD) > AAX-1.

Asphalt AAX (AC-20) has less conjugated material than all other MRL asphalts; asphalts AAZ, AAF-1 and AAQ are among the most highly conjugated. (The last-mentioned three asphalts are products of solvent deasphalting processes.)

Conjugation indices (CI_t) decrease in the order (AAX-1 > AAR-1 > AAZ-1 = AAC-1) > (AAF-1 > AAV-1) > (AAG-1 > ABD) in the range 0.26 - 0.34. It is important to keep in mind the distinction between CV and CI. For example, although asphalt AAX shows the lowest absorption due to conjugated entities (CV_t), the sizes of the chromophores responsible for the absorption (CI_t) are among the largest in Groups 1 and 2.

In other words, in spite of variations within the group in content of conjugated entities and in the sizes of the chromophores in those entities, the overall molecular size distributions are narrow, the molecules are relatively small and there is little if any evidence for self-assembly in Group 1 asphalts.

Data for Group 2 asphalts are given in Table 15 and Figures 30 and 31. These asphalts are characterized by strong shoulders in the LMS region such that the chromatogram peaks are clearly bimodal or trimodal. Initial elution times range from near 12 to about 13.5 minutes, indicating the presence of larger molecules and/or assemblies in Group 2 than in Group 1. Peak widths are also greater than in Group 1, reflecting a broader distribution of molecular sizes. CV_t decreases in the order: AAH > AAR > (AAT = AAS-1 = AAO > AAY = AAW = AAB-1) > (AAK-1 > AAL = AAU > AAE > AAN) > AAA-1 within the range 22.6×10^5 to 28.6×10^5 mAU.

Ranging between 0.260 and 0.350, CI_t values decrease in the order: AAH > AAS-1 > (AAO > AAB-1 > (AAR = AAY > AAW = AAN = AAT) > (AAU = AAE) > (AAL = AAK-1) > AAA-1. The % CV_{11-17} ranges from 12.7 - 27.5. The key distinguishing characteristics between Groups 1 and 2 are, (a) the presence or absence of large molecules or assemblages eluting before 14 minutes, (b) the presence or absence of a distinctive shoulder(s) representing a second (or third) population of molecular sizes which include intermolecular assemblies.

Table 15 contains information for the remaining MRL asphalts. Asphalt AAD-1 remains unique. It is characterized by a very wide molecular size distribution with a CV_t of only 20.8×10^5 , lower than all asphalts except AAX (AC-20), and a CI_t of 0.245, indicating a predominance of small chromophores. The distinguishing characteristic is the presence of a large peak centered about 23.0 min, representing smaller molecules with very small chromophores ($CI_{21-25} = 0.14$).

Group 4 contains four asphalts, including AAM-1, which are characterized by relatively narrow molecular size distributions leaning heavily to larger sizes. Their CV_t 's are lower than average for all MRL asphalts, whereas their CI_t values are higher than most others. That is, they have a low absorbance due to conjugated entities, but the sizes of the chromophores are relatively large. Asphalts ABA and AAP show more evidence for self-assembly by virtue of their trimodal peak shapes.

Table 14. HP-GPC characteristics of Group 1 asphalts

Asphalt	Approx Initial Elution Min.	Approx Peak Width Min.	CV_1 ($\times 10^5$)	CI_1	%CV 11-17 min	%CV 17-21 min	%CV 21-25 min	%CV 25-29 min	CI 11-17 min	CI 21-25 min
AAG-1	15.2	15.5	24.8	0.257	3.2	30.7	55.3	12.6	0.48	0.22
ABD	14.5	16.0	23.8	0.243	5.1	31.4	51.7	11.8	0.47	0.19
AAC-1	14.6	15.5	23.9	0.327	8.2	38.5	45.3	8.0	0.53	0.44
AAF-1 ⁽¹⁾	14.5	15.5	27.6	0.299	8.3	39.0	44.2	8.5	0.48	0.34
AAZ-1	14.2	17.0	26.8	0.328	8.2	38.2	44.3	9.3	0.51	0.43
AAV-1	14.0	15.5	24.3	0.288	10.2	37.7	42.9	9.3	0.49	0.34
AAX-1	14.0	17.0	17.7	0.340	9.5	43.0	38.9	8.6	0.50	0.42
AAQ-1 ⁽¹⁾	14.0	18.0	28.3	0.333	9.5	32.7	43.1	14.7	0.52	0.35

⁽¹⁾ Product of solvent deasphalting process

Bold face = SHRP core asphalt

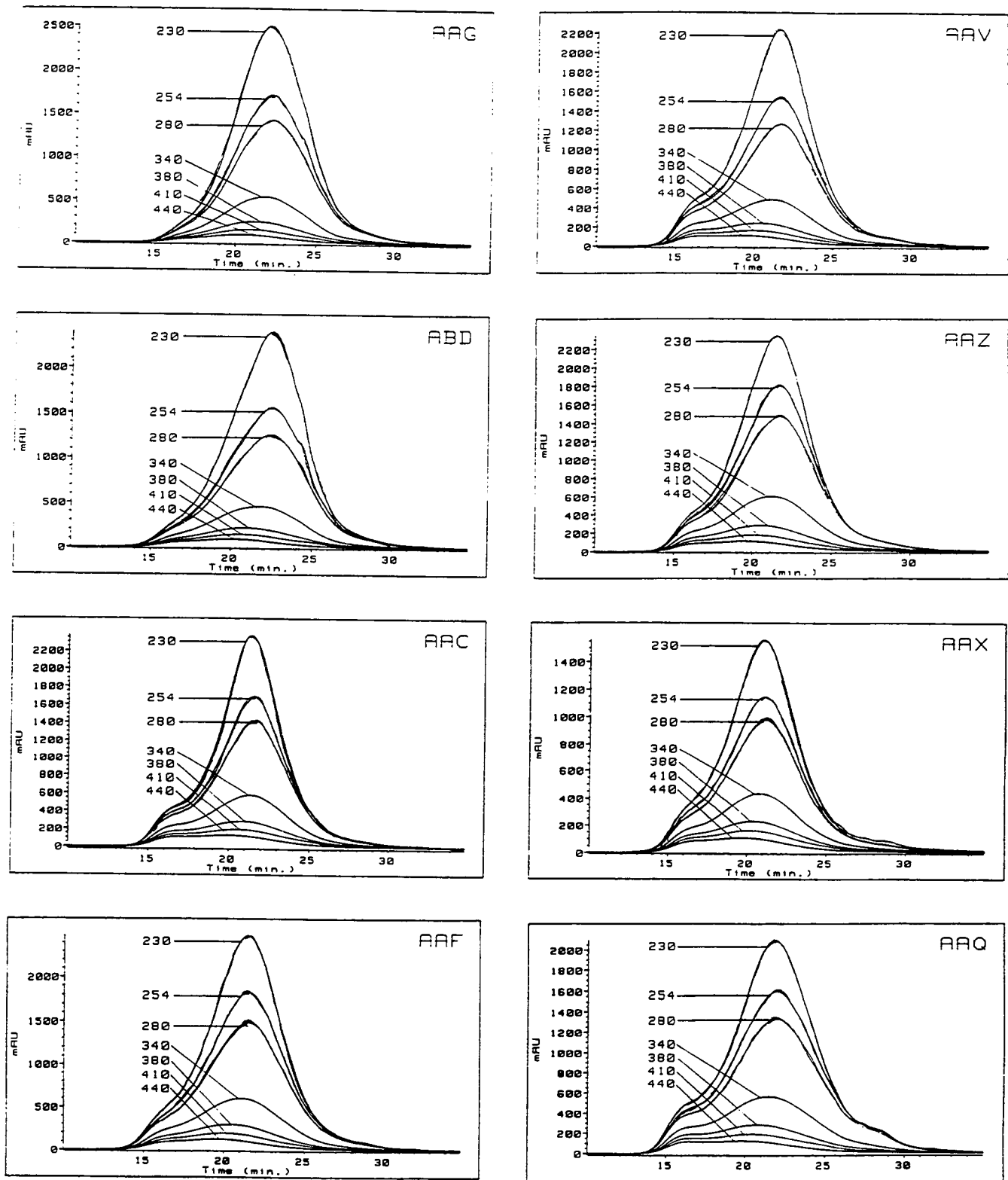


Figure 29. Seven-chromatogram plots of Group 1 asphalts.

Table 15. HP-GPC characteristics of Group 2 asphalts

Asphalt	Approx Initial Elution Time, Min.	Approx Peak Width, Min.	CV _t (x10 ⁵)	Cl _t	%CV 11-17 min	%CV 17-21 min	%CV 21-25 min	%CV 25- min	Cl 11-17 min	Cl 21-25 min
AAW	13.2	18.0	25.5	0.306	12.7	36.3	40.4	10.6	0.48	0.24
AAB-1	13.5	18.0	25.4	0.326	13.6	35.2	40.1	11.1	0.50	0.26
AAT	12.3	19.5	26.0	0.301	15.0	36.2	38.5	10.2	0.47	0.22
AAO	12.5	18.5	25.7	0.331	15.1	37.2	37.6	10.0	0.50	0.27
AAN	12.5	18.5	23.9	0.304	15.2	36.8	38.3	9.7	0.48	0.23
AAU	12.3	18.0	24.3	0.292	15.4	36.8	38.8	9.0	0.47	0.22
AAR	12.5	19.5	26.9	0.311	15.4	34.7	37.8	12.1	0.48	0.23
AAS-1	12.7	18.5	25.8	0.339	16.8	37.7	35.9	9.6	0.50	0.26
AAY	12.7	19.5	25.5	0.310	16.7	34.1	36.1	13.0	0.48	0.22
AAA-1	12.3	18.5	22.6	0.264	19.2	34.2	36.7	9.9	0.45	0.17
AAK-1	12.3	19.5	24.6	0.274	19.5	35.3	33.8	11.4	0.45	0.18
AAH	12.3	19.5	28.6	0.352	17.2	32.7	35.6	14.5	0.52	0.26
AAL	12.2	19.5	24.4	0.276	19.0	32.3	36.1	12.6	0.47	0.18
AAE ⁽¹⁾	12.1	19.5	24.1	0.290	27.5	31.1	32.3	9.1	0.48	0.17

⁽¹⁾ Air blown product

Bold face = SHRP core asphalt

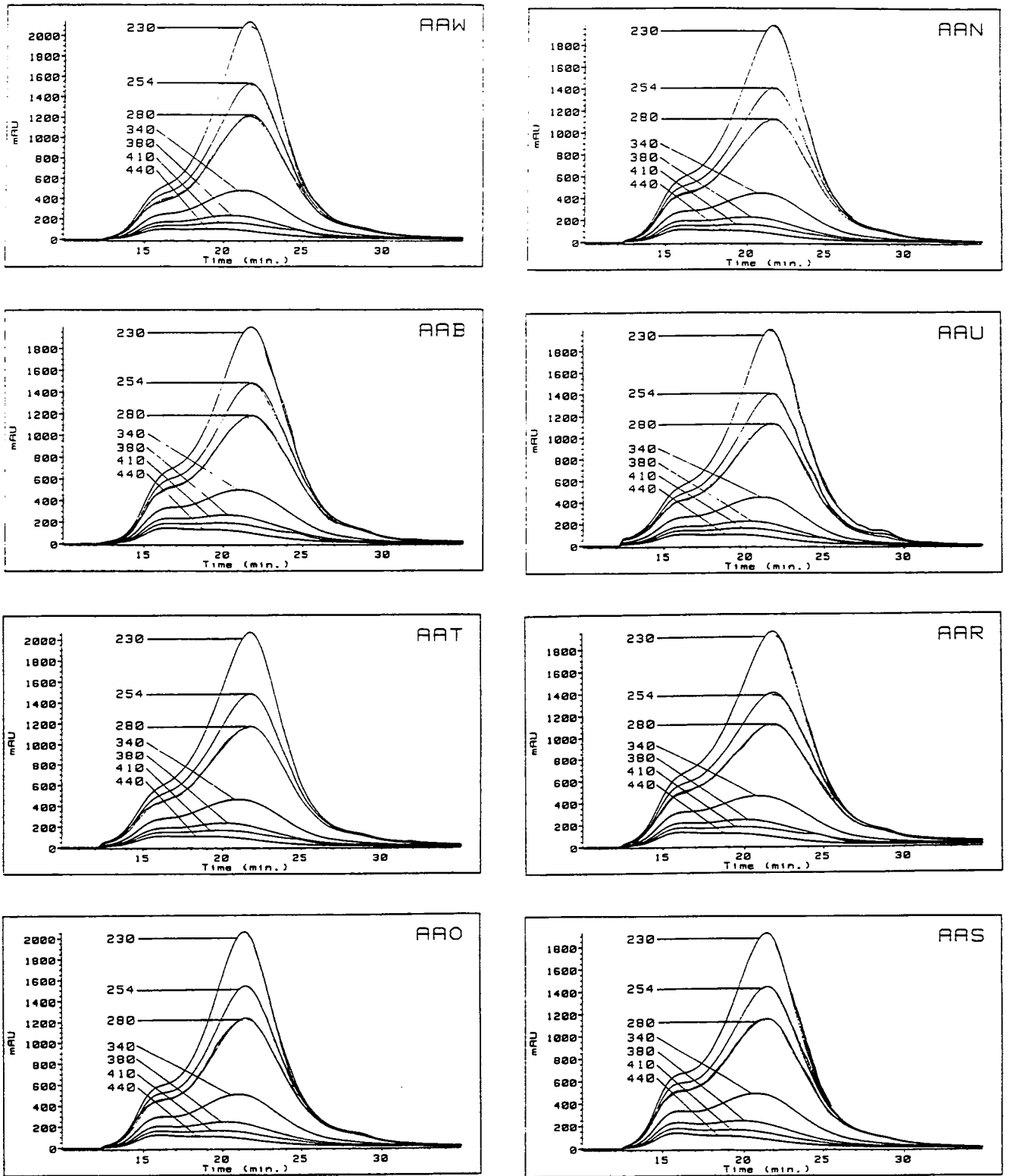


Figure 30. Seven-chromatogram plots of Group 2 asphalts

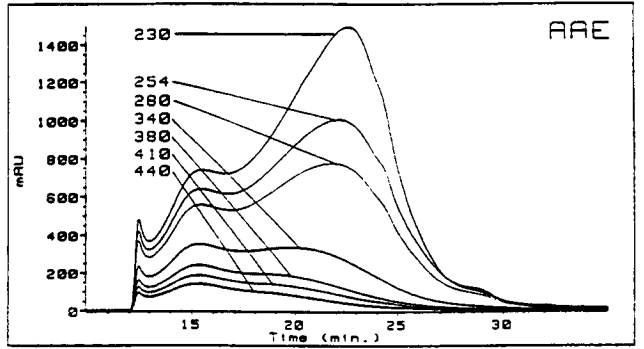
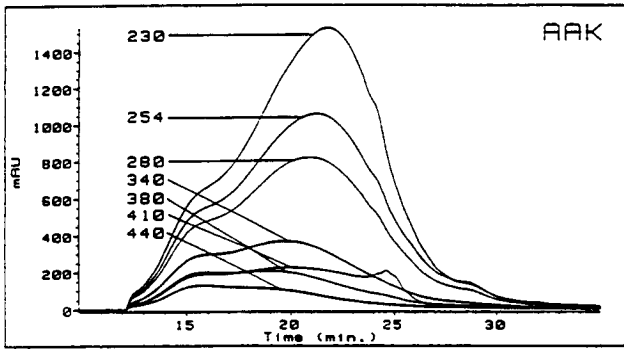
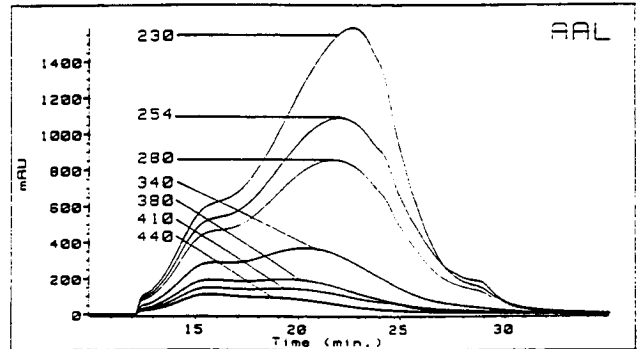
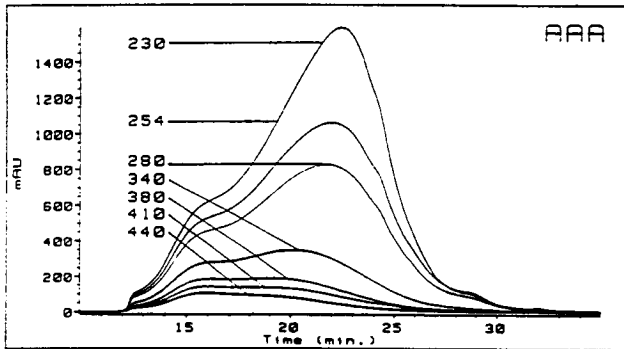
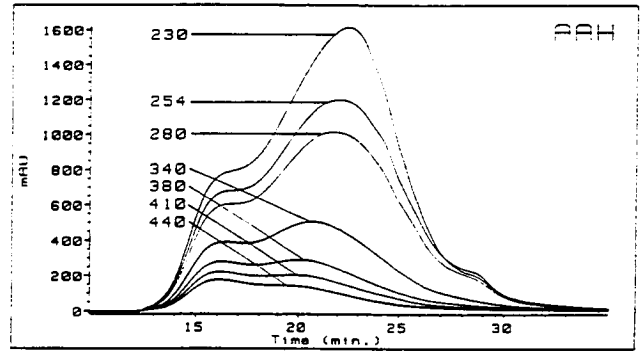
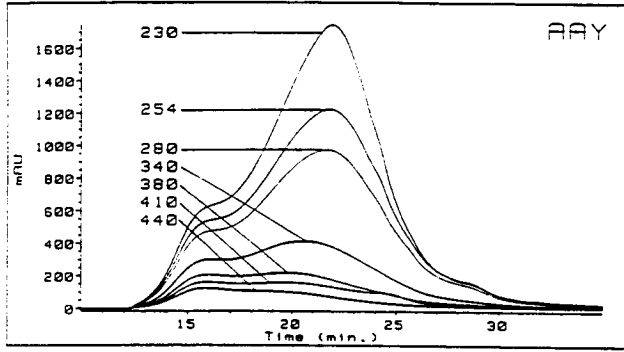


Figure 31. Seven-chromatogram plots of Group 2 asphalts (continuation of Figure 30).

Table 16. HP-GPC characteristics of Groups 3 and 4 asphalts

Asphalt	Approx Initial Elution Time, Min.	Approx Peak Width, Min. (x10 ⁵)	CV _t	CI _t	%CV 11-17 min	%CV 17-21 min	%CV 21-25 min	%CV 25-34 min	CI 11-17 min	CI 21-25 min
<u>Group 3</u>										
AAD-1	12.2	19.0	20.6	0.245	24.0	30.5	34.1	11.4	0.44	0.14
<u>Group 4</u>										
AAJ ⁽¹⁾	12.2	17.0	23.5	0.325	15.9	43.4	34.5	6.2	0.48	0.26
AAM ⁽¹⁾	12.2	18.3	23.5	0.345	20.1	44.0	29.4	6.5	0.43	0.33
ABA ⁽²⁾	12.2	16.8	22.7	0.321	25.9	39.3	30.7	4.1	0.51	0.23
AAP	12.2	16.8	22.7	0.325	26.2	43.8	26.0	4.0	0.49	0.25

(1) Solvent deasphalting (SDA) product

(2) Airblown product

Bold face = SHRP core asphalt

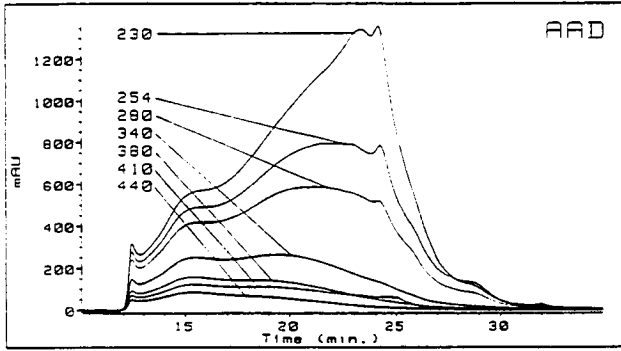


Figure 32. Seven-chromatogram plot of sole asphalt in Group 3.

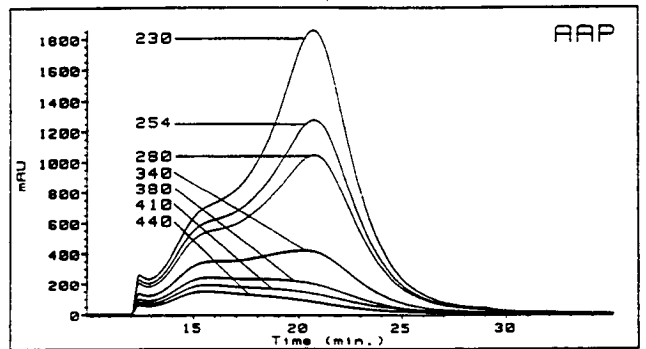
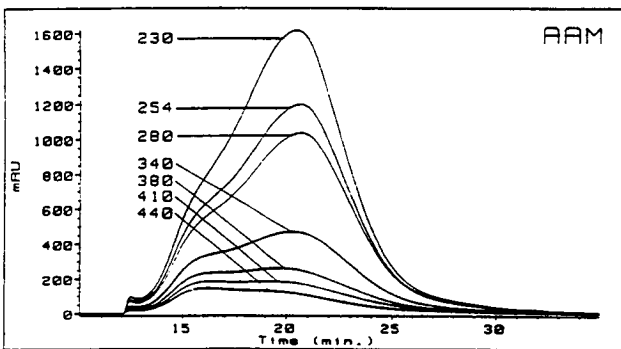
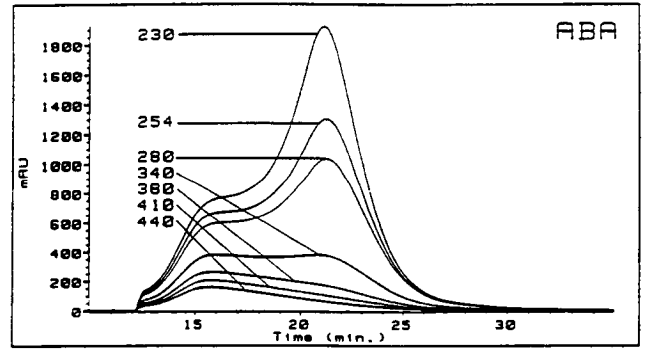
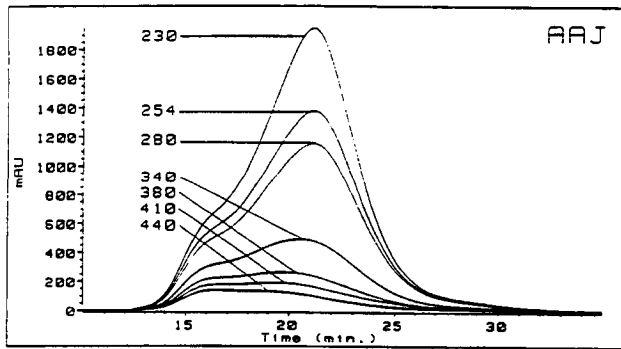


Figure 33. Seven-chromatogram plots of Group 4 asphalts.

Among these asphalts are some which are related by crude source, i.e., are derived from the same crude or have the same crude as a member of the crude slates. These are of interest because blending crudes may permit the production of superior asphalts.

Comparisons between asphalts ABD and AAG-1 are of interest because, although both are derived from the same crude source, caustic treatment was used in processing AAG-1 but not ABD. The differences between the two asphalts are small and are evidenced by a somewhat larger percentage of CV_t in the first two slices of ABD than of AAG-1 (Figure 29, Table 14). One would presume that the major difference between the two is the availability of RCOOH and ROH groups for hydrogen bonding in ABD. In AAG-1, these groups are bound up as salts and so are unavailable. If that is so, then hydrogen bonding does not contribute a great deal to self-assembly in this asphalt.

Asphalt AAE is an air-blown product from Lloydminster crude and, thus, is related to AAA-1. The chromatograms of AAE are more strongly trimodal than those of AAA-1, its conjugated volume is significantly higher and its conjugation index is somewhat higher than AAA-1. If the crudes are identical then the blowing process increases aromaticity (conjugation) and enlarges the average chromophore. It also increases molecular size and/or improves opportunities for self-assembly (Figures 30, 31, Table 15).

At first glance, the chromatograms of asphalts AAE and AAD-1 may seem to be identical. The most important difference between them is their conjugated volume

(20.6×10^5 for AAD-1 versus 24.1×10^5 for AAE). In addition, the elution time of the main peak is about 0.5 min later for AAD-1 (i.e., the components are smaller) and their conjugation index is somewhat lower (i.e., smaller chromophores) than for AAE.

Several asphalts include Maya in the blend of crude oils. For example, asphalt AAT (Figure 30) is produced from a blend of Maya and Lloydminster. Asphalt AAT has a somewhat narrower MSD than AAA-1 from Lloydminster (Figure 31) and has a lower % LMS (15% vs 19%). However, the CV_t of AAT is significantly greater than AAA-1. In other words, asphalt from a Maya-Lloydminster blend is somewhat smaller in molecular size but more highly conjugated than asphalt from Lloydminster alone.

A blend of Maya with Wyoming sour in asphalt AAR (Figure 30) produces a slightly greater % LMS (15.4 vs 13.6%) than asphalt AAB-1 (Figure 30, from Wyoming sour). Asphalt AAY (Figure 31), from a blend of Maya and Arabian heavy crudes, is remarkably similar to AAS-1 (Figure 30) from Arabian heavy. The main difference is in the % LMS and % CV_{25-29} which indicate that the Arabian crude contributes larger materials, Maya smaller. A final example is AAW (Figure 30) from a blend of Maya with West Texas sour. A comparison with AAF-1 (Figure 29, from West Texas sour) shows that the blend resulted in a decrease of CV_t (25.5 vs 27.6%) and an increase in % LMS (12.7 vs 8.3%).

The crudes for asphalts AAV (Figure 29, Alaska North Slope) and AAD-1 (Figure 32, California coastal) are blended in AAU (Figure 30, ANS and CA coastal). Although asphalt from the blend has somewhat more LMS material than AAV, it has no vestige of the main peak structure that is so dominant in AAD-1. In fact, although

AAV is in Group 1 and AAD-1 is unique in Group 3, asphalt AAU is typical of Group 2.

Asphalts AAO and AAS-1 (Figure 30) both from Arabian heavy crudes, are virtually identical in their HP-GPC characteristics except for some differences in % LMS (15.1 vs 16.8%, respectively) which could result from crude variability or processing differences.

West Texas sour is the crude source for asphalt AAF-1 (Figure 29). It appears in several blends. Asphalt AAW (Figure 30) from Maya and West Texas sour, was mentioned above. In AAZ (Figure 29) it is mixed with "coastal" crudes. Differences among these three are not particularly great. Asphalt AAW has most LMS material, AAF-1 the least; AAF-1 is the most highly conjugated, AAW the least.

These examples show how blending crudes induces considerable differences in the product asphalts and, moreover, suggests that the proper choice of crudes could be used to mitigate undesirable characteristics, once they are defined.

V. D. Asphalt AAX (AC-20) and ROSE fractions

In Table 17 and Figure 34 will be found HP-GPC data for six materials of particular interest to SHRP A-004 contractors. These are asphalt AAX (AC-20), its related ROSE fractions and AAX-F, a "flux" proposed for use for blending with the fractions. Both AAX (AC-20) and AAX-F are Group 1 asphalts. However, AAX-F is very highly conjugated, having the largest CV_1 of any MRL material tested to date. Nevertheless, it shows little tendency to form self-assemblies in THF and has no very

large molecules.

Fraction AAX-A, ROSE asphaltenes, is highly conjugated but does not show a great deal of % LMS material. Fraction AAX-R, the resins, has a narrow distribution of smaller molecules. The CV_t is about the same as AAX (AC-20).

In what is apparently an approximately 50:50 blend of AAX-A and AAX-R, the CV_t is 26.4×10^5 , which is similar to some Group 1 asphalts (e.g., AAZ-1). There is still little evidence for self-assembly. Blending AAX-A+R with AAX-F is not likely to change the HP-GPC characteristics of either by very much. It would tend to average the CV and CI values. This represents a good approach if asphalts of Group 1 type are found to be excellent performers, an unlikely event, unfortunately.

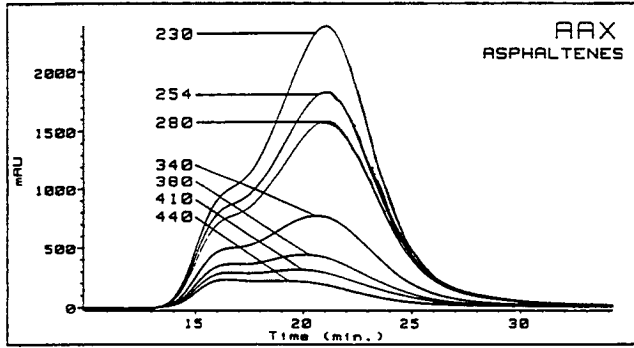
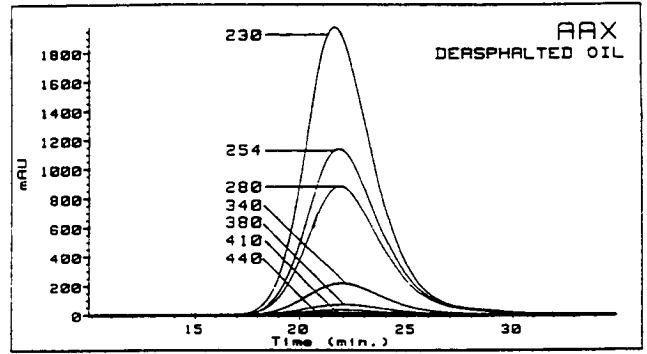
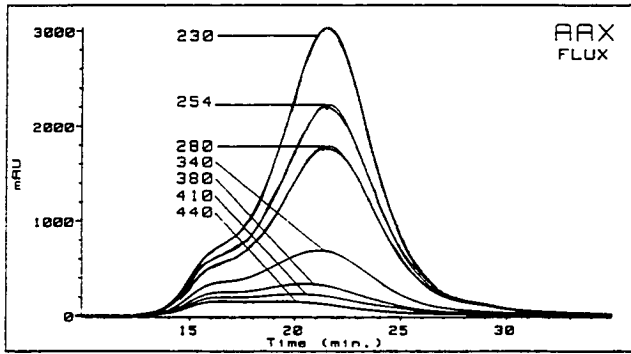
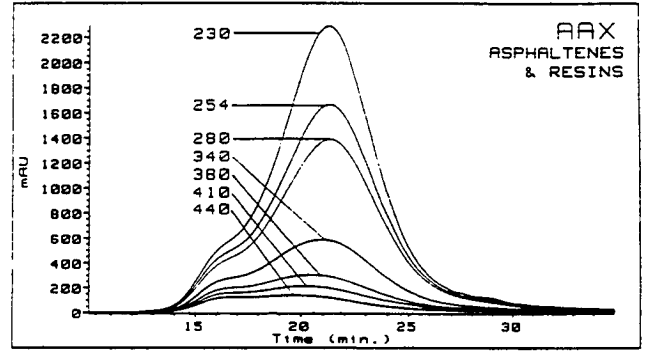
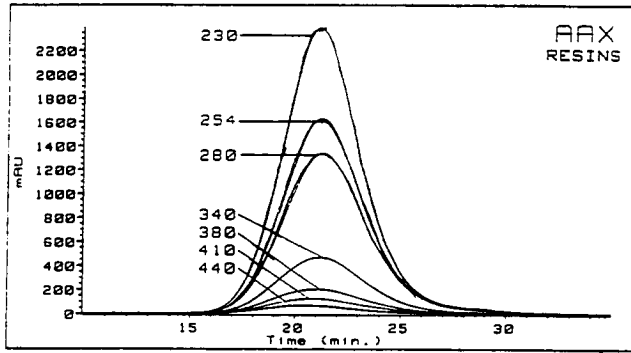


Figure 34. Seven-chromatogram plots of AAX - series materials.

Table 17. HP-GPC characteristics of AAX-series materials

Asphalt	Approx Initial Elution Time, Min.	Approx Peak Width, Min.	CV _t (x10 ⁵)	CI _t	%CV 11-17 min	%CV 17-21 min	%CV 21-25 min	%CV 25-31 min	CI 11-17 min	CI 21-25 min
AAX (AC-20)	14.0	17.0	17.7	0.340	9.5	43.0	38.9	8.6	0.50	0.42
AAX-A Asphaltenes	13.7	16.5	33.6	0.389	15.3	42.3	34.5	7.9	0.51	0.33
AAX-R Resins	16.2	13.0	17.7	0.225	1.0	43.2	50.4	5.4	0.35	0.22
AAX A + R	13.7	17.3	26.4	0.317	10.7	40.5	39.8	9.0	0.49	0.26
AAX-DO Deasphalted Oil	17.5	12.0	10.6	0.129	0.0	26.2	66.2	7.5	NA	0.13
AAX-F Flux	14.0	16.5	34.6	0.292	11.8	37.2	41.8	9.2	0.49	0.23

V.E. Relationships between data from HP-GPC analyses and other SHRP-generated information

Several laboratories around the country have studied the same sets of asphalts: the eight SHRP "core" asphalts and an extended group of asphalts. We have looked for relationships among these data and results from HP-GPC analyses. We have attempted correlations of only two variables and have done no multivariate analyses. It should be noted that data generated under other SHRP contracts has been extracted mostly from quarterly reports and may be subject to revision. Therefore, the correlations to be discussed should be regarded as preliminary indications of relationships.

V.E.1 HP-GPC and other chemical data

Early in this study a striking relationship between weight percent sulfur, or even weight percent nitrogen, oxygen and sulfur combined, was noted. For seven of the core asphalts (excluding AAM-1), the correlation coefficient for % LMS vs % sulfur is 0.93. This seemed to indicate a strong relationship between % LMS and potential polar functional groups. However, asphalt AAM-1 does not fit this pattern since it has a large "LMS" region but a lower weight percentage of heteroatoms than the other core asphalts. When the remaining MRL asphalts are included the other Group 4 asphalts also fall off the general trend. Nevertheless, the correlation coefficient is reduced to 0.55. Two conclusions may be drawn: first, the percent LMS material is only partly related to potential polarity; second, potential polarity seems to be even less involved in the large molecular size entities in Group 4 asphalts.

No significant correlations were noted between percent LMS material and the

concentrations of phenols and/or carboxylic acids (16), the concentrations of sulfoxide, the percent aromatic carbon, the conjugation index or the total conjugated volume, the weight percent of strong acids (17) or the weight percent of strong acids plus strong bases. Data for the weight percent of amphoteric materials is not complete at this time, but it appears that there will be little correlation between that and percent LMS. (A cursory examination indicates that the percentage of SEC I also is not directly related to any of the above factors.)

This indicates only that no single factor that has been measured is responsible for the intermolecular self-assembly observed in the LMS region. It does seem obvious that quantities or concentrations (weight percent strong acids or concentration of carboxylic acid groups, for example) are not so important to self assembly as is the overall ability of intermolecular bonds to form. This may involve considerations of the structure of individual molecules (rather than of averages or classes) – their planarity, their available functionality, their size – all of which is quite beyond reach at this time. Nevertheless, HP-GPC does indicate the tendency for strong intermolecular interactions to occur in an asphalt.

V.E.2 HP-GPC and physical properties

Because our earlier work had suggested a relationship between HP-GPC characteristics of an asphalt and that asphalt's ultimate behavior in a pavement, we have been interested in comparing HP-GPC data with some of the physical properties defined by SHRP.

PTI has listed values for ultimate strain at failure (-26° , 2 hr, %) (17). The correlation coefficient for linear regression analysis of percent LMS vs this failure strain value is only 0.59. However, it is noteworthy that all Group 1 asphalts except AAC-1 (i.e., AAF-1, AAG-1, AAQ, AAV, AAX, AAZ and ABD) have values at 1.3% or below. No other asphalts fall into this range.

Limiting stiffness values [200 MPa, S(t) @ 2 hr, $^{\circ}$ C, ibid] have a slight correlation with percent LMS : $r^2 = 0.65$. (Correlation coefficient for SEC I is 0.56.)

Values for G', G'' and tan δ from WRI and PTI (ibid) were also subjected to regression analyses with the following results.

for G' (WRI) vs % LMS, $r^2 = 0.85$

for G'' (WRI) vs % LMS, $r^2 = 0.83$

for tan δ (WRI) vs % LMS, $r^2 = 0.84$

for tan δ (PTI) vs % LMS, $r^2 = 0.78$

In all cases, asphalt V was omitted because of widely differing values for tan δ from WRI and PTI.

Finally, we have compared, to a limited extent, our predictions for field performance with that from the Grading of Asphalts According to SHRP Version 6 Binder Specification. Because that specification continues to undergo revision, extensive effort was not made with these correlations. However, it is of interest to compare PTI's predicted "failures" with our Group 1 asphalts, which we would expect to fail rapidly due to thermal sensitivity:

<u>PTI Grade - fail</u>	<u>MSU Group 1 - fail</u>
—	AAC-1
AAF-1	AAF-1
AAG-1	AAG-1
—	AAQ-1
AAT	—
AAU	—
—	AAV
AAW	AAW
AAX	AAX
AAZ	AAZ
ABD	ABD

Of eleven asphalts listed, the two approaches agree on six. It is worth noting that, of a number of asphalts with HP-GPC characteristics similar to asphalts AAT and AAU, and which are not listed as potential failures by PTI, we could find no chemical characteristics among data available to us to mark these two materials as "different."

V. F. Summary descriptions of SHRP core asphalts

In the next pages, information presented in this report for each of the SHRP core asphalts will be summarized.

Asphalt AAA-1 has a broad, tri-modal molecular size distribution. The strong acids derived therefrom have a bimodal distribution with most absorption occurring in the larger molecular size ranges. Solvent polarity studies indicate that both polar and nonpolar (probably pi-pi) interactions are important to this asphalt. Van der Waals interactions probably do not make a large contribution. Although it does not apparently undergo excessive oxidation (in terms of [OH+COOH] or percent aromatic

carbon) it does display a relatively rapid increase in % LMS after POV and TFO/POV treatment, suggesting that the associated change in physical properties may be significant. We would expect asphalt AAA-1 to perform well in relatively cold climates. As a representative of Group 2 asphalts, it should not exhibit thermal instability except at extreme temperatures. Its ability to form an intermolecular network could lead to cracking with time and under cold conditions, however.

Asphalt AAB-1 may be described as having a bimodal molecular size distribution of moderate width. It is comprised of materials which are more highly conjugated and have larger chromophores than all but one or two of the other core asphalts. The strong acids have a higher percentage of aromatic carbon than all other strong acids and contain the largest chromophores as well. Solvent polarity studies indicate that both polar and nonpolar associations may be important in AAB-1, but less so than in AAA-1. Although laboratory oxidation produced very small changes in percent aromatic carbon and [OH+COOH], above average increases in % LMS were produced. Asphalt AAB-1 exhibits somewhat less tendency to form self-assembled networks than does asphalt AAA-1. Therefore, it could be more susceptible to early cracking under strong thermal shock. On the other hand, once established, this same moderate network formation could provide longer service in cold climates than asphalt AAA-1.

Clearly asphalt AAC-1 is not "average". Its MSD is narrow with only slight bimodal character. Its chromophores are fairly large (similar to those of AAB-1) but it has an average percentage of aromatic carbon and so its conjugated volume is just average. It has less potential for polarity and more potential for van der Waals

interactions in the neat state. Changes in solvent polarity seem to indicate that neither polar nor nonpolar (pi-pi) interactions are strong contributors in this asphalt. The changes observed in percent aromatic carbon and [OH+COOH], although the latter is considerable, translate into a relatively small change in % LMS. We classify asphalt AAC-1 as a Group 1 asphalt, meaning that the potential for intermolecular network formation is too small to provide adequate resistance to thermal shock, and thus to provide adequate performances.

The findings about asphalt AAD-1 say that this, too, is an unusual material. It is characterized by a broad, trimodal molecular size distribution with an SMS peak indicating a high concentration of small materials with small chromophores. However, the chromophores among the larger materials are not much smaller than those in other asphalts. It has a high potential for polarity in the native state. Solvent polarity experiments show that this asphalt is subject to both polar and pi-pi associations to a greater degree than any other core asphalt. Nevertheless, the changes in percent aromatic carbon and [OH+COOH] upon oxidation correspond to an average increase in % LMS. The existence of the material in the SMS region leads us to anticipate a high loss-on-heating, which is borne out experimentally. The potential for strong network formation indicates that this is not a thermally sensitive material but the strength of that network would lead to eventual cracking in colder climates. This is a warm-climate material.

Asphalt AAF-1 is highly aromatic with its materials confined within a narrow molecular size range and average chromophore sizes. In spite of its relatively high

[OH+COOH], it shows very little propensity to increase its LMS absorption in nonpolar solvent. Nonpolar associations probably occur but large self-assembled entities do not occur. Further, little change in MSD is noted upon oxidation. Its high aromaticity makes it a prime candidate for compatibility with polymers containing aromatic units. But its inability to sustain network formation when used alone make it a Group 1 asphalt and, therefore, unsuitable for general use.

Asphalt AAG-1 is unusual in its very narrow molecular size distribution and, most important, in its apparent resistance to change in MSD with laboratory oxidation or solvent polarity (except for some dissociation in higher concentrations of toluene). That is, polar interactions appear to play a small role whereas nonpolar interactions may be somewhat more important in this asphalt. However, the inability of these interactions to sustain a stable network is the most important characteristic of this Group 1 asphalt. It is the "worst" of the Group 1 asphalts in this regard. We would not expect it to produce a satisfactory pavement.

To summarize the key characteristics of asphalt AAK-1, one must begin with the broad, trimodal molecular size distribution and the obvious presence of vanadyl porphyrins. Solvent polarity experiments demonstrate the importance of both polar and nonpolar (π - π) interactions. Not only is this asphalt subject to a large increase in [OH+COOH], it undergoes a significant increase in LMS on laboratory oxidation. The potential for network formation is quite strong in this asphalt and, therefore, it is not suitable for long-term cold climate use. It should perform well in warmer climates but may be subject to the effects of oxidative aging.

Asphalt AAM-1 is not an "average" asphalt. It is marked by very large molecules with large chromophores (but the second lowest percentage of aromatic carbon) and long, relatively unbranched aliphatic chains. It has a small concentration of heteroatoms and, thus, a low potential for polar interactions. In fact, non-polar interactions seem to be much more important in this asphalt than in any other SHRP core asphalt. Nevertheless, its intermolecular network may preclude its use in cold climates and make it a good candidate for hot climate use.

V. G. Miscellaneous topics

Several small experiments were conducted to enhance understanding of the HP-GPC experiment. Answers to several questions were sought:

- Does sample concentration affect the HP-GPC curve?
- Does the time the sample stands in solution affect the HP-GPC curve?
- How well does the uv-vis response relate to the amount of eluent eliciting that response?

These experiments will be discussed in the next pages.

V. G.1. Concentration effects

The authors and others have theorized that the absorption in the LMS shoulder(s) of asphalt is at least partly due to assemblies of smaller molecules. If this is so, then changing the concentration of asphalt in the sample should result in changes in the shape of the shoulder. Early in this research program a brief set of experiments was

done to test this supposition. Four of the core asphalts were analyzed at four concentrations in THF. The results are shown in Figure 35 and Table 18.

These data indicate that there are changes in the relative intensity of absorption in the chromatograms between their initial elution times and about 17 minutes in all four asphalts. However, the changes in AAG-1 are much less pronounced than in the other three asphalts, again showing the apparent reluctance of AAG-1 components to assemble.

Table 18. Effects of asphalt concentration on HP-GPC characteristics

Sample concentration	% LMS			
	0.1%	0.3%	0.5%	0.7%
Asphalt				
AAA-1	17.3	19.1	19.5	19.6
AAD-1	22.4	22.7	24.2	24.0
AAG-1	2.2	2.7	3.2	3.3
AAM-1	17.7	18.8	20.8	21.1

V. G.2. Effects of time in solution

The HP-GPC testing routine used in this laboratory requires that samples be analyzed as soon as they are prepared. When working with solvents of different polarities, however, it seemed possible that an equilibrium between disassembly and reassembly would not be reached in that time. For example, in toluene dissociation of pi-pi interactions might be slow even at low concentrations. Moreover, the ability of

polar entities to "find each other", so to speak, could be slow.

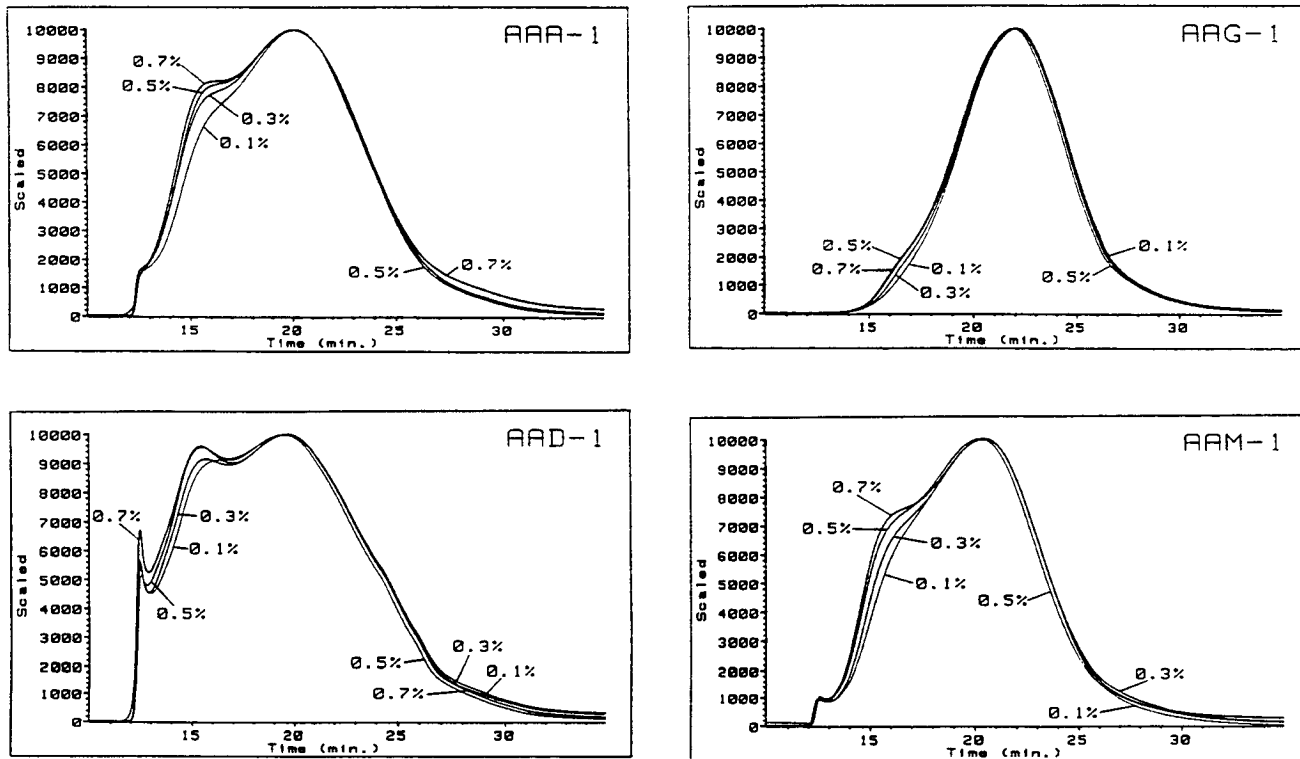


Figure 35. Effect of asphalt concentration on molecular size distribution.

Therefore, a brief series of experiments was conducted in which 0.5 percent solutions of each of the core asphalts in 80 percent toluene/THF were prepared, analyzed as usual and then allowed to stand (sealed) for 96 hours. Analyses were repeated at 24, 48 and 96 hours. The chromatograms in Figure 36 show that at least some increase in intensity of the LMS shoulder occurs with time in all of the core asphalts, presumably associated with increasing polar interactions. (It has not been

proven that no other reactions might be occurring in this solvent system. However, it is known that asphalts can stand in THF alone and not undergo such changes.)

Asphalts AAD-1 and AAK-1 show the largest increases with time. This is not surprising in light of the fact that their heteroatom content is highest among the core asphalts. In contrast, asphalts AAG-1 and AAF-1, with very low heteroatom contents, show very little LMS increase with time. However, asphalts AAM-1 and AAC-1 which also have few heteroatoms, show more LMS increase. Perhaps these asphalts, which have very long aliphatic chains, undergo a reequilibration based on van der Waals interactions.

Asphalts AAA-1 and AAB-1, which have similar and "average" heteroatoms contents, appear to respond somewhat differently. In AAB-1, a gradual increase in the peak centered about 15.5 minutes is observed. Asphalt AAA-1 increases the relative intensity of absorption in the first two populations after 24 hours and remains essentially unchanged until at least 48 hours before once again showing a relative LMS increase at 96 hours.

That the observed increases are likely to be related to polar interactions is supported by chromatograms in Figure 37. These compare similar time-in-solution experiments with asphalts AAG-1 and ABD. These asphalts are derived from the same crude source but AAG-1 was treated with lime during the refining process, thus presumably reducing the potential for hydrogen bonding by producing salts from carboxylic acids and phenols. No lime was used in the production of asphalt ABD, so hydrogen bonding potential should exist. Indeed, a greater increase in LMS is observed

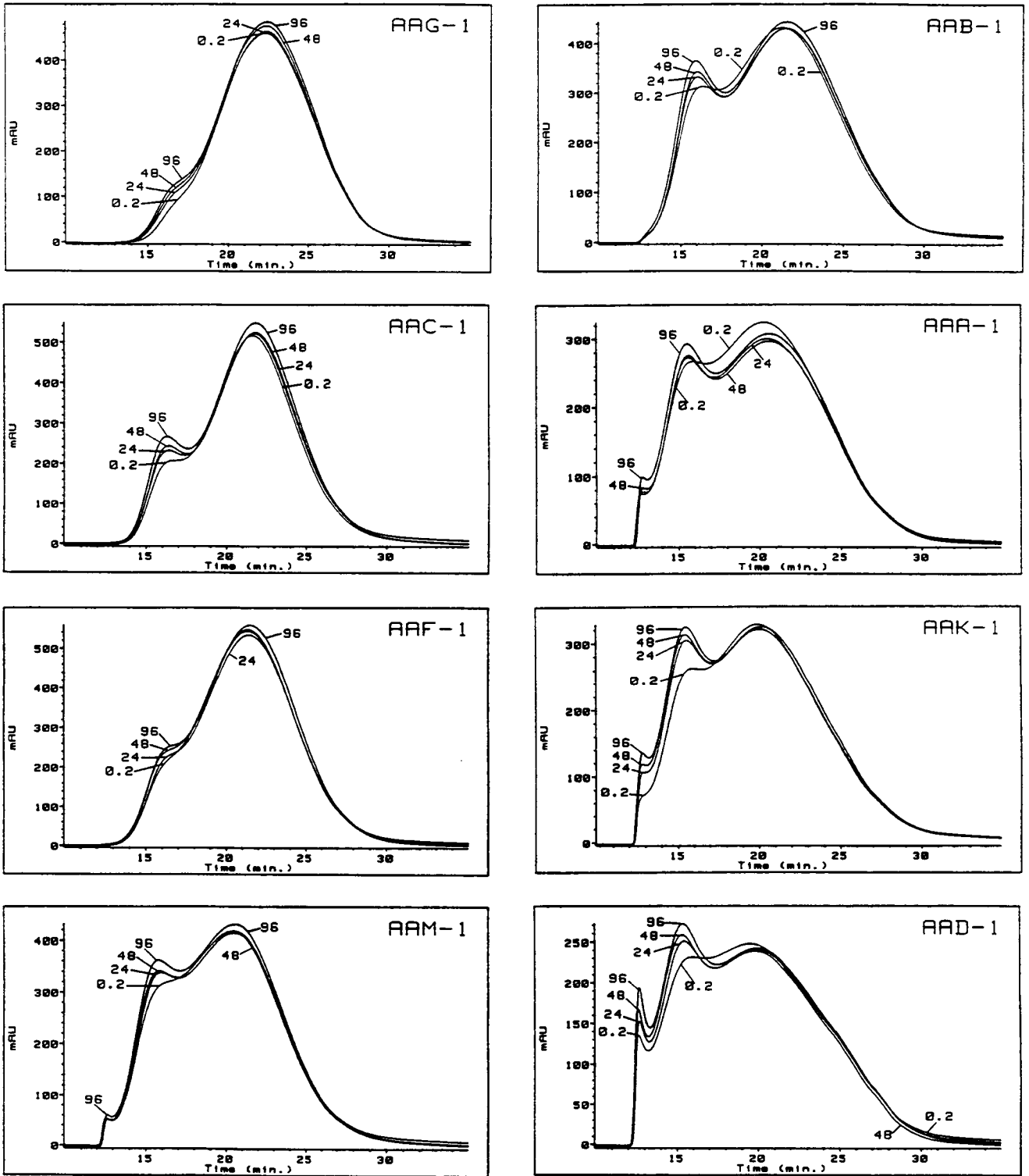


Figure 36. Changes in apparent molecular size distribution with time (hours) in 80 percent toluene/THF solution.

in ABD than in AAG-1. However, ABD remains a Group 1 asphalt.

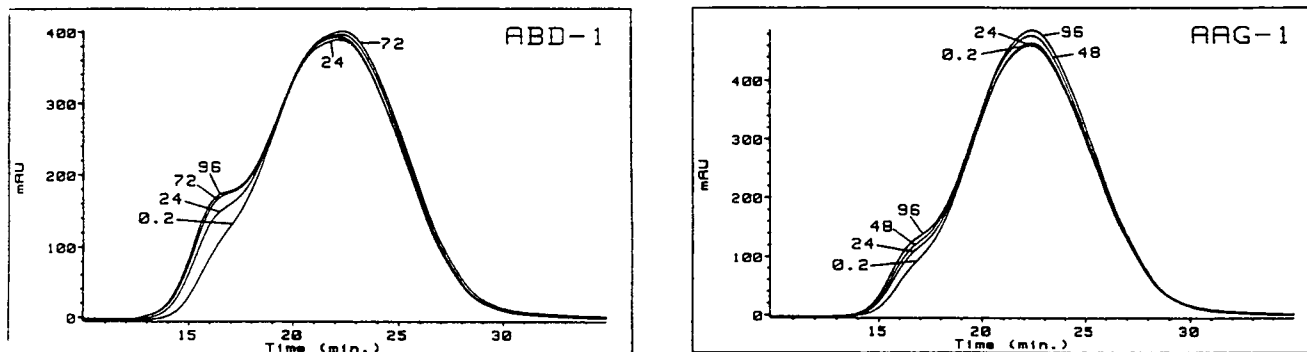


Figure 37. Difference in response to time (hours) in solution for asphalts AAG-1 and ABD-1.

V. G.3. Relationship of sample mass to detector response

As stated early in this report, no "perfect detector" is available for the analysis of asphalt by HP-GPC. Brûlè (3) reported that neither refractive index nor single-wavelength ultraviolet-visible detection mirrored the mass of material yielding the response precisely. The authors have recognized this limitation even with the diode array detector, because of the differences in uv-vis absorption among aromatic molecules and because of the lack of absorption by aliphatic materials.

To obtain an indication of the potential disparity between the amount of asphalt and the detector response for which it is responsible, four of the SHRP core asphalts were analyzed. In these experiments the eluent in five fractions was collected, the solvent removed and the fraction weighed. The resulting information is given in Table 19. Up to about 19 minutes, the percentage of detector response is proportionally "too

large" for the percentage of asphalt responsible; after that time, the opposite is true.

This can be attributed to the larger proportion of non-absorbing aliphatic material eluting later in the MSD. (Recall the low conjugation indices of the neutrals fractions and their smaller molecular sizes.)

Table 19. Relationship of sample mass to detector response

Elution time range, minutes	%weight recovered	%CV _t	%area 230 nm
<u>AAD-1</u>			
10-15	6.0	11.6	11.7
15-19	17.1	26.4	27.1
19-23	41.0	34.3	34.5
23-29	35.9	26.1	25.1
29-35	0.0	1.6	1.6
<u>AAG-1</u>			
10-15	0.0	0.3	0.2
15-19	3.1	11.2	10.3
19-23	52.6	51.9	50.6
23-29	42.3	34.4	36.7
29-35	2.1	2.2	2.1
<u>AAK-1</u>			
10-15	1.1	7.3	6.9
15-19	17.1	28.0	27.9
19-23	50.9	39.6	39.8
23-29	30.8	22.6	22.8
29-35	0.0	2.5	2.6
<u>AAM-1</u>			
10-15	1.0	6.5	6.0
15-19	28.9	33.4	31.5
19-23	55.7	44.2	45.5
23-29	13.4	14.0	15.1
29-35	1.0	1.9	1.8

VI. SUMMARY

The purpose of the research under the SHRP-AIIR-14 project has been to enhance the HP-GPC technique by exploration of the use of more advanced analytical column types with a diode array detector and then to apply that technique to study of the chemical composition of the SHRP core asphalts and their modes of intermolecular interaction.

New, highly-crosslinked styrene-divinylbenzene column packing material proved to be remarkably (although not perfectly) stable in solvents of different polarities. This permitted exploration of the effects of polarity on the asphalt's ability to form self-assembled units. However, tetrahydrofuran (THF) was the solvent of choice for most analyses.

Using this analytical system, it has been possible to compare the core asphalts with respect to the following characteristics:

- 1) overall apparent molecular size distribution (MSD)
- 2) relative content of conjugated (e.g., aromatic) components (CV_t)
- 3) relative size of the chromophores in the aromatic components (CI)
- 4) MSD, CV_t and CI of fractions from ion exchange chromatography (IEC) and size exclusion chromatography (SEC) in toluene
- 5) changes in MSD resulting from laboratory oxidation
- 6) effects of solvent polarity which indicate the relative importance of polar and nonpolar interactions.

Using HP-GPC in THF, the SHRP asphalts (including the eight core asphalts as

well as the extended group collected in the SHRP materials Reference Library) were classified into four broad groups on the basis of their molecular size distributions, the likelihood of the presence of intermolecular associations as indicated by a bi- or trimodal curve shape and the relative elution time of the major peak. Other HP-GPC characteristics may vary within each group.

Group 1 contains just eight asphalts, including three of the core asphalts (AAC-1, AAF-1 and AAG-1). These materials are characterized by narrow molecular size distributions with no large molecules and little, if any, indication of self-assembly in the whole asphalt. Strong acids from the three core asphalts in this group vary in overall MSD but remain in a narrow range with most of the absorption among smaller materials. In general, these core asphalts do not respond strongly to change in solvent polarity, indicating that neither polar nor nonpolar interactions are very important. **Group 1 asphalts, because they possess little potential for formation of sufficient intermolecular network, are expected to be very thermally susceptible and unacceptable as paving materials.**

However, there are differences within the group that can be determined by HP-GPC alone. For example, asphalt AAC-1 has rather large chromophores but not so much aromatic content overall. The presence of disruptable pi-pi (in strong acids) and van der Waals interactions are suggested. Oxidation causes an increase in the absorption in the LMS region of about 3 percent -- more than either of the other core asphalts in this group.

Asphalt AAG-1 has the narrowest MSD and responds least to solvent polarity

changes, to oxidation, concentration changes, etc. There is apparently an effect from the lime treatment in its refining process in reducing the potential for hydrogen-bonding since an asphalt derived from the same crude oil but without lime treatment does exhibit a slight increase in LMS. Nevertheless, it remains a Group 1 asphalt.

Asphalt AAF-1 is very highly aromatic but its chromophores are of "average" size, thus giving it a unique place in Group 1. It is more likely than other core asphalts to be compatible with highly aromatic polymers.

Fourteen asphalts were placed in Group 2 which is characterized by a wider MSD than Group 1 and bi- or trimodal peak shapes. In the authors experience, these are the "common" asphalts. The three core asphalts in this group (AAA-1, AAB-1, AAK-1) respond noticeably to changes in solvent polarity, to oxidation, and to changes in sample concentration. Their strong acids fractions contain predominantly large materials (except AAB-1). These should be much less thermally susceptible than Group 1 asphalts and be limited more by the fact that extensive network formation may eventually lead to cracking in colder regimes.

Nevertheless, there are unique characteristics among these core asphalts as well. Asphalt AAB-1, in addition to showing a strong acids MSD more like Group 1 than Group 2, has a bimodal distribution of moderate width as a whole asphalt. It is more highly aromatic and has larger chromophores than the other Group 2 core asphalts, and is somewhat less influenced by solvent polarity.

The HP-GPC chromatograms of AAK-1 display a strong absorbance about 410 nm resulting from the presence of vanadyl porphyrins. (Asphalts AAB-1 and AAD-1

have a similar, but much less intense, absorbance.)

Only one asphalt can be placed in Group 3, that is AAD-1. Its HP-GPC characteristics include a very wide, trimodal molecular size distribution. The unique feature is the strong absorption among smaller molecular size materials with small chromophores while still having more large molecular size material than any other core asphalt. This asphalt is most responsive to changes in solvent polarity and concentration but less so to oxidation. It is subject to loss of the lighter components and, in colder climates, may be subject to eventual cracking.

Group 4 includes five asphalts, only one of which is from the core samples (AAM-1). These are marked by somewhat narrower MSD's than Groups 2 and 3 but are composed overall of much larger molecules and/or assemblies. They have lower absorbances due to conjugated entities but the chromophores are relatively large. That is, one can envision large aromatic ring systems with a large amount of aliphatic material in association. Asphalt AAM-1 is somewhat affected by changes in solvent polarity and changes in the LMS region in response to oxidation. It is more subject to nonpolar association than the other asphalts; it is probably best suited to use in warmer regions.

Other, more detailed information is included in this report. It may well be useful in differentiating asphalts within the groups suggested and to help in defining shades of difference in performance. However, the authors suggest that these groups will be related to broad performance characteristics. Group 1 asphalts may be unable to assemble an effective intermolecular network incorporating polar and nonpolar

interactions. Thus, they may exhibit "tenderness" and lack the ability to resist early cracking due to rapid temperature changes.

Group 2 and Group 3 asphalts are likely to be able to assemble very effective polar-nonpolar networks. In fact, with time these networks may become "too effective", depending on the climate in which they are used, and lead to long-term, age-related cracking. Asphalts like AAD-1 may be subject to volatile loss on heating.

VII. APPENDIX

EXPERIMENTAL PROCEDURES

A. Short-term phase transfer methylation

A 100 mg aliquot of asphalt was dissolved in 100 mls of freshly distilled THF (tetrahydrofuran), in a 250 ml Erlenmeyer flask equipped with a magnetic stir bar. 0.2 ml of aqueous tetrabutylammonium hydroxide, (TBAH, 40% by weight; Aldrich), was slowly added, dropwise, while the mixture was stirred, under nitrogen at room temperature, for 20 minutes. Then 0.20 ml of 45% (v/v) solution of carbon 13 enriched iodomethane (99.4 atom % ^{13}C ; Aldrich) in carbon tetrachloride was added to the reaction flask and stirred overnight, under nitrogen, at room temperature.

Any THF remaining the next morning was removed by rotoevaporation at 30° C. The residue was dissolved in 100 mls of chloroform and then rigorously extracted, first with 150-200 ml portions of a 1-5% (wt) aqueous solution of sodium nitrate (total volume 1 L), and then by washes of 150-200 mls of distilled water (total volume 4 L). Washes were tested for the presence of ionic iodide with a few drops of aqueous (21%) silver nitrate (Alfa). No iodide was detectable after 6-7 washings.

Chloroform was removed by roto-evaporation at 30° C and for an additional 0.5 hour at 70° C. The final product was then dried at 70-80° C and ≤ 1 mm Hg for 2 hours on a high vacuum pump.

B. Friedel-Crafts acylation

A 100 mg aliquot of asphalt was dissolved in approximately 15 mls of methylene chloride in a 50 ml round bottom boiling flask with stir-bar. The flask was flushed with nitrogen for a moment and immediately an excess of anhydrous ferric chloride added, (i.e., an excess being greater than 1 equivalent where $1 \text{ eq.} = 0.100 \text{ g asphalt} \times \# \text{ g asphalt/mol}$). The flask was then placed in an ice bath and, while stirring, 1.1 to 1.5 equivalents of acetylchloride added alowly. A trap was attached to the reaction vessel and the HCl gas evolution monitored. Once bubbling stopped the sample was removed from the ice bath and allowed to warm to room temperature (approximately 30 minutes). Ice was then added to quench the mixture.

The organic phase was isolated from the aqueous using a separatory funnel and then filtered through glass fiber filters to remove excess FeCl_3 . Solvent was removed using roto-evaporation at 40°C and 100°C to remove any residual solvent trace.

C. HP-GPC analysis of asphalt samples

The HP-GPC technique performed by our research group utilized the following instrumentation:

- a Waters 6000A series chromatography pump capable of delivering solvent at a rate of 0.1 to 10.0 mls per minute,
- an in-line flow rate meter by Phase Sep capable of measuring flows of 0.1 to 10.0 mls per minute within 1% accuracy, (Phase Sep; Hauppauge, NY),
- a model 6K injector fitted with an appropriate sample loop,

- a diode array detector (DAD) by Hewlett Packard capable of simultaneous detection of any eight wavelengths from 200 to 600 nm, (Hewlett Packard 1040A HPLC-Detection System),
- a 9000 Series 300 Hewlett Packard computer with HP79988A HPLC Chemstation software, Rev. 5.1, for data acquisition, storage/retrieval, and manipulation, plus hard copy output devices,
- a Jordi GPC-GEL 10^3 angstrom, 10 mm ID x 50 cm (crosslinked styrene divinylbenzene) column, (Jordi Assoc. Inc.; Bellingham, MA). An in-line pre-column filter was also used,
- a closed water-circulation system to maintain a constant column temperature of 24° C,
- and a solvent reservoir with dry nitrogen or helium purge.

System operating parameters include a mobile phase pump flow rate for sample and standard analyses at 0.9 ml per minute. The column temperature was maintained at $24^\circ \pm 1^\circ$ C. Eight wavelengths were selected for detection by the DAD; 210, 230, 254, 280, 340, 380, 410, and 440 nm, all with a 4 nm bandwidth. The sampling interval was 3520 milliseconds with a peakwidth setting of 0.5 minutes. Elution times for samples were completed within 35 minutes.

Calibration of the system was performed with a set of polystyrene standards available from Waters. Six polystyrene standards - 1125K, 240K, 50K, 9K, 3.6K, and 1.8K, and toluene, were combined as a mixed standard to monitor system functions and column characteristics in each solvent type.

Equilibration of the HP-GPC system was determined by successive injections of the same asphalt until identical runs obtained. These were then compared with previous runs for precision. Usually several hours is required at the start of each day for these systems to equilibrate, i.e., temperature, flow rate, and pressure, before repeatable data is observed.

Solvent changes were performed according to the column manufacturer's instructions, the procedure usually requiring from 24 to 72 hours for equilibration with the new solvent.

All solvents used were high purity (HPLC Grade or better), free of water and stabilizers. THF was distilled by spinning band reflux column with sodium metal and benzophenone as indicator prior to use to remove water and other impurities.

Sample preparation for the HP-GPC technique consisted of taking aliquots of each sample transferred to glass vials and, immediately prior to injection, diluted with the mobile phase solvent to obtain a 0.5 percent solution by weight. Before injection the sample solution was centrifuged to isolate insoluble material which may act in plugging and potentially damaging the column. Rarely was any insoluble material seen collected at the bottom of the centrifuge tube.

HP-GPC injection sizes were generally 100 μ ls, depending on sample type. Injection sizes for the IEC Strong Acids and SEC-1 fraction were smaller due to their high concentration, a result of the techniques used to isolate and concentrate them from the whole asphalt cement.

Integrations of the chromatograms were performed using the HP Chemstation software program. An events table was established to integrate the chromatograms at specific times, dividing each wavelength into nine time-segments. A moderately sensitive threshold (mAV/mV) and a baseline hold from 10 to 35 minutes were used.

VIII. REFERENCES

1. Yapp, M.T.; Durrani, A.Z. and Finn, F.N. "HP-GPC and Asphalt Characterization Literature Review", SHRP document TM-ARE-A-003A-90-2.
2. Brûlé, B.; Such and Baluja-Santos, "Characterization of a Road Asphalt by Chromatographic Techniques (GPC and HPLC)", *J. Liquid Chromatography* 2, 437 (1979).
3. Brûlé, B.; "Contribution of Gel Permeation Chromatography (GPC) to the Characterization of Asphalts", in *Liquid Chromatography of Polymers and Related Materials II*. Cazes and Delamore, Eds., Dekker, 1980.
4. Brûlé, B.; Ramond, G.; Such, C. "Relationships between Composition, Structure and Properties of Road Asphalts: State of Research at French Laboratoire Central des Ponts Chaussees" for TRB, 1986.
5. Beazley, P.M.; Hawseg, L.E. and Plummer, M.A., "Size Exclusion Chromatography and Nuclear Magnetic Resonance Techniques for Predicting Asphalt Yields and Viscosities from Crude Oil"; *Transportation Research Record*, 1987, 1115, 46.
6. Plummer, M.A., et al., *Asphalt Paving Technology*, 1984. 53, 138.
7. Jennings, P.W.; Pribanic, J.A.S. and Dawson, K.R., "Use of HPLC to Determine the Effects of Various Additives and Fillers on the Characterization of Asphalt", U.S. Department of Transportation, Federal Highway Administration Report No. FHWA/MT-82/001. 1982.
8. Jennings, P.W. and Pribanic, J.A.S., "Prediction of Asphalt Performance by HP-GPC", *Proceedings Association of Asphalt Paving Technologists*, 1985, 54, 635.
9. Jennings P.W., "Asphalt Chemistry: A Perspective on the Use of HP-GPC", Symposium held in Wichita, Kansas, November 1987 to be published in *Fuel Science and Technology*, in press.
10. Pribanic, J.A.S.; Emmelin, M. and King, G.N., "Use of a Multiwave UV-VIS Detector with HP-GPC to Give a Three-Dimensional View of Bituminous Materials", in *Transportation Research Record* 1228, TRB, National Research Council, Washington D.C., 1989, 168.

11. Petersen, J.C., "Chemical Composition of Asphalt as Related to Asphalt Durability - State of the Art...", in *Transportation Research Record*, TRB, National Research Council, Washington D.C. 1984.
12. Garrick, N.W. and Wood, L.E., "Relationship between High Pressure Gel Permeation Chromatography Data and the Rheological Properties of Asphalts", in *Transportation Research Record* 1096, TRB, National Research Council, Washington D.C., 1986, p. 35.
13. Speight, J.G. and Moschopedis, S.E., "On the Molecular Nature of Petroleum Asphaltenes" in *Chemistry of Asphaltenes*, J.W. Bunger and N.C. Li, eds., *Advances in Chemistry Series* 195, 1981, ACS.
14. Branthaver, J.F., et al., "Separation of SHRP Asphalts by Ion Exchange Chromatography," *PREPRINTS*, Div. Petrol. Chem., ACS, 35 (3) 376 (1990).
15. Branthaver, J.F., et al., "Separation of SHRP Asphalts by Preparative Size Exclusion Chromatography," *PREPRINTS*, Div. of Petrol. Chem., ACS, 35, (3) 407 (1990).
16. Jennings, P.W. et al., "Binder Characterization and Evaluation by NMR Spectroscopy" SHRP A-002C Final Report, February 1991.
17. MRL Asphalt Properties List, revision 4/29/92. SHRP contract A-001.

Asphalt Advisory Committee

Chairman

Thomas D. Moreland
Moreland Altobelli Associates, Inc.

Vice Chairman

Gale C. Page
Florida Department of Transportation

Members

Peter A. Bellin
*Niedersachsisches Landesamt
für Strassenbau*

Campbell Crawford
National Asphalt Paving Association

Joseph L. Goodrich
Chevron Research Company

Eric Harm
Illinois Department of Transportation

Charles Hughes
Virginia Highway & Transportation Research Council

Robert G. Jenkins
University of Cincinnati

Anthony J. Kriech
Heritage Group Company

Richard Langlois
Universite Laval

Richard C. Meiningner
National Aggregates Association

Nicholas Nahas
EXXON Chemical Co.

Charles F. Potts
APAC, Inc.

Ron Reese
California Department of Transportation

Donald E. Shaw
Georgia-Pacific Corporation

Scott Shuler
The Asphalt Institute

Harold E. Smith
City of Des Moines

Thomas J. Snyder
Marathon Oil Company

Richard H. Sullivan
Minnesota Department of Transportation

Haleem A. Tahir
*American Association of State Highway
and Transportation Officials*

Jack Telford
Oklahoma Department of Transportation

George A. West
Shell Oil Company

Liaisons

Avery D. Adcock
United States Air Force

Ted Ferragut
Federal Highway Administration

Donald G. Fohs
Federal Highway Administration

Fredrick D. Hejl
Transportation Research Board

Aston McLaughlin
Federal Aviation Administration

Bill Weseman
Federal Highway Administration

12/22/92

ETG members

Ernest Bastian
Federal Highway Administration

Don O'Connor
Texas Department of Highways and Public Transportation

Brian Chollar
Federal Highway Administration

Ken Grzybowski
PRI Asphalt Technologies, Inc.

Robert Jester
Federal Highway Administration

Gerhard Kennepohl
Ontario Ministry of Transport

Ron Reese
California Department of Transportation